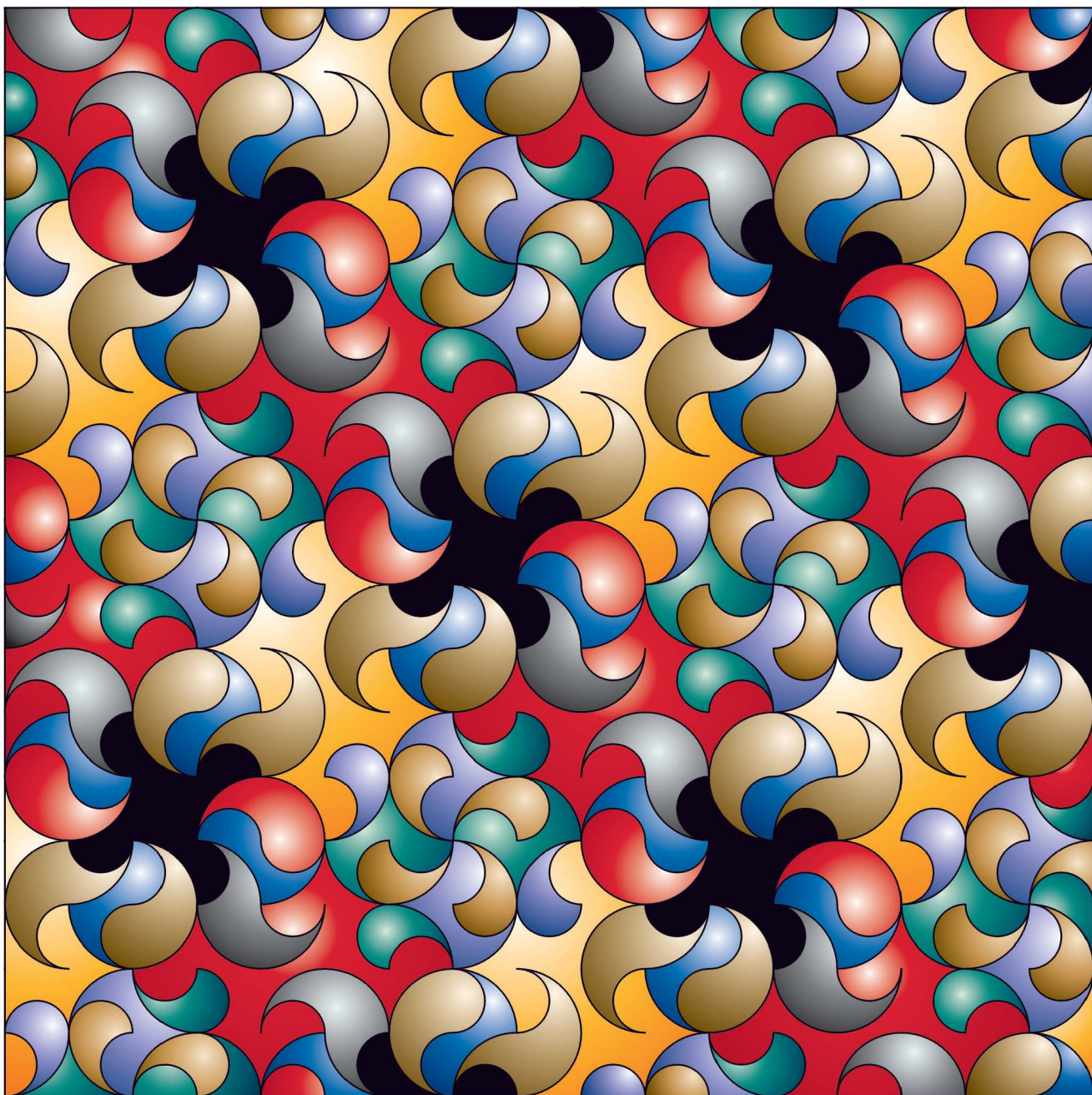
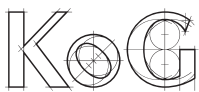


KoG

No. 11, 2007
ISSN 1331-1611

SCIENTIFIC-PROFESSIONAL JOURNAL OF
CROATIAN SOCIETY FOR GEOMETRY AND GRAPHICS





Official publication of the Croatian Society for Geometry and Graphics publishes scientific and professional papers from the fields of geometry, applied geometry and computer graphics.

Founder and Publisher

Croatian Society for Geometry and Graphics

Editors

SONJA GORJANC, Faculty of Civil Engineering, University of Zagreb, Croatia (Editor-in-Chief)

JELENA BEBAN-BRKIĆ, Faculty of Geodesy, University of Zagreb, Croatia

EMA JURKIN, Faculty of Mining, Geology and Petroleum Engineering, University of Zagreb, Croatia (young editor)

MARIJA ŠIMIĆ, Faculty of Architecture, University of Zagreb, Croatia (young editor)

Editorial Board

SONJA GORJANC, Faculty of Civil Engineering, University of Zagreb, Croatia

MILJENKO LAPAINE, Faculty of Geodesy, University of Zagreb, Croatia

EMIL MOLNÁR, Institute of Mathematics, Technical University of Budapest, Hungary

LIDIJA PLETENAC, Faculty of Civil Engineering, University of Rijeka, Croatia

HELLMUTH STACHEL, Institute of Geometry, Technical University of Vienna, Austria

NIKOLETA SUDETA, Faculty of Architecture, University of Zagreb, Croatia

VLASTA SZIROVICZA, Faculty of Civil Engineering, University of Zagreb, Croatia

VLASTA ŠČURIĆ - ČUDOVAN, Faculty of Geodesy, University of Zagreb, Croatia

GUNTER WEISS, Institute of Geometry, Technical University of Dresden, Germany

Design

Miroslav Ambruš-Kiš

Layout

Sonja Gorjanc, Ema Jurkin

Cover Illustration

Tamás F. Farkas, *Drawings* (see the last page)

Print

“O-TISAK”, d.o.o., Zagreb

URL address

<http://www.hdgg.hr/kog>

<http://hrcak.srce.hr>

Edition

250

Published annually

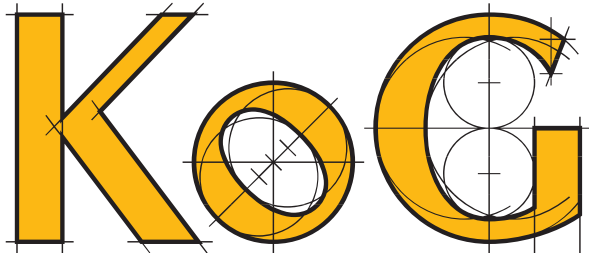
Guide for authors

Please, see the pages 53, 54

KoG is cited in: Mathematical Review, MathSciNet, Zentralblatt für Mathematik

This issue has been financially supported by The Ministry of Science, Education and Sport of the Republic of Croatia.

ISSN 1331-1611



SCIENTIFIC AND PROFESSIONAL JOURNAL OF
CROATIAN SOCIETY FOR GEOMETRY AND GRAPHICS

No. 11

Zagreb, 2007

CONTENTS

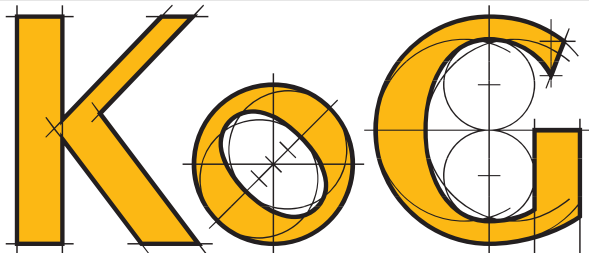
ORIGINAL SCIENTIFIC PAPERS

- Ibrahim Günaltılı*: On the Projectively Extended Linear Spaces 3
Ivanka Babić, Ana Sliepčević: Regular Polygons in the Projectively Extended Hyperbolic Plane 7
Friedrich Manhart: Affine Geometry of Minkowski Minimal Surfaces in \mathbb{R}^3_1 15
Radimir Viher: On the Multiple Roots of the 4th Degree Polynomial 25

PROFESSIONAL PAPERS

- Tatiana Olejníková*: Cyclical Surfaces Created by a Conical Helix 33
Hans Günther Kopetzky, Hans Sachs: Quadratic Cones and AutoCAD 39
Daniela Velichová: Knotted Tori 43
Željko Gjuranić: Terrain Modelling by Using Delaunay Triangulation 49

ISSN 1331-1611



BROJ 11
Zagreb, 2007

ZNANSTVENO-STRUČNI ČASOPIS
HRVATSKOG DRUŠTVA ZA GEOMETRIJU I GRAFIKU

SADRŽAJ

ORIGINALNI ZNANSTVENI RADOVI

<i>Ibrahim Günaltılı:</i> O projektivno proširenim linearnim prostorima	3
<i>Ivanka Babić, Ana Sliepčević:</i> Pravilni poligoni u projektivno proširenoj hiperboličkoj ravnini	7
<i>Friedrich Manhart:</i> Afina geometrija minimalnih ploha Minkowskog u \mathbb{R}^3_1	15
<i>Radimir Viher:</i> O višestrukim korijenima polinoma 4. stupnja	25

STRUČNI RADOVI

<i>Tatiana Olejníková:</i> Kružne plohe izvedene pomoću zavojnice na stošcu	33
<i>Hans Günther Kopetzky, Hans Sach:</i> Stošci 2. stupnja i AutoCAD	39
<i>Daniela Velichová:</i> Torusni čvorovi	43
<i>Željko Gjuranić:</i> Modeliranje terena pomoću Delaunayeve triangulacije	49

Original scientific paper
Accepted 28.11.2007.

IBRAHIM GÜNALTLİ

On the Projectively Extended Linear Spaces

On the Projectively Extended Linear Spaces

ABSTRACT

In this article, we show that a linear space whose parameters are those of the complement of a subset in a finite projective plane π of order n such that no line is removed and a sufficient number of lines lost only one point, is projectively extended linear space.

Key words: linear space, projective plane, affine plane, semiextension, parallel class, projectively extended linear space.

MSC 2000: 51E20, 51A45

1 Introduction

The complementation problem with respect to a projective plane is the following:

Remove a certain subset of points and lines from the projective plane. Determine the parameters of the resulting space. Now assume that you are starting with a space having these parameters. Does this somehow force this subset to reappear, thus giving an embedding in the original projective plane? A number of people have considered complementation problems ([1], [2], [3], ..., [10]). In 1970, Dickey solved the problem for the case where the configuration removed was a unital [6].

Let us first recall some definitions and results. For more details, see [5].

Definition 1.1 A *finite linear space* is a pair $(\mathcal{P}, \mathcal{L})$, where \mathcal{P} is a finite set of points and \mathcal{L} is a family of proper subsets of \mathcal{P} , which are called *lines*, such that

- (L1) Any two distinct points lie on exactly one line,
- (L2) Any line contains at least two points.

Definition 1.2 A finite linear space $S = (\mathcal{P}, \mathcal{L})$ is called a *non-trivial $(n+1)$ -regular linear space*, $n \geq 1$, if

- (i) Every point is on $n+1$ lines
- (ii) No line contains all points of S .

O projektivno proširenim linearnim prostorima

SAŽETAK

U ovom članku se pokazuje da je projektivno prošireni linearni prostor onaj linearni prostor čiji parametri su parametri komplementa podskupa konačne projektivne ravnine π reda n tako da niti jedan pravac nije odstranjen, a dovoljan broj pravaca gubi samo jednu točku.

Ključne riječi: linearni prostor, projektivna ravnina, afina ravnina, poluproširenje, paralelna klasa, projektivno prošireni linearni prostor

Definition 1.3 Let $S = (\mathcal{P}, \mathcal{L})$ be a finite linear space. If there exists at least one parallel class in S , this class is called **ideal point** of S . We construct a new structure $S^* = (\mathcal{P}^*, \mathcal{L}^*)$ which consists of the points of S along with the ideal points and the lines of S which are extended by those parallel classes to which belong. This structure S^* is called **semiextension** of S . S is called **projectively extended linear space** if S^* is a projective plane.

The cardinality of \mathcal{P} (resp. \mathcal{L}) will be denoted by v (resp. b). The *degree* of a point p is the number $b(p)$ of lines on which it lies. The integer n , where $n+1 = \max \{b(p) : p \in \mathcal{P}\}$, is called the *order* of the space. The *size* or *degree* $v(l)$ (also denoted by $|l|$) of a line l is the number of points it contains. A k -line is a line of size k .

The difference between $n+1$ and the number of points on l is called a *deficiency* of l denoted $d(l)$ for any line l . Two lines l and l' are *parallel* (respectively *disjoint*) if $l = l'$ or $l \cap l' = \emptyset$ (respectively if $l \neq l'$ and $l \cap l' = \emptyset$).

A *parallel class* in the linear space $(\mathcal{P}, \mathcal{L})$ is a subset of \mathcal{L} with the property that each point of \mathcal{P} is on a unique element of this subset.

A *finite projective plane* of order n , $n \geq 2$, is a non-trivial $(n+1)$ -regular linear space in which all lines have the same size $n+1$.

A *finite affine plane* of order n , $n \geq 2$, is a non-trivial $(n+1)$ -regular linear space in which all lines have the same size n .

In this paper, for any two disjoint lines l and l' which have size less than n in a finite linear space we will use $m(l, l')$ and $m_n(l, l')$ to denote respectively the total number of lines and n -lines meeting l or l' without l and l' are themselves included.

$$\mu = \min\{n+1 - v(l) \mid l \in \mathcal{L}, v(l) \leq n\} \text{ and}$$

$$\lambda = \max\{n+1 - v(l) \mid l \in \mathcal{L}, v(l) \leq n\}.$$

$$M_n = \max\{m_n(l, l') \mid l', l \in \mathcal{L}, v(l) \leq n, v(l') \leq n\}.$$

The positive integers μ and λ will denote the minimum and maximum of *deficiencies* of lines of \mathcal{S} which have size less than n , respectively.

Lemma 1.1 [5, Lemma 3.3] Suppose that $\mathcal{S} = (\mathcal{P}, \mathcal{L})$ is a non-trivial $(n+1)$ -regular linear space with $n^2 + n + 1$ lines and $n^2 + n + 1 - s$ points.

(i) If b_n is the number of lines of size n , $b_n \geq s(n+2-s)$. In particular, $n^2 + 1 \leq v \leq n^2 + n - 1$, $b_n \geq 2n$.

(ii) If there is no line of size n ,

$$\sum_{l \in \mathcal{L}} d(l)(d(l) - 2) = s(s - 2 - n).$$

2 Main Results

Lemma 2.1 If $\mathcal{S} = (\mathcal{P}, \mathcal{L})$ is a non-trivial $(n+1)$ -regular linear space with $n^2 + n + 1$ lines which contains at least one n -line, $n \geq 2$, the semiextension of \mathcal{S} is linear space.

Proof. Let $\mathcal{S}^* = (\mathcal{P}^*, \mathcal{L})$ be a semiextension of \mathcal{S} . Fix an n -line l . Then the number of lines missing l is n . Hence each n -line induces a parallel class of $n+1$ lines. Since \mathcal{S} is a $(n+1)$ -regular linear space which contains sufficient number of n -lines, \mathcal{S} contains at least one parallel class of lines.

It is clear that two old points (points of \mathcal{P}) or an old and a new point are on a unique line of \mathcal{L} .

Let x and y be new points. We must show that they determine a unique line of \mathcal{L} . Let l_x and l_y be n -lines which determine the parallel classes corresponding to x and y . If l_x and l_y do not meet, then $x = y$ which is a contradiction. So l_x and l_y meet. Each point of l_y is on a unique line of the parallel class determined by l_x . This leaves precisely one line of the parallel class parallel to both l_x and l_y . Therefore \mathcal{S}^* is a linear space.

Lemma 2.2 Let \mathcal{S} be a non-trivial $(n+1)$ -regular linear space with $n^2 + n + 1$ lines in which all lines in semiextension of \mathcal{S} meet. Then semiextension of \mathcal{S} is a projective plane of order n , $n \geq 2$.

Proof. Let \mathcal{S}^* be semiextension of \mathcal{S} . Then each line in \mathcal{S}^* contains $n+1$ points since all lines in \mathcal{S}^* meet. Therefore \mathcal{S}^* is a linear space with $n^2 + n + 1$ lines and $n^2 + n + 1$ points. Hence \mathcal{S}^* is a projective plane of order n .

Lemma 2.3 Let \mathcal{S} be a non-trivial $(n+1)$ -regular linear space with $b = n^2 + n + 1$ lines and $v(l) = n + 1 - d(l)$ for every line l of \mathcal{S} . Then

- (i) The number of lines parallel to a line l is $d(l).n$
- (ii) If l and l' intersect, the number of lines parallel to two lines l and l' is $d(l).d(l')$, and it is $(n-1) + (d(l)-1)(d(l')-1)$, if l and l' are parallel.
- (iii) If M is the set of lines parallel to a given line l , $(v - v(l)).d(l) = \sum_{k \in M} v(k)$

Proof. It is trivial.

Lemma 2.4 Let $\mathcal{S} = (\mathcal{P}, \mathcal{L})$ be an $(n+1)$ -regular linear space with $b = n^2 + n + 1$ lines and v points having the property each point on an $n+1-d(l)$ -line, $d(l) \geq 0$, is on at most $b-v-d(l)$ lines of size n .

- (i) If $b-v \leq 2\mu-1$, $M_n \leq 2(n+1-\mu)(b-v-\mu)$.
- (ii) If $b-v \geq 2\lambda-1$, $M_n \leq (n+1-\mu)(b-v-1)$.

Proof. Suppose that l is an $n+1-d(l)$ -line and l' is a $n+1-d(l')$ -line, $d(l) \leq d(l')$. By all the assumptions of lemma, there are at most $(n+1-d(l))(b-v-d(l))$ lines of size n and $(n+1-d(l'))(b-v-d(l'))$ lines of size n meeting l and l' , respectively. Let the number of n -lines which are (meeting l and missing l'), (meeting l' and missing l) or (meeting l and l') be x, y or z , respectively. Then $m_n(l, l') = x+y+z$. On the otherhand $y+z \leq (n+1-d(l'))(b-v-d(l'))$, since $d(l) \leq d(l')$.

If $b-v \leq 2\mu-1$, $b-v-d(l) \leq d(l')-1$ and $b-v-d(l') \leq d(l)-1$ since $d(l) \leq d(l')$ and $2\mu-1 \leq d(l)+d(l')-1$. Hence

$$\begin{aligned} x &\leq (n+1-d(l))(b-v-d(l)) \\ &\leq (n+1-\mu)(b-v-\mu) \\ y+z &\leq (n+1-d(l'))(b-v-d(l')) \\ &\leq (n+1-\mu)(b-v-\mu). \end{aligned}$$

Thus

$$M_n \leq 2(n+1-\mu)(b-v-\mu).$$

If $b-v \geq 2\lambda-1$, $b-v-d(l) \geq d(l')-1$, $b-v-d(l) \geq d(l')-1$, since $d(l) \leq d(l')$ and $2\lambda-1 \geq d(l)+d(l')-1$.

Therefore,

$$\begin{aligned} (n+1-d(l))(b-v-d(l)) &\geq (n+1-d(l))(d(l')-1) \\ \text{and} \\ (n+1-d(l'))(b-v-d(l')) &\geq (n+1-d(l'))(d(l)-1). \end{aligned}$$

Hence

$$\begin{aligned} x &\leq (n+1-d(l))(d(l')-1) \\ y+z &\leq (n+1-d(l'))(b-v-d(l')) \\ &\leq (n+1-d(l))(b-v-d(l')). \end{aligned}$$

Therefore, $M_n \leq (n+1-\mu)(b-v-1)$, since

$$m_n(l, l') \leq (n+1-d(l))(b-v-1) \text{ and } \mu \leq d(l) \leq d(l') \leq \lambda.$$

Theorem 2.1 Let \mathcal{S} be a non-trivial $(n+1)$ -regular linear space with n^2+n+1 lines and v points. Let the total number of n -lines in \mathcal{S} be b_n . If $b_n > M_n$, \mathcal{S} is projectively extended space of order n .

Proof. Let \mathcal{S}^* be semiextension of \mathcal{S} . By Lemma 2.1, \mathcal{S}^* is a linear space. It follows from our method of construction that each point of \mathcal{S}^* is on $n+1$ lines. Finally we prove that any two lines of \mathcal{S}^* always meet. Let l and l' be lines of \mathcal{S}^* which don't meet in \mathcal{S} . To prove that they meet in \mathcal{S}^* , it suffices to find an n -line parallel to both.

If either l or l' is an n -line, we are done (and clearly neither can be an $n+1$ -line)

Suppose that l is an $n+1-d(l)$ -line and l' is an $n+1-d(l')$ -line, $2 \leq d(l) \leq d(l')$. Since $b_n > M_n$, and there is at most M_n lines of size n which intersect at least one of two parallel lines l and l' , there is at least another n -line. Thus l and l' meet in \mathcal{S}^* . Therefore, by Lemma 2.2, \mathcal{S}^* is a projective plane of order n .

Theorem 2.2 Let $\mathcal{S} = (\mathcal{P}, \mathcal{L})$ be an $(n+1)$ -regular linear space with $b = n^2+n+1$ lines and v points having the property each point on an $n+1-d(l)$ -line, $d(l) \geq 0$, is on at most $b-v-d(l)$ lines of size n . If $b_n > 2(n+1-\mu)(b-v-\mu)$, \mathcal{S} is projectively extended space of order n .

Proof. By Lemma 2.1, semiextension of \mathcal{S} is linear space. Fix an n -line l . Then the number of lines missing l is n . Hence each n -line induces a parallel class of $n+1$ lines. Let \mathcal{S}^* be a semiextension of \mathcal{S} . We must show that any two lines in \mathcal{S}^* intersect. Let l and l' be lines of \mathcal{S}^* which don't meet in \mathcal{S} . To prove that they meet in \mathcal{S}^* , it suffices to find an n -lines parallel to both.

If either l or l' is an n -line, we are done. (and clearly neither can be an $n+1$ -line).

Suppose that l is a $n+1-d(l)$ -line and l' is a $n+1-d(l')$ -line, $2 \leq d(l) \leq d(l')$. By all the assumptions of theorem, there are at most $(n+1-d(l))(b-v-d(l))$ n -lines and $(n+1-d(l'))(b-v-d(l'))$ n -lines meeting l and l' , respectively. Let the number of n -lines which are (meeting l and missing l'), (meeting l' and missing l) or (meeting l and l') be x, y or z , respectively. Then $y+z \leq (n+1-d(l'))(b-v-d(l'))$, since $2 \leq d(l) \leq d(l')$. Hence

$$\begin{aligned} x &\leq (n+1-d(l))(b-v-d(l)) \\ &\leq (n+1-\mu)(b-v-\mu) \\ y+z &\leq (n+1-d(l'))(b-v-d(l')) \\ &\leq (n+1-\mu)(b-v-\mu). \end{aligned}$$

Therefore, the number of n -lines which intersect at least one of lines l and l' , the number of n -lines is at most $2(n+1-\mu)(b-v-\mu)$ and there is at least one n -line missing l and l' . Thus l and l' meet in \mathcal{S}^* . So by the Lemma 2.2, \mathcal{S}^* is a projective plane of order n .

Corollary 2.1 Let $\mathcal{S} = (\mathcal{P}, \mathcal{L})$ be an $(n+1)$ -regular linear space with $b = n^2+n+1$ lines and v points having the property each point on an $n+1-d(l)$ -line, $d(l) \geq 0$, is on at most $b-v-d(l)$ lines of size n .

If $b_n \geq 1$ and $n \geq (b-v-\mu)(b-v-1)$, \mathcal{S} is projectively extended space of order n

Proof. Let $b_n \geq 1$ and $n \geq (b-v-\mu)(b-v-1)$. By Lemma 1.1, $b_n > (b-v)(n+2-(b-v))$.

Since $n \geq (b-v-\mu)(b-v-1)$,

$$(b-v)(n+2-(b-v)) > 2(n+1-\mu)(b-v-\mu).$$

Therefore, by the Theorem 2.2, \mathcal{S} is projectively extended space of order n .

Theorem 2.3 Let $\mathcal{S} = (\mathcal{P}, \mathcal{L})$ be an $(n+1)$ -regular linear space with $b = n^2 + n + 1$ lines and at most $n^2 + n + 2 - 2\lambda$ points having the property each point on an $n+1-d(l)$ -line, $d(l) \geq 0$, is on at most $b-v-d(l)$ lines of size n .

If $b_n > (n+1-\mu)(b-v-1)$ then \mathcal{S} is projectively extended space of order n .

Proof. By Lemma 2.1, the semiextension of \mathcal{S} is linear space. Fix an n -line l . Then the number of lines missing l is n . Hence each n -line induces a parallel class of $n+1$ lines. Let \mathcal{S}^* be a semiextension of \mathcal{S} . We must show that all lines in \mathcal{S}^* intersect. Let l and l' be lines which do not meet in \mathcal{S} . To prove that they meet in \mathcal{S}^* , it suffices to find an n -line parallel to both in \mathcal{S} .

If either l or l' is an n -line, we are done (and clearly neither can be an $n+1$ -line).

Suppose that l is an $n+1-d(l)$ -line and l' is an $n+1-d(l')$ -line, $2 \leq d(l) \leq d(l')$. By all the assumptions of this theorem, there are at most $(n+1-d(l))(b-v-d(l))$ n -lines and $(n+1-d(l'))(b-v-d(l'))$ n -lines meeting l and l' , respectively. Hence,

$$n+1-d(l') \leq n+1-d(l) \text{ and } b-v-d(l') \leq b-v-d(l).$$

$$(n+1-d(l))(b-v-d(l)) \geq (n+1-d(l'))(b-v-d(l'))$$

$b-v \geq 2\lambda-1$, since $v \leq n^2+n+2-2\lambda$ and $b=n^2+n+1$. Therefore, the number of n -lines meeting l or l' is at most $(n+1-\mu)(b-v-1)$, by Lemma 2.4(ii). Thus all lines in \mathcal{S}^* intersect, since \mathcal{S} contains at least $(n+1-\mu)(b-v-1)+1$ lines of size n . Hence, \mathcal{S}^* is a projective plane of order n , by the Lemma 2.2

References

- [1] I. GÜNALTI, §. OLGUN, On the embedding some linear spaces in finite projective planes, J.geom. 68 (2000), pp. 96-99.
- [2] I. GÜNALTI, Pseudo-complements in finite projective planes, Ars Combinatoria, to appear
- [3] I. GÜNALTI, P. ANAPA, §. OLGUN, On the embedding of complements of some hyperbolic planes. Ars Combin. 80 (2006), pp. 205-214
- [4] J. TOTTEN, Embedding the complement of two lines in a finite projective plane, J.Austral.Math.Soc. 22 (Series A) (1976), pp 27-34.
- [5] L. M. BATTE, A. BEUTELSPACHER, *Combinatorics of points and lines*, Cambridge University Press, 1993
- [6] L. J. DICKEY, Embedding the complement of a unital in a projective plane, Atti del convegno di Geometria Combinatoria e sue Applicazioni, Perugia, 1971, pp. 199-203
- [7] P. DE WITTE, The exceptional case in a Theorem of Bose and Shrikhande, J. Austral. Math. Soc. Ser. A 24 (1977), pp. 64-78
- [8] R. H. BRUCK, Existence problems for classes of finite projective planes, Lectures delivered to the Canadian Math. Congress, Sask., Aug. 1963
- [9] R.C. BOSE, S.S. SHRIKHANDE, Embedding the complement of a oval in a projective plane of even order, Discrete Math. 6 (1973), pp. 305-312
- [10] R. KAYA, E. ÖZCAN, On the construction of B-L planes from projective planes, Rendiconti del Seminario Matematico Di Bresciot (1984), pp. 427-434

Ibrahim Günaltılı

Osmangazi University, Department of Mathematics
26480 Eskişehir-Türkiye
e-mail:igunalti@ogu.edu.tr

Originelle wissenschaftliche Arbeit
Angenommen am 19.12.2007.

IVANKA BABIĆ, ANA SLIEPČEVĆ

Regelmäßige Polygone in der projektiv-erweiterten hyperbolischen Ebene

Regular Polygons in the Projectively Extended Hyperbolic Plane

ABSTRACT

Regular, semi-regular and polygons with right angles are constructed in Cayley-Klein's model of the projectively extended hyperbolic plane (H -plane). Some of the construction are analogous with the Euclidean ones. The ones for which there are not Euclidean analogues are carried out in original way characteristic for a H -plane. The construction of the defect of an equilateral triangle is of a special interest having the construction of the regular heptagon as its consequence.

Key words: hyperbolic plane, regular polygons, orthogon

MSC 2000: 51M09, 51M10, 51M15, 14H50

Pravilni poligoni u projektivno proširenoj hiperboličkoj ravnini

SAŽETAK

Na Cayley-Kleinovom modelu projektivno proširene H -ravnine konstruiraju se pravilni, polupravilni i pravokutni poligoni, odnosno ortogoni. Neke su konstrukcije potpuno analogne euklidskima, a one za koje ne postoje euklidski analogoni, izvode se na originalne načine svojstvene H -ravnini. Posebno je zanimljiva konstrukcija defekta jednakostraničnog trokuta, što ima za posljedicu konstrukciju pravilnog sedmerokuta.

Ključne riječi: hiperbolička ravnina, pravilni poligon, ortogon

Einleitung

Zur Erklärung der verschiedenen planimetrischen Konstruktionen in der projektiv erweiterten hyperbolischen Ebene (i.w. H -Ebene) zieht man zweckmäßig das klassische, projektive Modell dieser Ebene von F. Klein und A. Cayley heran. Dieses Modell benutzt eine mit einer hyperbolischen absoluten Polarität ausgestattete projektive Ebene, in der dann die (im Außengebiet des absoluten Kegelschnittes liegenden) hyperbolisch uneigentlichen Punkte zur Konstruktion mit herangezogen werden können. Die übliche Wahl eines euklidischen Kreises als absolutem Kegelschnitt a erlaubt zusätzliche Vereinfachungen. Dennoch ist zu beachten, dass die planimetrischen Konstruktionen mittels euklidischer Werkzeuge ausgeführt werden müssen, dass wir also nicht über einen "hyperbolischen Zirkel" verfügen.

Unter Benützung der Grund-Konstruktionen, wie Strecken- und Winkelsymmetralen, sowie von H -Kreisen [1], [7], [8], [9] werden in diesem Artikel einige Konstruktionen für regelmäßige und rechtwinklige Polygone in der H -Ebene angegeben.

Wir betrachten zwei Klassen von Polygonen:

- Die Klasse der *vollständig regelmäßigen* Polygone; das sind solche Polygone, die gleiche Seiten und gleiche Eckenwinkel haben. Sie besitzen einen Innenkreis und einen Umkreis, wie auch in der euklidischen Ebene.
- Die Klasse der Polygone für welche gilt, daß je zwei aufeinanderfolgende Seiten normal zueinander stehen. Diese Polygone heißen *vollständige Orthogone*.

Bekanntlich haben in der euklidischen Ebene nur Rechtecke die Eigenschaft, dass alle vier Eckenwinkel rechte sind. Demgegenüber existiert in der H -Ebene kein solches Viereck mit vier rechten Winkeln; hingegen existieren vollständige n -Orthogone für jedes $n \geq 5$.

In diesem Artikel werden nun Polygone aus jeder der Klassen im Cayley-Kleinschen Modell der projektiv erweiterten H -Ebene konstruiert, wobei der absolute (fundamentale) Kegelschnitt durch einen Kreis a gegeben wird. Man

bemerkt, dass nur das gleichseitige Dreieck, das dann automatisch auch gleichwinkelig ist, analog zum euklidischen Fall konstruiert werden kann. Andere regelmäßige Polygone, wie auch vollständige Orthogone, wurden auf andere Weisen konstruiert.

1 Regelmäßige Polygone

1.1. Dreieck

Das gleichseitige Dreieck ist das einfachste regelmäßige Polygon. In der Fig. 1 ist ein solches Dreieck durch die Seite \overline{AB} gegeben.

Die Konstruktion wurde ganz analog zur euklidischen Konstruktion durchgeführt. Die dritte Ecke C des Dreiecks ABC ist als Schnittpunkt der Seitensymmetrale s und des H-Kreises $k(A, \overline{AB})$ mit dem Mittelpunkt A und Radius \overline{AB} konstruiert. Um den Punkt C konstruktiv zu erreichen, wurde die perspektive Kollineation (O, o, B, B_1) angewendet. Durch diese Kollineation bildet sich der H-Kreis k in den absoluten Kreis a ab, und die Symmetrale s in die Gerade s_1 [9]. Die Ecke C des gesuchten Dreiecks ABC ist dabei dem Schnittpunkt $C_1 = a \cap s_1$ zugeordnet. Man bemerkt, dass noch ein solches Dreieck ABH existiert, welches symmetrisch zum ersten bezüglich AB liegt.

1.2. Vierecke

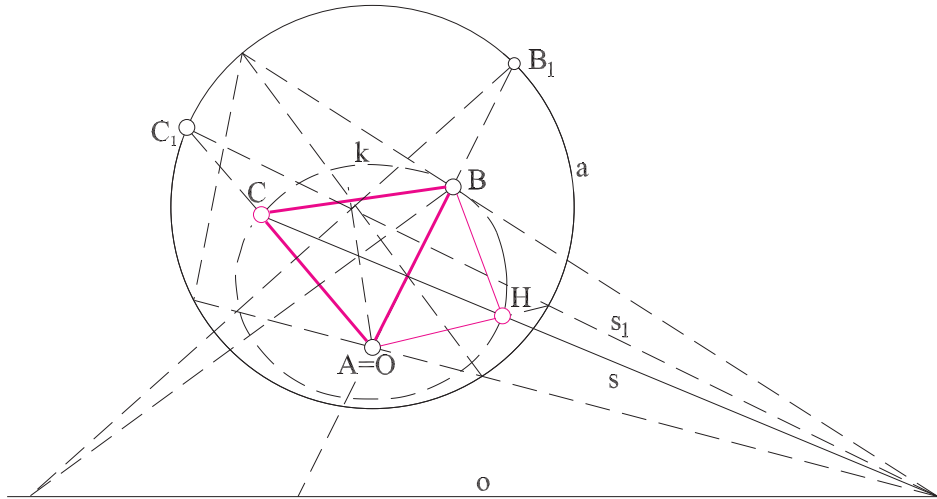
1.2.1. H - Rhombus

Das Dreieckspaar ABC und ABH in der Fig. 1 stellt ein gleichseitiges Viereck $ACBH$ mit kongruenten Pa-

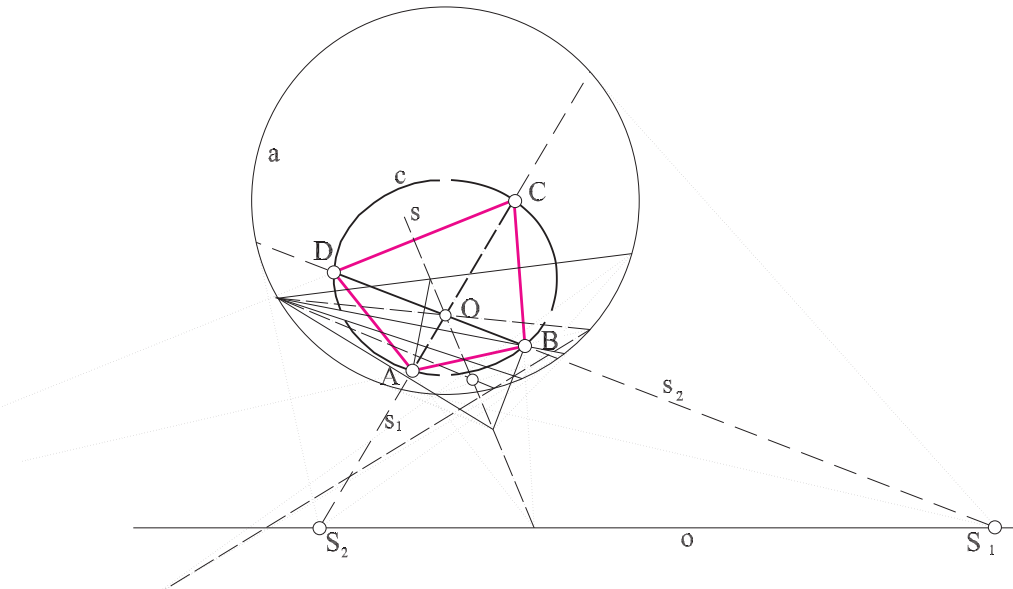
ren gegenüberliegender Winkel und hyperparallelen gegenüberliegenden Seitenpaaren dar. Die Diagonalen des Vierecks stehen senkrecht zueinander und halbieren sich, sind aber nicht kongruent. Da die gegenüberliegende Winkelsymmetralenpaare zusammen fallen, besitzt dieses Viereck einen Inkreis. Da kein Vierecksumkreis existiert, handelt es sich hier um ein “halbregelmäßiges” Viereck, das ein Analogon zur euklidischen Rhombus ist.

1.2.2. Pseudoquadrat

In der H-Ebene kann man ein regelmäßiges H-Viereck konstruieren, welches vier kongruente Winkel und Seiten, wie auch senkrechtstehende kongruente Diagonalen hat. Dieses wird “Pseudoquadrat” der H-Ebene genannt, weil es bis auf die Rechtwinkligkeit aufeinanderfolgender Seiten die gleichen Eigenschaften, wie das euklidische Quadrat hat. Die Konstruktion des solchen durch die Diagonale \overline{AC} gegebenen Vierecks ist in Fig. 2a gegeben. Zuerst konstruiert man den Kreis c mit dem Durchmesser \overline{AC} . Der zum \overline{AC} senkrechtstehende Durchmesser schneidet den Kreis c in den anderen beiden Ecken B, D des gesuchten Vierecks $ABCD$. Es ist zentral- und achsensymmetrisch in Bezug auf die Achsensymmetrien (S_1, s_1, B, D) und (S_2, s_2, A, C) [1], [8], aber auch in Bezug auf die gemeinsamen Seitensymmetralen der Gegenseitenpaare. Da dieses Viereck offensichtlich einen Inkreis hat, der zum Umkreis c konzentrisch ist, handelt es sich um ein vollständig regelmäßiges H-Viereck, eben ein Pseudoquadrat.



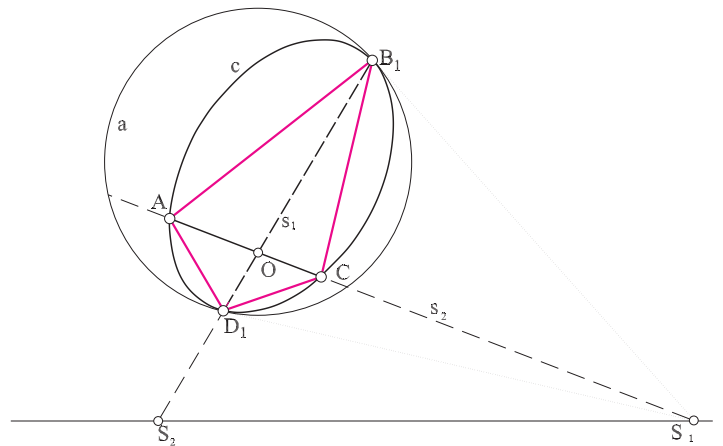
Figur 1: Gleichseitiges Dreieck

Figur 2a: *Pseudoquadrat*

Das Pseudoquadrat ist auch durch eine vorgegebene Seite \overline{AB} festgelegt. Zur Konstruktion bestimmt man zunächst die (eigentliche) Seitensymmetrale s von \overline{AB} . Ordnet man jeder Geraden des Geradenbüschels (A) die H-orthogonale Gerade des Geradenbüschels (B) zu, so schneiden solche projektiv zugeordnete Geradenbüschel die Symmetrale s in zwei kollokalen Punktreihen. Die Doppelpunkte dieser kollokalen Projektivität (s) sind die Mittelpunkte zweier Pseudoquadrate. Die Angabe ist damit auf die vorherige zurückgeführt, die anderen zwei Ecke konstruiert man dann mittels Zentralsymmetrie (O, o, C, A).

Bemerkung:

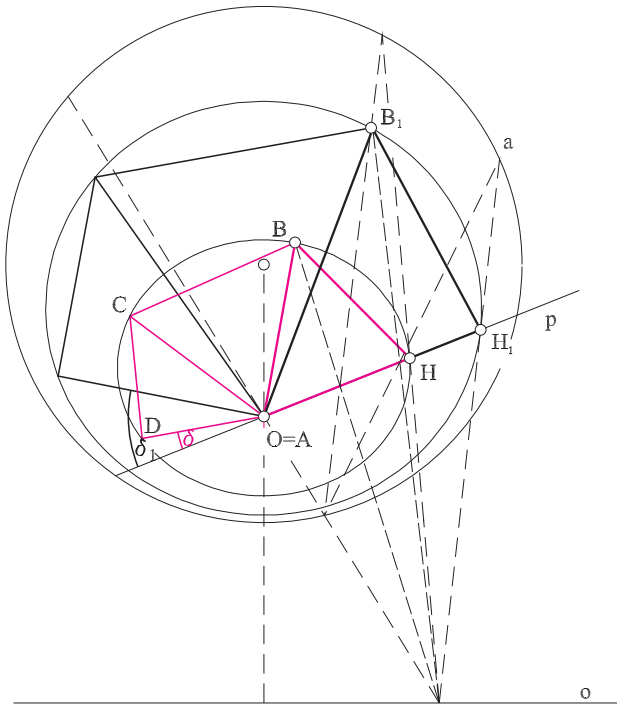
Durch den Durchmesser \overline{AC} ist noch ein spezieller H-Kreis - ein Hyperzykel mit dem uneigentlichen Mittelpunkt S_1 gegeben. Auf die beschriebene Art kann man in diesen Hyperzykel ein spezielles Viereck einschreiben (Fig. 2b). Es ist ein sogenanntes "Pseudorhombus" mit zwei Paaren parallelen Nebenseiten und hyperparallelen gegenüberliegenden Seiten. Es hat normalstehende nicht-kongruente Diagonalen und besitzt auch einen Inkreis. Es existiert kein Analogon eines solchen Vierecks in der euklidischen Ebene.

Figur 2b: *Pseudorhombus*

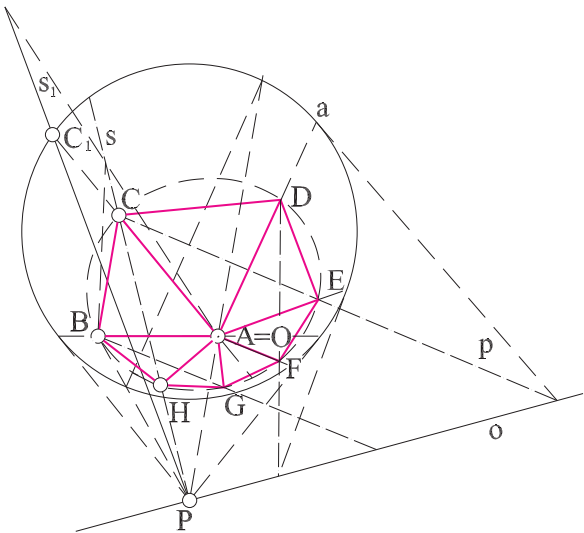
1.3. Sechsecke

Konstruiert man in der Fig. 1 noch ein zum Dreieck ABC , bzw. ABH kongruentes Dreieck ACD mit der Seite \overline{AC} , so sollten diese drei Dreiecke, gemäß der euklidischen Logik die Hälfte eines regelmäßigen Sechsecks bilden. Es ist aber anders in der H-Ebene, weil die Summe der drei Winkel bei der Ecke $O = A$ weniger als π beträgt (Fig. 3a). Da nämlich, ein Winkel in einem gleichseitigen Dreieck weniger als $\frac{\pi}{3}$ beträgt, können die drei erwähnten kongruenten Dreiecke keine Hälfte des in den Kreis k eingeschriebenen regelmäßigen Sechsecks bilden. Das regelmäßige Sechseck in der H-Ebene besteht nämlich nicht aus sechs gleichseitigen, sondern aus gleichschenkeligen Dreiecken. Die Rosette aus sechs gleichseitigen Dreiecken mit einer ge-

meinsamen Ecke im H-Kreiszentrum O erfüllt keinen vollen Winkel. Der Rest bis zum vollen Winkel hängt vom so genannten Defekt des Grunddreiecks ABC ab. Wie man in der Fig. 3a sieht, hängt der Dreiecksdefekt von der Länge und der Lage der Dreiecksseite ab. Je kleiner die Dreiecksseite, desto kleiner ist der Dreiecksdefekt δ . Somit ist eine didaktisch brauchbare Möglichkeit gegeben, den Defekt eines gleichseitigen H-Dreiecks anschaulich darzustellen.



Figur 3a: *Defekt des gleichseitigen Dreiecks*



Figur 3b: *Regelmäßiges Siebeneck*

Der Dreiecksdefekt kann speziell gerade die Hälfte des Eckenwinkels eines gleichseitigen H-Dreiecks betragen. In diesem Fall erfüllen sieben gleichseitige Dreiecke ein in den Kreis k eingeschriebenes *gleichseitiges Siebeneck* (Fig. 3b). Es zeigt sich, dass die Dreiecksseite so lange sein kann (also der Defekt so groß), dass acht (bzw. mehr) kongruente gleichseitige Dreiecke ein regelmäßiges Achteck (bzw. n -Eck) bilden.

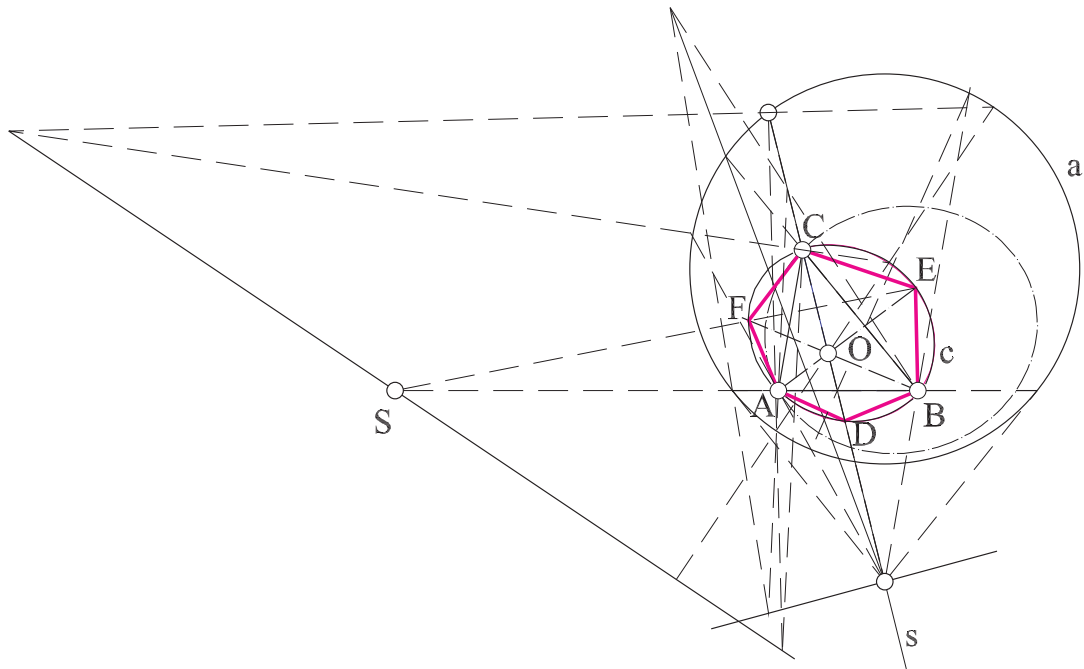
In der H-Ebene kann man auch ein durch eine Seite gegebenes regelmäßiges Sechseck konstruieren. Für die Konstruktion werden einige Kongruenztransformationen verwendet, welche das Lösungs-Sechseck in ein regelmäßiges Sechseck, dessen Mittelpunkt in dem absoluten Mittelpunkt liegt, verbinden. In der Fig. 4 ist eine Konstruktion des durch die kürzere Diagonale \overline{AB} gegebenen regelmäßigen Sechsecks gezeichnet. Zuerst konstruiert man das gleichseitige Dreieck ABC wie in der Fig. 1. Der Mittelpunkt O des Dreiecksumkreises c ist auch sein Orthozentrum und eines der vier Inkreiszentren. Eine von Seiten symmetrale jeder Dreiecksseite stellt gleichzeitig die Höhe dieser Seite, wie auch eine der Winkelsymmetralen des ihr gegenüberliegenden Winkels dar. Die drei Seitensymmetralen schneiden den Dreiecksumkreis c in den restlichen Ecken D, E, F des gesuchten regelmäßigen Sechsecks $ADBECF$ (Fig. 4). Das regelmäßige Sechseck besteht aus den sechs kongruenten, gleichschenkeligen Dreiecken mit der gemeinsamen Ecke O .

Bemerkung:

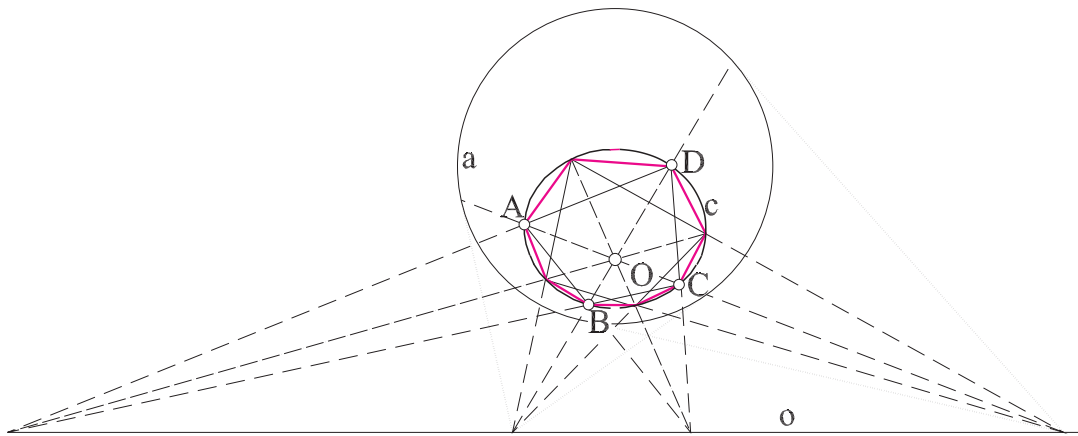
Man kann die Frage stellen, ob mit der kürzeren Diagonale ("Nebendiagonale") \overline{AB} ein einziges regelmäßiges Sechseck gegeben ist? Bekanntlich besitzt das Dreieck ABC noch weitere drei H-Umkreise [8]. Konstruiert man die Schnittpunkte der eigentlichen Seitensymmetralen des Dreiecks ABC mit jedem der Umkreise, bekommt man noch drei Dreiecke, die mit dem Dreieck ABC noch drei weitere Sechsecke bilden. Diese zusätzlichen Sechsecke sind aber nicht vollständig regelmäßig; sie bestehen aus drei kongruenten Deltoiden.

1.4. Achteck

Ein regelmäßiges Achteck kann z.B. durch seine das Zentrum enthaltende Hauptdiagonale \overline{AC} angegeben werden (siehe Fig. 5). Mit dem Duchmesser \overline{AC} konstruiert man zuerst den Kreis c und dann das Pseudoquadrat $ABCD$ wie in der Fig. 2. Die anderen vier Ecken des gesuchten Achtecks sind die Schnittpunkte der Seitensymmetralen des Pseudoquadrats mit dem Kreis c (Fig. 5). Da die Winkel-symmetrale der gegenüberliegenden Winkel des Achtecks mit den Seitensymmetralen des Pseudoquadrats zusam-menfallen, handelt es sich hier um ein solches regelmäßigs Achteck, das einen zum Umkreis c konzentrischen Innenkreis besitzt. Das Achteck besteht aus den gleichschenkeligen Dreiecken.



Figur 4: *Regelmäßiges Sechseck, gegeben durch eine nicht durch den Sechseck-Mittelpunkt gehende Nebendiagonale*



Figur 5: *Regelmäßiges Achteck*

Bemerkung:

Wie im euklidischen Fall kann durch fortgesetztes Halbieren des Zentralwinkels aus jedem n -Eck ein $2^k n$ -Eck erzeugt werden. Auch in der H-Ebene stellt sich die Frage, welche regelmäßigen n -Ecke mit Zirkel und Lineal allein konstruiert werden können. Sei ein solches n -Eck durch den Mittelpunkt M und eine Ecke A gegeben. Dann existiert eine (keineswegs eindeutige) H-Spiegelung derart, dass M in die (euklidische) Mitte des absoluten Kreises a gelangt. Das zu konstruierende regelmäßige H-Vieleck erscheint dann auch als euklidisch reguläres n -Eck. Somit folgt unmittelbar:

Ein hyperbolisch regelmäßiges n -Eck ist genau dann mit Zirkel und Lineal konstruierbar, wenn es das euklidisch regelmäßige n -Eck ist.

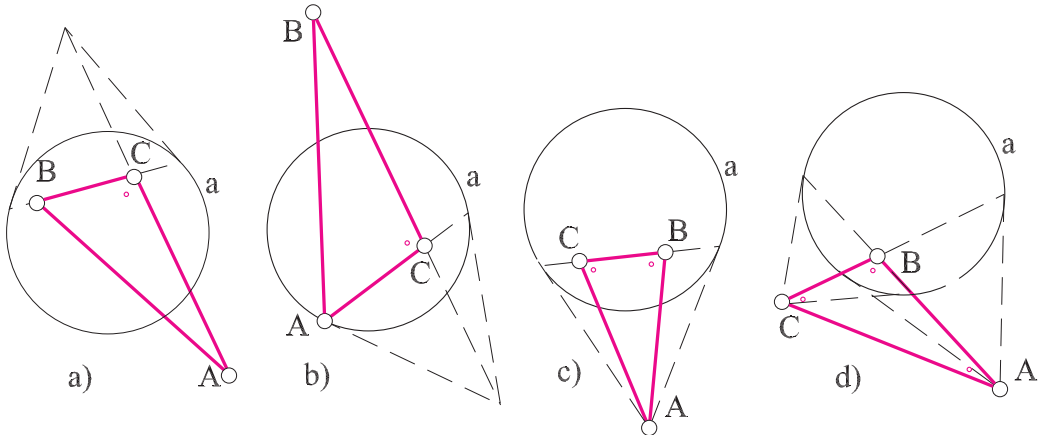
Es wäre also eine interessante und vielleicht lohnende Aufgabe, nach einer unmittelbaren Konstruktion eines hyperbolisch regulären Fünfecks zu suchen.

2 Rechtwinkelige Polygone

Wie bekannt hat ein Dreieck in der euklidischen Ebene höchstens einen rechten Winkel. Demgegenüber kann ein Dreieck in der projektiv-erweiterten H-Ebene (und in der

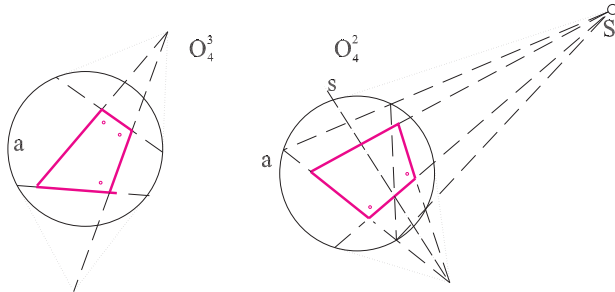
elliptischen Ebene) entweder einen, zwei oder im speziellen Fall sogar alle drei rechte Winkel besitzen. Die Dreiecke in der Fig. 6a und 6b haben einen rechten Winkel bei der Ecke C. Zwei-rechtwinklig ist das Dreieck in Fig. 6c, und ein spezielles Dreieck mit drei rechten Winkeln ist in der Fig. 6d gegeben. Bei diesem Dreieck ist jede der

Dreiecksseiten die absolute Polare der gegenüberliegenden Ecke. Es ist ein sogenanntes “autopolares Dreieck”; es besitzt naturgemäß nur eine eigentliche Ecke, die beiden anderen liegen im Außengebiet von a . Ein Dreieck mit drei eigentlichen Ecken kann offensichtlich nur einen einzigen rechten Winkel haben.



Figur 6: Rechtwinkelige Dreiecke

In der euklidischen Ebene existieren Vierecke mit lauter rechten Eckenwinkeln. In der H-Ebene gilt anderes: Da nämlich zwei beliebige Geraden in dieser Ebene eine einzige Normale haben, existiert kein Viereck mit nur rechten Winkeln. Das bekannteste Viereck mit drei rechten Winkeln ist das *Viereck vom J.H. Lambert*. Das *Viereck von G.G. Saccheri* ist hingegen zwei-rechtwinklig und gleichschenkelig (Fig. 7).



Figur 7: Vierecke vom J.H. Lambert und G.G. Saccheri

Ein ebenes Polygon mit mindestens einem rechten Eckenwinkel nennt man unabhängig von der Metrik in seiner Trägerebene “Orthogon”. Ein Orthogon mit lauter rechten Winkeln heißt *vollständiges Orthogon*. Sei mit O_n^m , ($m \leq n$), ein n -Orthogon mit m rechten Winkeln bezeich-

net. Es ist bekannt, dass für jede $n \geq 5$ das vollständige Orthogon O_n^n existiert [4].

Die Konstruktion der eigentlichen Orthogone kann man beispielsweise durch eine spezielle Modifikation des n -Ecks ($n \geq 3$) mit mindestens einer Idealecke durchführen. Jede Idealecke eines n -Ecks transformiert sich durch die absolute Polarität in eine eigentliche Gerade, die zum bestimmten Seitenpaar des n -Ecks orthogonal steht, bzw. jede Idealecke definiert im Allgemeinen zwei rechte Winkel. Transformiert man ein n -Eck mit nur Idealecken und nur eigentlichen Seiten, dass man jeder der Idealecken ihre absolute Polare ordnet, entsteht ein Orthogon mit $2n$ Seiten und $m = 2n$ rechten Winkeln. Im Fall eines n -Ecks mit $k = 1, 2, \dots, (n-1)$ eigentlichen Ecken bekommt man ein Orthogon mit $2n-k$ Seiten und mit $m \leq 2n-k$ rechten Winkeln. Die Seiten des Orthogons liegen dabei entweder auf den eigentlichen Seiten des n -Ecks oder auf der absoluten Polaren der Idealecken des n -Ecks.

Beispielsweise, aus den Dreiecken mit drei bzw. zwei Idealecken und alle drei eigentlichen Seiten wurden auf die beschriebene Weise die vollständige Orthogone O_6^6 bzw. O_5^5 konstruiert, wobei O_5^5 aus dem rechtwinkeligen Dreieck entsteht (Fig. 8).

Aus einem allgemeinen Dreieck mit zwei Idealecken bekommt man ein vier-rechtwinkeliges Fünfeck. Aus einem asymptotischen Dreieck mit zwei Idealecken und ei-

ner Grenzecke bekommt man ein asymptotisches, vier-rechtwinkeliges Fünfeck mit einer Grenzecke. Das drei-rechtwinkelige Viereck vom Lambert O_4^3 kann durch die Modifikation des rechtwinkeligen Dreiecks 6a) bzw. 6b) entstehen (Fig. 7). Die zwei-rechtwinkeligen Vierecke O_4^2 erstes Typs modifizieren sich aus den Dreiecken mit einer Idealecke. Unter diesen Vierecken ist auch ein gleich-schenkeliges Saccherisches Viereck (Fig. 7). Ein zwei-rechtwinkeliges Viereck O_4^2 des zweiten Typs entsteht aus einem Dreieck mit zwei Idealecken, wobei zwei Dreiecksseiten auf eigentlichen Geraden liegen und eine liegt auf einer Idealgeraden oder einer Grenzgeraden (Fig. 9).

Bemerkung:

In [8] wurde bewiesen, dass 28 Dreieckstypen existieren. Zwölf Paare der Dreieckstypen stehen dual zueinander, und 4 Dreieckstypen sind selbstdual. Für die beschriebene Modifikation sind nur die Dreiecke mit Idealecken interessant. Dabei induziert jedes Dreieck eines dualen Dreieckspaares das gleiche Orthogon (Fig 10).

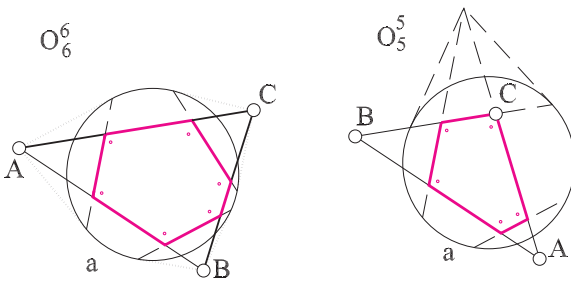
Durch die Modifikation eines Vierecks mit vier, drei, zwei bzw. eine Idealecke und allen Seiten auf eigentlichen Geraden entstehen die Orthogone O_8^m, O_7^m, O_6^m bzw. O_5^m , die auch vollständig sein können. Es ist einfach zu sehen, dass man durch die Modifikation eines Vierecks mit einer Idealecke Orthogone O_5^2, O_5^3, O_5^4 oder O_5^5 konstruieren kann.

Im Allgemeinen kann ein n -Eck, $n > 3$, durch die beschriebene Modifikation in die vollständigen Orthogone O_{2n-k}^{2n-k} ($k = 0, 1, \dots, n-1$) transformiert werden. Jedes der vollständigen Orthogone kann als ein Vertreter des Mengentyps $O_{2n-k}^{2n-2k+j}$ ($k = 0, 1, \dots, n-1; j = 0, 1, \dots, k$) betrachtet werden. Mit k ist die Zahl der eigentlichen Ecken des n -Ecks bezeichnet. Z. B. für $n = 5$ und $k = 0, 1, 2, 3, 4$ kann man von einem Fünfeck die vollständigen Orthogone $O_{10}^{10}, O_9^9, O_8^8, O_7^7, O_6^6$ ableiten. Dabei ist, z.B., ein vollständiges Orthogon O_7^7 nur ein Vertreter des Mengentyps O_7^{4+j} ($j = 0, 1, 2, 3$).

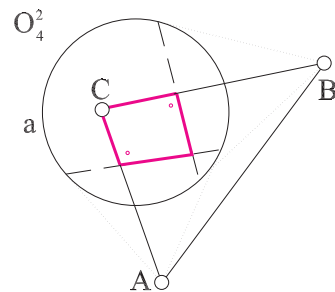
Natürlich lassen sich manche der Orthogone auch auf andere Weise konstruieren.

Literatur

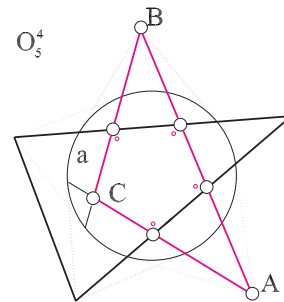
- [1] BABIĆ, I., *Neke kolineacije H-ravnine*, KoG 9, (2005), 1-5
- [2] BACHMANN, F., *Aufbau der Geometrie aus dem Spiegelungsbegriff*, 2. Auflage, Springer Verlag (Berlin-Heidelberg-New York, 1973)



Figur 8: *Vollständige Orthogone*



Figur 9: *Zweirechtwinkeliges Viereck des II Typs*



Figur 10: *Duale Dreiecke modifizieren das gleiche Orthogon*

- [3] KAGAN, V. F., *Osnovanja geometrii*, č.1. Geometrija Lobačevskogo i jejo predistorija, Moskva - Lenjograd, 1949
- [4] KLEIN, F., *Vorlesungen über nicht-euklidische Geometrie*, Berlin, Springer-Verlag, 1928., Nachdruck 1968

- [5] KOSTIN, V. I., *Osnovanija geometrii*, Moskva-Lenjingrad, 1946
- [6] MÓLNAR, E., *Inversion auf der Idealebene der Bachmannschen metrischen Ebene*, Acta Mathematica Scientiarum Hungaricae, 37 (4), (1981), 451-470
- [7] RAJČIĆ, L., *Obrada osnovnih planimetrijskih konstrukcija geometrije Lobachevskog sintetičkim sredstvima*, Glasnik mat. Fiz. Astr. 5 (1950), 57-120
- [8] SLIEPČEVIĆ, A., BABIĆ, I., *Charakteristische Dreieckpunkte in der projektiv-erweiterten hyperbolischen Ebene*, Teaching Mathematics and Computer Science, Debrecen, (im Druck)
- [9] SLIEPČEVIĆ, A., KOS-MODOR, J., *Neke planimetrijske konstrukcije u H-ravnini*, KoG 9, (2005), 1-3

Ivana Babić

Technische Hochschule, Abteilung für Bauwesen
Zagreb

e-mail: ibabic@tvz.hr

Ana Sliepčević

Fakultät für Bauwesen, Zagreb
e-mail: anas@master.grad.hr

Original scientific paper
Accepted 20.12.2007.

FRIEDRICH MANHART

Affine Geometry of Minkowski Minimal Surfaces in \mathbb{R}^3_1

Dedicated to Professor Hellmuth Stachel on occasion of his 65th birthday

Affine Geometry of Minkowski Minimal Surfaces in \mathbb{R}^3_1

ABSTRACT

On the one hand we give results concerning affine invariants of the focal surfaces of Minkowski minimal surfaces. Secondly we investigate the behavior of affine invariants in case of association of Minkowski minimal surfaces.

Key words: Minkowski minimal surfaces, focal surfaces, associated surfaces

MSC 2000: 53A15, 53B30

There are many results on affine geometry of Euclidean minimal surfaces in \mathbb{R}^3 . Several results concern the *focal surfaces* of a minimal surface. Denoting K_e the Gauss-curvature, in case of minimal surfaces the principal curvatures (eigenvalues of the shape operator) are $\varphi(-K_e)^{1/2}$ ($\varphi = \pm 1$).

Theorem 1 (P. FRANCK [5]). *Let $f: U \subseteq \mathbb{R}^2 \rightarrow f(U) =: \Phi \subset \mathbb{R}^3$ be a minimal immersion with $K_e \neq 0$ in U . The two sets of focal points Ψ_1 and Ψ_{-1} of $f(U) = \Phi$ are parametrized by $z = f + \varphi(-K_e)^{-1/2} n_e$, where n_e denotes the normal vector and Ψ_1 and Ψ_{-1} correspond to $\varphi = 1$ and $\varphi = -1$ respectively. Then the following holds for $\varphi \in \{1, -1\}$:*

- (a) *If Ψ_φ is a regular surface, then $K_e(\Psi_\varphi) = -1/4 K_e$, where $K_e(\Psi_\varphi)$ denotes the Gauss-curvature of Ψ_φ .*
- (b) *If Ψ_φ is a regular surface the affine normal of Ψ_φ intersects the affine normal of Φ orthogonally.*
- (c) *If Ψ_φ is a regular surface then it is an affine minimal surface.*
- (d) *If Ψ_1 and Ψ_{-1} are both regular surfaces, then $K_a(\Psi_1) : K_a(\Psi_{-1}) = H_e(\Psi_1)^4 : H_e(\Psi_{-1})^4$, where $K_a(\Psi_1), K_a(\Psi_{-1})$ and $H_e(\Psi_1), H_e(\Psi_{-1})$ are the affine Gauss-curvature and the Euclidean mean curvature of Ψ_1 and Ψ_{-1} respectively.*

Afina geometrija minimalnih ploha Minkowskog u \mathbb{R}^3_1

SAŽETAK

S jedne strane mi dajemo rezultate vezane uz afine invariante žarišnih ploha minimalnih ploha Minkowskog, dok s druge istražujemo karakteristike afinih invarijanata u slučaju pridruživanja kod minimalnih ploha Minkowskog.

Ključne riječi: minimalne plohe Minkowskog, žarišne plohe, pridružene plohe

Results concerning the behavior of affine quantities by association are contained in

Theorem 2 (P. FRANCK [5], F. MANHART [9]). *Let Φ be a regular minimal surface with $K_e \neq 0$ and Ψ_1 and Ψ_{-1} the sets of focal points as above. Denoting $(^\lambda)\Phi$ the pencil of associated minimal surfaces to Φ the following holds:*

- (a) *The affine normal vector $n_a(\Phi)$ of Φ is invariant: $n_a((^\lambda)\Phi) = n_a(\Phi)$.*
- (b) *The affine Gauss-curvature of Φ is invariant: $K_a((^\lambda)\Phi) = K_a(\Phi)$.*
- (c) *If Ψ_1 and Ψ_{-1} are regular surfaces then denoting by $n_a(\Psi_1)$ and $n_a(\Psi_{-1})$ the affine normal vector of Ψ_1 and Ψ_{-1} respectively, the figure of the three affine normals spanned by $n_a(\Phi), n_a(\Psi_1), n_a(\Psi_{-1})$ is invariant by translation along the orbit (ellipse).*

In the present paper we will prove analogous results for minimal surfaces in Minkowski space and give some examples.

1 Preliminaries

A *Minkowski* (or *Lorentz*) 3-space \mathbb{R}^3_1 is $(\mathbb{R}^3, \langle x, y \rangle)$, where $\langle x, y \rangle$ is the scalar product

$$\langle x, y \rangle := x_1 y_1 + x_2 y_2 - x_3 y_3, x = (x_1, x_2, x_3). \quad (1)$$

A vector $x \in \mathbb{R}^3_1$ is called

$$\begin{aligned} \text{spacelike} &\iff \langle x, x \rangle > 0, \\ \text{timelike} &\iff \langle x, x \rangle < 0, \\ \text{isotropic (lightlike)} &\iff \langle x, x \rangle = 0, \quad x \neq 0. \end{aligned}$$

The (*Minkowski*-) *length* of a vector x is defined by

$$\|x\| := \sqrt[+]{|\langle x, x \rangle|} \geq 0. \quad (2)$$

The (*Minkowski*-) *crossproduct* is

$$x \times y \text{ with } \langle x \times y, z \rangle = \det(x, y, z). \quad (3)$$

A surface Φ in \mathbb{R}^3_1 is locally parametrized by $f : U \subseteq \mathbb{R}^2 \rightarrow \mathbb{R}^3$. The local coordinates are denoted by (u, v) or $(u^1 := u, u^2 := v)$. Partial derivatives of a function $b : \mathbb{R}^2 \rightarrow \mathbb{R}$ or $b : \mathbb{R}^2 \rightarrow \mathbb{R}^3$ are denoted by

$$b_{,j} := \frac{\partial}{\partial u^j} b, \quad b_{,jk} := \frac{\partial^2}{\partial u^j \partial u^k} b.$$

The scalar product $\langle \cdot, \cdot \rangle$ in \mathbb{R}^3_1 induces a (pseudo-)Riemannian metric on U , the *first fundamental form* (*I*) with components

$$g_{jk} := \langle f_{,j}, f_{,k} \rangle : U \rightarrow \mathbb{R}. \quad (4)$$

Denoting $\Delta := \det(g_{jk})$ a surface $\Phi = f(U)$ is called

$$\begin{aligned} \text{spacelike} &\iff \Delta > 0 \quad \text{in } U, \\ \text{timelike} &\iff \Delta < 0 \quad \text{in } U. \end{aligned}$$

Points with $\Delta = 0$ are excluded. For $T \subset U$ a Jordan measurable set the *Minkowski surface area* is

$$O(f(T)) := \int_T \sqrt{|\Delta|} du dv. \quad (5)$$

The normal vector is

$$n := \frac{f_{,1} \times f_{,2}}{\|f_{,1} \times f_{,2}\|} = \frac{f_{,1} \times f_{,2}}{\sqrt{|\Delta|}}. \quad (6)$$

Because of $\Delta \neq 0$, n is a well defined non null vector in U . In the following we denote $\varepsilon := \langle n, n \rangle$. So in case of spacelike and timelike surfaces we have $\varepsilon = -1$ and $\varepsilon = 1$ and the *spherical image* $n(U)$ is part of the two-sheet hyperboloid $\langle x, x \rangle = -1$ and the one-sheet hyperboloid

$\langle x, x \rangle = 1$, respectively. The *second fundamental form* (*II*) and the *shape operator* S are related by $(II)(f_{,j}, f_{,k}) = \varepsilon \langle S(f_{,j}), f_{,k} \rangle$. The components of (*II*) and S are

$$\begin{aligned} h_{jk} &:= (II)(f_j, f_k) = \varepsilon \langle n, f_{,jk} \rangle = \\ &= \frac{\varepsilon}{\sqrt{|\Delta|}} \det(f_{,1}, f_{,2}, f_{jk}), \end{aligned} \quad (7)$$

$$S(f_{,j}) := -n_{,j} =: h_{j,s}^s \quad \text{with} \quad h_j^s = \varepsilon h_{jk} g^{ks}. \quad (8)$$

Mean curvature and *Gauss-curvature* are

$$H := \frac{1}{2} \operatorname{tr} S = \frac{\varepsilon}{2\Delta} (h_{11} g_{22} - 2h_{12} g_{12} + h_{22} g_{11}), \quad (9)$$

$$K := \varepsilon \det S = \varepsilon \frac{\det(h_{jk})}{\Delta}. \quad (10)$$

In case of K we use the sign convention used in [10], [4] and [8]. The eigenvalues of S (principal curvatures of Φ) are

$$k_{1,2} = H \pm \sqrt{H^2 - \varepsilon K}. \quad (11)$$

The integrability conditions of Codazzi and the Theorema egregium read as usual:

$$Co : \quad h_{js,k} - h_{jk,s} = \Gamma_{jk}^p h_{ps} - \Gamma_{js}^p h_{pk}, \quad (12)$$

$$Ga : \quad R_{pjks} = R_{jks}^t g_{pt} = h_{jk} h_{sp} - h_{js} h_{kp}. \quad (13)$$

Remark 1 From (7) and (10) an easy calculation gives $\Delta^2 K = -\Delta_e^2 K_e$ where Δ_e is the determinant of the components of the Euclidean metric. Thus Euclidean and Minkowski Gauss-curvature have different sign.

We need some basics from affine differential geometry. For details see for instance [13], [2]. From affine point of view a surface $f(U)$ is *nondegenerate* if

$$D := \det(D_{jk}) \neq 0, \quad D_{jk} := \det(f_{,1}, f_{,2}, f_{,jk}). \quad (14)$$

By (7) and (10) we have $D \neq 0 \iff K \neq 0$. Assuming f to be regular and nondegenerate, it is said to be an *equiaffine immersion*. Then the components of the *affine metric* of $f(U)$ are

$$G_{jk} := |D|^{-1/4} D_{jk}, \quad (15)$$

and the *affine normal vector* of $\Phi = f(U)$ is

$$n_a := (1/2) \Delta G f, \quad (16)$$

where Δ_G is the Laplacian with respect to the affine metric. The *affine shape operator* B defined by $B(f_{,j}) = -n_{a,j}$ has components B_j^k defined by

$$n_{a,j} =: -B_j^k f_{,k}. \quad (17)$$

Affine curvature K_a and affine mean curvature H_a are defined by

$$K_a := \det(B), H_a := (1/2)\text{tr}(B). \quad (18)$$

In case of a constant affine normal vector the surface Φ is called an *improper affine sphere* and we have $K_a = H_a = 0$.

2 Minimal Surfaces and their focal surfaces

A regular surface $\Phi = f(U) \subset \mathbb{R}^3_1$ is called a (*Minkowski-*) *minimal surface* iff $H = 0$ in U . There are many investigations on these surfaces, for instance [1], [3], [4], [6], [7], [10], [11], [12], [14], [15]. Although a spacelike surface locally maximizes the surface area defined by (5), as E.CALABI proved in [3], and timelike minimal surfaces neither maximize nor minimize surface area (see [11]), we speak of minimal surfaces.

As we want to study properties of affine geometry too, we exclude points with $K = 0$ on Φ . Denoting by $k_{1,2}$ the eigenvalues of the shape operator S of Φ , the *focal surfaces* of $\Phi = f(U)$ are parametrized by $z = f + (1/k_{1,2})n$. So the focal points are real iff $k_{1,2}$ are real. From (11) the eigenvalues are in case of $H = 0$

$$k_{1,2} = \pm \sqrt{-\varepsilon K}. \quad (19)$$

In case of a spacelike minimal surface ($\varepsilon = -1$) the Gauss-curvature is positive (cf. [7, p. 298], [4, p. 518]), so we have two different real eigenvalues $\pm \sqrt{K}$. A timelike minimal surface ($\varepsilon = 1$) has real focal surfaces iff $K < 0$ that means by Remark 1 Φ is locally strongly convex. So in both cases locally we can take the lines of curvature as parametric lines.

Lemma 1 (T. WEINSTEIN [14, p. 160]). *Let Φ be a minimal surface in \mathbb{R}^3_1 with $K \neq 0$ and real focal surfaces. Then locally there is a parametrization $f : U \rightarrow \mathbb{R}^3_1$, $f(U) = \Phi$, so that*

$$\begin{aligned} g &:= g_{11} > 0, g_{22} = -\varepsilon g, g_{12} = 0, \\ h_{11} &= 1, h_{22} = \varepsilon, h_{12} = 0, \end{aligned}$$

where $\varepsilon = -1$ and $\varepsilon = 1$ refers to spacelike and timelike surfaces respectively.

The coordinate functions of (I) and (II) in Lemma 1 fulfil the Codazzi condition *Co* (12). The Theorema egregium (13) reads

$$g(g'' - \varepsilon \dot{g} + 2) = g'^2 - \varepsilon \dot{g}^2, \quad (20)$$

where here as in the following the derivatives of $g : U \subseteq \mathbb{R}^2 \rightarrow \mathbb{R}$ are denoted by

$$\dot{g} := \frac{\partial g}{\partial u}, \ddot{g} := \frac{\partial^2 g}{\partial u^2}, g' := \frac{\partial g}{\partial v}, g'' := \frac{\partial^2 g}{\partial v^2}, \dot{g}' := \frac{\partial^2 g}{\partial u \partial v}.$$

Theorem 3 *Let $f(U) = \Phi \subset \mathbb{R}^3_1$ be a regular minimal surface with $K \neq 0$ in U . The two sets of focal points Ψ_1 and Ψ_{-1} of $\Phi = f(U)$ are parametrized by $z = f + \varphi(-\varepsilon K)^{-1/2}n$, where n denotes the normal vector and Ψ_1 and Ψ_{-1} correspond to $\varphi = 1$ and $\varphi = -1$ respectively. Then the following holds for $\varphi \in \{1, -1\}$:*

- (a) *If Ψ_φ is a regular surface, then $K(\Psi_\varphi) = -1/4K$, where $K(\Psi_\varphi)$ denotes the Gauss-curvature of Ψ_φ .*
- (b) *If Ψ_φ is a regular surface, then it is non degenerate and the affine normal of Ψ_φ intersects the affine normal of Φ orthogonally.*
- (c) *If Ψ_φ is a regular surface then it is an affine minimal surface.*
- (d) *If Ψ_1 and Ψ_{-1} are both regular surfaces, then*

$$K_a(\Psi_1) : K_a(\Psi_{-1}) = (-\varepsilon)H(\Psi_1)^4 : H(\Psi_{-1})^4,$$

where $K_a(\Psi_\varphi)$ and $H(\Psi_\varphi)$ are the affine Gauss-curvature and the Minkowski mean curvature of Ψ_φ respectively.

Proof

- (a) Using the parameters of Lemma 1 we calculate the Gauss-curvature

$$K = \frac{-\varepsilon}{g^2}, \quad (21)$$

and the Gauss equations

$$\begin{aligned} f_{,11} &= \gamma_1 f_{,1} + \varepsilon \gamma_2 f_{,2} + n, \\ f_{,12} &= \gamma_2 f_{,1} + \gamma_1 f_{,2}, \\ f_{,22} &= \varepsilon \gamma_1 f_{,1} + \gamma_2 f_{,2} + \varepsilon n, \end{aligned} \quad (22)$$

where

$$\gamma_1 := \frac{\dot{g}}{2g}, \gamma_2 := \frac{g'}{2g}.$$

The Weingarten equations are

$$n_{,1} = \frac{-\varepsilon}{g} f_{,1}, n_{,2} = \frac{\varepsilon}{g} f_{,2}. \quad (23)$$

The parametrizations of the focal surfaces (sets of focal points) are

$$z = f + \varphi g n, \varphi \in \{1, -1\}. \quad (24)$$

Expressing the derivatives of z by the derivatives of f and n we get

$$\begin{aligned} z_{,1} &= (1 - \varepsilon\varphi)f_{,1} + \varphi\dot{g}n, \\ z_{,2} &= (1 + \varepsilon\varphi)f_{,2} + \varphi g'n, \\ z_{,11} &= (1 - 3\varepsilon\varphi)\gamma_1 f_{,1} + (\varepsilon - \varphi)\gamma_2 f_{,2} + (1 - \varepsilon\varphi + \varphi\dot{g})n, \\ z_{,12} &= (1 - \varepsilon\varphi)\gamma_2 f_{,1} + (1 + \varepsilon\varphi)\gamma_1 f_{,2} + \varphi\dot{g}'n, \\ z_{,22} &= (\varepsilon + \varphi)\gamma_1 f_{,1} + (1 + 3\varepsilon\varphi)\gamma_2 f_{,2} + (\varepsilon + \varphi + \varphi g'')n. \end{aligned} \quad (25)$$

Using (25) we calculate the metric $g_{jk}^* := \langle z_{,j}, z_{,k} \rangle$ of the focal surfaces

$$\begin{aligned} g_{11}^* &= 2g(1 - \varepsilon\varphi) + \varepsilon\dot{g}^2, \\ g_{12}^* &= \varepsilon\dot{g}g', \\ g_{22}^* &= -2\varepsilon g(1 + \varepsilon\varphi) + \varepsilon g'^2, \\ \Delta^* &= \det(g_{jk}^*) = 2g[\varepsilon g'^2(1 - \varepsilon\varphi) - \dot{g}^2(1 + \varepsilon\varphi)]. \end{aligned} \quad (26)$$

The determinants $D_{jk}^* := \det(z_{,1}, z_{,2}, z_{,jk})$ (according to (14)) for the focal surfaces are

$$\begin{aligned} D_{11}^* &= (1 + \varepsilon\varphi)g^2 + (\varepsilon - \varphi)g'^2 \\ D_{12}^* &= 0, \\ D_{22}^* &= (\varepsilon\varphi - 1)g'^2 - (\varepsilon + \varphi)\dot{g}^2 \\ D^* &= \det(D_{jk}^*) = -2(\varepsilon + \varphi)\dot{g}^4 - 2(\varepsilon - \varphi)g'^4. \end{aligned} \quad (27)$$

From (26) and (27) a focal surface is non degenerate iff it is regular. In case of $\varepsilon\varphi = 1$ or $\varepsilon\varphi = -1$ this requires $\dot{g} \neq 0$ or $g' \neq 0$ respectively. From (7), (10) and (14) the Gauss-curvature of a focal surface $K(\Psi_\varphi)$ is

$$K(\Psi_\varphi) = \varepsilon^* \frac{\det(h_{jk}^*)}{\Delta^*} = \varepsilon^* \frac{D^*}{|\Delta^*|\Delta^*} = -\varepsilon^* \frac{D^*}{\Delta^{*2}}, \quad (28)$$

because of $\text{sgn}(\Delta^*) = -\langle n^*, n^* \rangle = -\varepsilon^*$, where n^* is the normal vector of the focal surface. Calculating $K(\Psi_\varphi)$ from (28) using (26) and (27) gives $K(\Psi_\varphi) = -1/4K$ from (21).

(b) From (15) the components of the affine metric of Φ are

$$G_{11} = \varepsilon\sqrt{g}, G_{12} = 0, G_{22} = \sqrt{g}. \quad (29)$$

Using (29) the affine normal vector of Φ is from (16)

$$n_a(\Phi) = \frac{1}{2g^{3/2}}(\varepsilon\dot{g}f_{,1} + g'f_{,2} + 2\varepsilon gn). \quad (30)$$

In case of spacelike surfaces ($\varepsilon = -1$) we calculate the affine metric of the focal surfaces Ψ_φ

$$\begin{aligned} \varphi = 1 &: G_{11}^* = G_{22}^* = -\sqrt{2}|g'|, G_{12}^* = 0, \\ \varphi = -1 &: G_{11}^* = G_{22}^* = \sqrt{2}|\dot{g}|, G_{12}^* = 0 \end{aligned}$$

and the affine normal

$$\begin{aligned} \varphi = 1 &: n_a(\Psi_1) = \frac{1}{|g'|}(\frac{-1}{\sqrt{2}g})[\dot{g}f_{,1} - g'f_{,2} + \frac{1}{2}(\dot{g}^2 + g'^2)n], \\ \varphi = -1 &: n_a(\Psi_{-1}) = \frac{1}{|\dot{g}|}(\frac{-1}{\sqrt{2}g})[\dot{g}f_{,1} - g'f_{,2} + \frac{1}{2}(\dot{g}^2 + g'^2)n]. \end{aligned} \quad (31)$$

In case of timelike surfaces ($\varepsilon = 1$) we get

$$\begin{aligned} \varphi = 1 &: G_{11}^* = \sqrt{2}|\dot{g}|, G_{12}^* = 0, G_{22}^* = -\sqrt{2}|\dot{g}|, \\ \varphi = -1 &: G_{11}^* = \sqrt{2}|g'|, G_{12}^* = 0, G_{22}^* = -\sqrt{2}|g'| \end{aligned}$$

and the affine normal

$$\begin{aligned} \varphi = 1 &: n_a(\Psi_1) = \frac{1}{|\dot{g}|}(\frac{-1}{\sqrt{2}g})[\dot{g}f_{,1} + g'f_{,2} - \frac{1}{2}(\dot{g}^2 - g'^2)n], \\ \varphi = -1 &: n_a(\Psi_{-1}) = \frac{1}{|g'|}(\frac{-1}{\sqrt{2}g})[\dot{g}f_{,1} + g'f_{,2} - \frac{1}{2}(\dot{g}^2 - g'^2)n]. \end{aligned} \quad (32)$$

In both cases we have used (20). From (31) and (32) the affine normals of Ψ_1 and Ψ_{-1} are parallel and using (30), (31) and (32) it follows $\langle n_a(\Phi), n_a(\Psi_\varphi) \rangle = 0$. So (b) is proved.

(c) From (31) and (32), using (22) and (23) a straightforward calculation gives the components B_j^{*k} of the affine shape operator B^* of the focal surfaces Ψ_φ .

In case of spacelike surfaces ($\varepsilon = -1$) we get

$$\begin{aligned} \varphi = 1 &: \left(B_j^{*k} \right) = \frac{\text{sgn}(g')}{2\sqrt{2}g} \begin{pmatrix} \dot{P} & P' \\ P' & -\dot{P} \end{pmatrix}, \\ P &:= \frac{\dot{g}}{g'}, (g' \neq 0), \end{aligned} \quad (33)$$

$$\begin{aligned} \varphi = -1 &: \left(B_j^{*k} \right) = \frac{\text{sgn}(\dot{g})}{2\sqrt{2}g} \begin{pmatrix} Q' & -\dot{Q} \\ -\dot{Q} & -Q' \end{pmatrix}, \\ Q &:= 1/P, (\dot{g} \neq 0). \end{aligned} \quad (34)$$

In case of timelike surfaces ($\varepsilon = 1$) we get with P, Q as above

$$\varphi = 1 : \left(B_j^{*k} \right) = -\frac{\text{sgn}(\dot{g})}{2\sqrt{2}g} \begin{pmatrix} Q' & \dot{Q} \\ -\dot{Q} & -Q' \end{pmatrix}, \quad (35)$$

$$\varphi = -1 : \left(B_j^{*k} \right) = -\frac{\text{sgn}(g')}{2\sqrt{2}g} \begin{pmatrix} \dot{P} & P' \\ -P' & -\dot{P} \end{pmatrix}. \quad (36)$$

From (33)-(36) the focal surfaces Ψ_φ are affine minimal surfaces.

(d) From (33)-(36) the affine Gauss-curvatures of the focal surfaces are related by

$$\varepsilon = -1 : K_a(\Psi_1) = (\frac{\dot{g}}{g'})^4 K_a(\Psi_{-1}) \quad (37)$$

$$\varepsilon = 1 : K_a(\Psi_1) = -(\frac{g'}{\dot{g}})^4 K_a(\Psi_{-1}). \quad (38)$$

The components of the second fundamental form of the focal surfaces are

$$\varepsilon = -1, \varphi = 1 : h_{11}^* = h_{22}^* = -\frac{|g'|}{\sqrt{g}}, h_{12}^* = 0, \quad (39)$$

$$\varepsilon = -1, \varphi = -1 : h_{11}^* = h_{22}^* = \frac{|\dot{g}|}{\sqrt{g}}, h_{12}^* = 0, \quad (40)$$

$$\varepsilon = 1, \varphi = 1 : h_{11}^* = -h_{22}^* = \frac{|\dot{g}|}{\sqrt{g}}, h_{12}^* = 0, \quad (41)$$

$$\varepsilon = 1, \varphi = -1 : h_{11}^* = -h_{22}^* = \frac{|g'|}{\sqrt{g}}, h_{12}^* = 0. \quad (42)$$

Calculating the mean curvature of the focal surfaces from (39)–(42) using (26) together with (37) and (38) proves (d).

□

3 Associated spacelike minimal surfaces

On a spacelike minimal surface in $\Phi \subset \mathbb{R}^3_1$ there are always global (I)-isothermal coordinates (see [14, p.184]), for instance the normalized ones of Lemma 1:

$$g := g_{11} = g_{22} > 0, g_{12} = 0,$$

$$h_{11} = 1, h_{22} = -1, h_{12} = 0.$$

Consequently we have

$$H = 0 \iff h_{11} + h_{22} = 0 \iff f_{,11} + f_{,22} = 0 \iff \Delta_{(I)} f = 0, \quad (43)$$

so the coordinate functions $f^\alpha : U \subseteq \mathbb{R}^2 \rightarrow \mathbb{R}$, ($\alpha = 1, 2, 3$) are harmonic. Then the conjugate harmonic functions are

$$\bar{f}^\alpha : U \subseteq \mathbb{R}^2 \rightarrow \mathbb{R}, (\alpha = 1, 2, 3),$$

related to f^α by

$$f_{,1}^\alpha = \bar{f}_{,2}^\alpha, \quad f_{,2}^\alpha = -\bar{f}_{,1}^\alpha \quad (\alpha = 1, 2, 3). \quad (44)$$

Then the one parameter family $(\lambda)\Phi$ of associated minimal surfaces is parametrized by

$$(\lambda)f(u, v) := \cos \lambda f(u, v) - \sin \lambda \bar{f}(u, v), \lambda \in \mathbb{R}. \quad (45)$$

If $|\lambda_2 - \lambda_1| = \pi/2$ the surfaces $(\lambda_1)\Phi$ and $(\lambda_2)\Phi$ are called *adjoined*. It is well known that the surfaces of the pencil $(\lambda)\Phi$ share metric (I), normal vector and Gauss-curvature as in the Euclidean situation (see [14, p.184]).

Theorem 4 Let Φ be a spacelike minimal surface in \mathbb{R}^3_1 with $K \neq 0$ and $(\lambda)\Phi$ the family of the associated minimal surfaces. Then the following holds.

(a) The affine normal vector $n_a(\Phi)$ of Φ is invariant: $n_a((\lambda)\Phi) = n_a(\Phi)$,

(b) The affine Gauss-curvature of Φ is invariant: $K_a((\lambda)\Phi) = K_a(\Phi)$

(c) Assuming the focal surfaces Ψ_1 and Ψ_{-1} of Φ not to be degenerate and denoting by $n_a(\Psi_1)$ and $n_a(\Psi_{-1})$ the affine normal vectors of Ψ_1 and Ψ_{-1} respectively, the figure of the three affine normals spanned by $n_a(\Phi)$, $n_a(\Psi_1)$, $n_a(\Psi_{-1})$ is invariant by translation along the orbit.

Proof

(a) We use the coordinates according to Lemma 1. From (45) we calculate the derivatives of $(\lambda)f$ and from this

$${}^{(\lambda)}g_{jk} = g_{jk}, \quad (46)$$

$${}^{(\lambda)}D_{11} = -g \cos \lambda, {}^{(\lambda)}D_{12} = g \sin \lambda, {}^{(\lambda)}D_{22} = g \cos \lambda, \quad (47)$$

where (46) expresses the well known isometry. Further we get the components of the affine metric

$${}^{(\lambda)}G_{11} = -\sqrt{g} \cos \lambda, {}^{(\lambda)}G_{12} = \sqrt{g} \sin \lambda, {}^{(\lambda)}G_{22} = \sqrt{g} \cos \lambda. \quad (48)$$

Using this the affine normal is

$$n_a((\lambda)\Phi) = \frac{1}{2g^{3/2}}(-\dot{g}f_{,1} + g'f_{,2} - 2gn). \quad (49)$$

Because of $\varepsilon = -1$, comparison with (30) proves (a).

(b) Denoting the components of the affine shape operator of f and $(\lambda)f$ by B_j^k and $(\lambda)B_j^k$ respectively, we get

$$\left({}^{(\lambda)}B_j^k \right) = \begin{pmatrix} B_1^1 \cos \lambda + B_1^2 \sin \lambda & B_2^1 \cos \lambda + B_2^2 \sin \lambda \\ -B_1^1 \sin \lambda + B_1^2 \cos \lambda & B_2^1 \cos \lambda - B_2^2 \sin \lambda \end{pmatrix}. \quad (50)$$

From this we get

$$K_a((\lambda)\Phi) = \det \left({}^{(\lambda)}B_j^k \right) = K_a(\Phi).$$

(c) From (46) we have $(\lambda)K = K$. Together with the invariance of the normal $n(\Phi)$ and the affine normals $n_a(\Phi)$ and $n_a(\Psi_1)$, $n_a(\Psi_{-1})$ this gives the invariance of the figure of the three affine normals. □

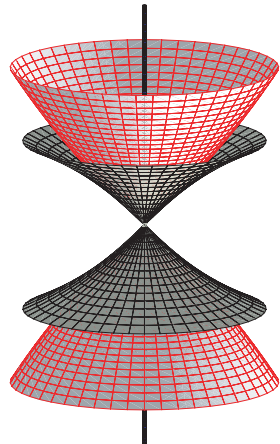


Figure 1a

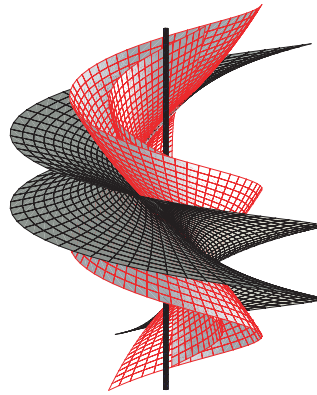


Figure 1b

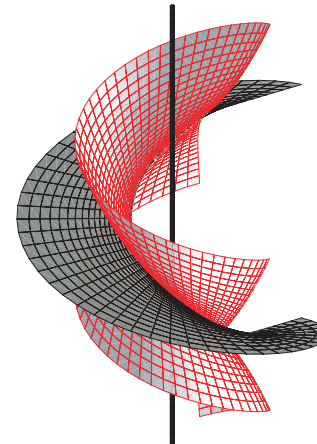


Figure 1c

Figure 1. Associated spacelike surfaces and their focal surfaces (in red color).

In figure 1 the dark surfaces are associated minimal surfaces (to the so called *elliptic catenoid* (62)). Starting with the elliptic catenoid (left figure) the adjoined surface is the spacelike portion of a right helicoid (right figure). It is well known, that the surfaces are *screw surfaces* in \mathbb{R}^3_1 ((see [12])). The red surfaces are the focal surfaces. The focal surface on the left is the surface (69), which is an improper affine sphere. Because of Theorem 4 the focal surfaces of every surface of the pencil is an improper affine sphere.

4 Associated timelike minimal surfaces

A timelike minimal surface in $\Phi \subset \mathbb{R}^3_1$ admits locally a representation in isotropic coordinates

$$f(u, v) = g(u) + h(v), \quad g : I \in \mathbb{R} \rightarrow \mathbb{R}^3_1, h : J \in \mathbb{R} \rightarrow \mathbb{R}^3_1, \quad (51)$$

where $g(I)$ and $h(J)$ are isotropic curves

$$\langle \dot{g}, \dot{g} \rangle = \langle h', h' \rangle = 0; \quad \dot{g} := \frac{dg}{du}, \quad h' := \frac{dh}{dv}$$

(see [14, p.184] or [6, p.338]). So it is

$$g_{11} = g_{22} = 0, \quad g_{12} = \langle \dot{g}, h' \rangle \neq 0. \quad (52)$$

This means a timelike minimal surface is locally a surface of translation with isotropic generating curves. The conjugate minimal surface $\bar{\Phi}$ is locally parameterized by

$$\bar{f}(u, v) = g(u) - h(v), \quad (53)$$

and the family of associated minimal surfaces ${}^{(\lambda)}\Phi$ is given by

$${}^{(\lambda)}f(u, v) = \cosh f(u, v) + \sinh \bar{f}(u, v), \quad \lambda \in \mathbb{R}. \quad (54)$$

Remark 2 : It is ${}^{(0)}f = f$. Obviously the surface $\bar{f}(U)$ does not belong to the family of associated surfaces ([6, p.338]).

Analogous to Theorem 4 we have

Theorem 5 Let Φ be a timelike minimal surface in \mathbb{R}^3_1 with $K \neq 0$ and ${}^{(\lambda)}\Phi$ the family of the associated minimal surfaces. Then the following holds.

- (a) The affine normal vector $n_a(\Phi)$ of Φ is invariant: $n_a({}^{(\lambda)}\Phi) = n_a(\Phi)$,
- (b) The affine Gauss-curvature of Φ is invariant: $K_a({}^{(\lambda)}\Phi) = K_a(\Phi)$
- (c) Assuming the focal surfaces Ψ_1 and Ψ_{-1} of Φ not to be degenerate and denoting by $n_a(\Psi_1)$ and $n_a(\Psi_{-1})$ the affine normal vectors of Ψ_1 and Ψ_{-1} respectively, the figure of the three affine normals spanned by $n_a(\Phi)$, $n_a(\Psi_1)$, $n_a(\Psi_{-1})$ is invariant by translation along the orbit.

Proof

(a) We use the isotropic coordinates from above. From (54) we calculate the derivatives of ${}^{(\lambda)}f$ and from this

$${}^{(\lambda)}g_{jk} = g_{jk}, \quad (55)$$

$${}^{(\lambda)}D_{11} = (\cosh \lambda + \sinh \lambda) D_{11},$$

$${}^{(\lambda)}D_{12} = 0, \quad (56)$$

$${}^{(\lambda)}D_{22} = (\cosh \lambda - \sinh \lambda) D_{22},$$

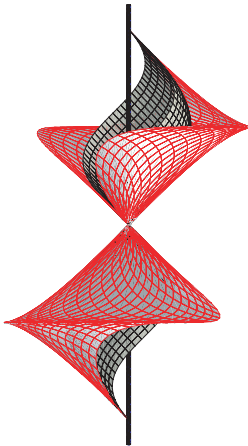


Figure 2a

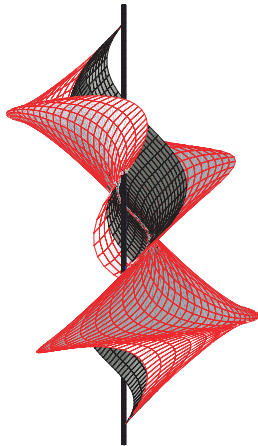


Figure 2b



Figure 2c

Figure 2. Associated timelike surfaces to the surface of rotation (65) and their focal surfaces (in red color).

where (55) expresses the well known isometry. The components of the affine metric are

$$\begin{aligned} {}^{(\lambda)}G_{11} &= (\cosh\lambda + \sinh\lambda)G_{11}, \\ {}^{(\lambda)}G_{12} &= 0, \\ {}^{(\lambda)}G_{22} &= (\cosh\lambda - \sinh\lambda)G_{22}. \end{aligned} \quad (57)$$

Calculating the affine normal by (16) yields $n_a({}^{(\lambda)}\Phi) = n_a(\Phi)$.

(b) Denoting the components of the affine shape operator of f and ${}^{(\lambda)}f$ by B_j^k and ${}^{(\lambda)}B_j^k$ respectively, we get

$$\left({}^{(\lambda)}B_j^k \right) = \begin{pmatrix} e^{-\lambda}B_1^1 & e^{-\lambda}B_1^1 \\ e^{\lambda}B_1^2 & e^{\lambda}B_2^2 \end{pmatrix}. \quad (58)$$

Thus it is

$$K_a({}^{(\lambda)}\Phi) = \det \left({}^{(\lambda)}B_j^k \right) = K_a(\Phi).$$

(c) The argument is as in the proof of Theorem 4. \square

5 Further Examples

A well known class of minimal surfaces in Minkowski space is that of rotation surfaces, that means surfaces admitting a one parameter family of isometries in \mathbb{R}^3_1 fixing the points of a straight line. If the axis is timelike (x^3 – axis) or spacelike (x^1 – axis) or isotropic ($x^1 = x^3, x^2 = 0$)

representations of this rotations are

$$\begin{pmatrix} x^1 \\ x^2 \\ x^3 \end{pmatrix} \mapsto \begin{pmatrix} \cos v & -\sin v & 0 \\ \sin v & \cos v & 0 \\ 0 & 0 & 1 \end{pmatrix} \begin{pmatrix} x^1 \\ x^2 \\ x^3 \end{pmatrix}, \quad (59)$$

$$\begin{pmatrix} x^1 \\ x^2 \\ x^3 \end{pmatrix} \mapsto \begin{pmatrix} 1 & 0 & 0 \\ 0 & \cosh v & \sinh v \\ 0 & \sinh v & \cosh v \end{pmatrix} \begin{pmatrix} x^1 \\ x^2 \\ x^3 \end{pmatrix}, \quad (60)$$

$$\begin{pmatrix} x^1 \\ x^2 \\ x^3 \end{pmatrix} \mapsto \begin{pmatrix} 1 - \frac{v^2}{2} & v & \frac{v^2}{2} \\ -v & 1 & v \\ -\frac{v^2}{2} & v & 1 + \frac{v^2}{2} \end{pmatrix} \begin{pmatrix} x^1 \\ x^2 \\ x^3 \end{pmatrix}. \quad (61)$$

There are seven types of minimal surfaces with rotational symmetry (see [1], [6], [7], [10], [15]).

The following surfaces are spacelike ($\varepsilon = -1$)

$$f(u, v) = (\sinh u \cos v, \sinh u \sin v, u), \quad (62)$$

$$f(u, v) = (u, \sin u \sinh v, \sin u \cosh v), \quad (63)$$

$$f(u, v) = (u^3 + u - uv^2, -2uv, u^3 - u - uv^2). \quad (64)$$

where the rotation axis is timelike, spacelike or isotropic respectively.

In case of timelike surfaces we have

$$f(u, v) = (\sin u \cos v, \sin u \sin v, u), \quad (65)$$

$$f(u, v) = (u, \sinh u \sinh v, \sinh u \cosh v), \quad (66)$$

$$f(u, v) = (u, \pm \cosh u \cosh v, \cosh u \sinh v), \quad (67)$$

$$f(u, v) = (-u^3 + u - uv^2, -2uv, -u^3 - u - uv^2). \quad (68)$$

where in case of surfaces (65) and (68) the rotation axis is timelike and isotropic respectively. Surfaces (66) and (67) have a spacelike rotation axis. Clearly we have to exclude discrete values of u in order to have regular surfaces.

Calculation of the focal surfaces gives in case of surfaces (62), (63) and (64)

$$f(u, v) = (2 \sinh u \cos v, 2 \sinh u \sin v, u + \sinh u \cosh u), \quad (69)$$

$$f(u, v) = (u + \cos u \sin u, 2 \sin u \sinh v, 2 \sin u \cosh v), \quad (70)$$

$$f(u, v) = (-2u^3 + 2u - 2uv^2, -4uv, -2u^3 - 2u - 2uv^2). \quad (71)$$

and in case of surfaces (65), (66), (67) and (68)

$$f(u, v) = (2 \sin u \cos v, 2 \sin u \sin v, u + \cos u \sin u), \quad (72)$$

$$f(u, v) = (u + \cosh u \sinh u, 2 \sinh u \sinh v, 2 \sinh u \cosh v), \quad (73)$$

$$f(u, v) = (u - \cosh u \sinh u, \pm 2 \cosh u \cosh v, 2 \cosh u \sinh v), \quad (74)$$

$$f(u, v) = (2u^3 + 2u - 2uv^2, -4uv, 2u^3 - 2u - 2uv^2). \quad (75)$$

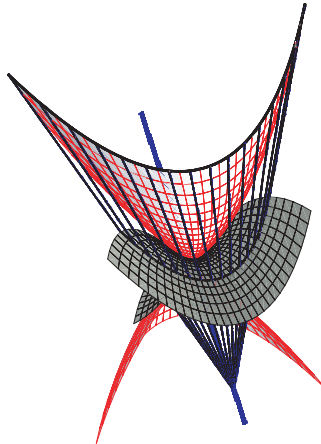


Figure 3a

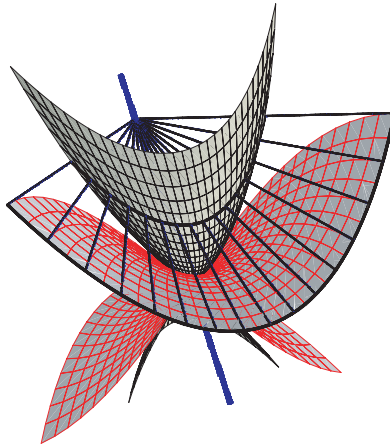


Figure 3b

Figure 3. Surfaces of rotation with isotropic axis: Timelike (spacelike) surface as focal surface (in red color) of a spacelike (timelike) surface.

References

- [1] ALIAS, L.J., CHAVES, R.M.B., MIRA, P., *Björling problem for maximal surfaces in Lorentz-Minkowski space*, Math. Proc. Camb. Phil. Soc. **134** (2003), 289–316.
- [2] BLASCHKE, W., *Vorlesungen über Differentialgeometrie, Band II : Affine Differentialgeometrie*, Springer, Berlin (1923).
- [3] CALABI, E., *Examples of Bernstein problems for some non-linear equations*, Proc. Symp. Pure Math. **15** (1970), 223–230.
- [4] ESTUDILLO, F.J.M., ROMERO A., *Generalized maximal surfaces in Lorentz-Minkowski space \mathbb{L}^3* , Math. Proc. Camb. Phil. Soc. **111** (1992), 515–524.
- [5] FRANCK, P., *Über paraboloidische Flächen. 4. Mitteilung. Die Minimalflächen und ihre Zentraflächen*, Jahresberichte DMV **33** (1923), 33–44.
- [6] INOGUCHI, J., TODA, M., *Timelike Minimal Surfaces via Loop Groups*, Acta Appl. Math. **83** (2004), 313–355.
- [7] KOBAYASHI, O., *Maximal surfaces in the 3-dimensional Minkowski space L^3* , Tokyo J. of Math. **6** (1983), 297–309.
- [8] KÜHNEL, W., *Differentialgeometrie*, 2.Auflage, Vieweg, Braunschweig (2003).
- [9] MANHART, F., *Zur affinen Krümmungstheorie euklidischer Minimalflächen*, In: Röschel, O. (ed.) et al., Geometrie-Tagung “107 Jahre Drehfluchtprinzip”, Vorau, Österreich, 1. Juni-6. Juni 1997. Tagungsband. Vorau: TU Graz, 121–130 (1999).

- [10] McNERTNEY, L., *One-parameter families of surfaces with constant curvature in Lorentz 3-space*, Ph.D. thesis Brown University (1980) (unpublished).
- [11] KLOTZ MILNOR, T., *Entire Timelike Minimal Surfaces in $E^{3,1}$* , Michigan Math. J. **37** (1990), 163–177.
- [12] MIRA, P., PASTOR, J.A., *Helicoidal Maximal Surfaces in Lorentz-Minkowski Space*, Monatsh. Math. **140** (2003), 315–334.
- [13] NOMIZU, K., SASAKI, T., *Affine differential geometry*, Cambridge University Press (1994).
- [14] WEINSTEIN, T., *An Introduction to Lorentz Surfaces*, De Gruyter expositions in mathematics; 22, de Gruyter, Berlin (1996).
- [15] VAN DE WOESTIJNE, I., *Minimal Surfaces in 3-dimensional Minkowski space*, In: *Geometry and Topology of submanifolds II*, M.Boyom et al.,eds., Singapore: World scientific (1990), 344–369.

Friedrich Manhart

Technische Universität

Wiedner Hauptstraße 8–10/1131, A–1040 Wien
Austria

e-mail: manhart@geometrie.tuwien.ac.at

Original scientific paper
Accepted 29.12.2007.

RADIMIR VIHER

On the Multiple Roots of the 4th Degree Polynomial

On the Multiple Roots of the 4th Degree Polynomial

ABSTRACT

In this article we investigate the connection between the multiple roots of the 4th degree polynomial $P_4(x)$ and its Descartes's cubic resolvent $P_3(x)$. The multiple roots of $P_4(x)$ are classified according to the position of all roots of the corresponding $P_3(x)$. Seven types are obtained.

Key words: 4th degree polynomial, Descartes's cubic resolvent, types of roots

MSC 2000: 14H45

In the previous article (see [6]), it is shown that we get the Descartes's cubic resolvent of the reduced polynomial of the fourth degree

$$P_4(x) \equiv x^4 + a_2x^2 + a_1x + a_0 \quad (a_i \in \mathbf{R}, i = 0, 1, 2), \quad (1)$$

by factorization of $P_4(x)$

$$x^4 + a_2x^2 + a_1x + a_0 \equiv (x^2 + Ax + B)(x^2 + Cx + D) \quad (2)$$

and then seek the equation for deriving the value of A . By multiplying those two quadratic polynomials on the right side of (2) and then equating the coefficients of the same powers of x we get the following system of four equations with four unknowns

$$\begin{aligned} A &+ C &= 0 \\ AC &+ B &+ D &= a_2 \\ AD &+ BC &= a_1 \\ BD &= a_0. \end{aligned} \quad (3)$$

When we solve this system we obtain the following equation (Descartes's cubic resolvent)

$$P_3(t) \equiv t^3 + 2a_2t^2 + (a_2^2 - 4a_0)t - a_1^2 = 0, \quad (4)$$

O višestrukim korijenima polinoma 4. stupnja

SAŽETAK

U članku se istražuje veza između višestrukih korijena polinoma 4. stupnja $P_4(x)$ i njegove Descartesove kubne rezolvante $P_3(x)$. Višestruki korjeni polinoma $P_4(x)$ razvrstani su ovisno o položaju svih korijena pripadne $P_3(x)$. Dobiveno je sedam tipova.

Ključne riječi: polinom 4. stupnja, Descartesova kubna rezolventa, tipovi korijena

where $t = A^2$. Further in the above mentioned article there are the theorems about correspondences between the types of the roots of $P_3(t)$ and $P_4(x)$, and about characterizations of those types of roots of $P_3(t)$ formulated and proved. For the sake of further results we shall repeat the main definitions and formulations of those two theorems. As the free member of $P_3(t)$ is $-a_1^2$ and the coefficient of the greatest power of t is 1 we have three main possibilities for the types of roots of $P_3(t)$.

In the **first case**, $P_3(t)$ has only one real non-negative root and two conjugate complex roots or one real non-negative root and one real negative double root.

In the **second case**, $P_3(t)$ has one real non-negative root and two different real non-positive roots (the case of double root at zero is included in this case).

In the **third case**, $P_3(t)$ has three real non-negative roots (the cases of double and triple roots are included in this case).

Now we shall give the formulations of the theorem 1 and the theorem 2 of [6].

Theorem 1.

- 1st case $\iff P_4(x)$ has two real and two complex roots
 2nd case $\iff P_4(x)$ has only complex roots
 3rd case $\iff P_4(x)$ has only real roots.

Theorem 2.

- 1st case $\iff D_1 > 0$ or ($D_1 = 0$ and ($a_2^2 - 4a_0 < 0$ or ($a_2^2 - 4a_0 > 0$ and $a_2 > 0$)))
 or ($D_1 = 0$ and $a_2^2 - 4a_0 = 0$ and $a_2 > 0$ and $a_1 \neq 0$)
 2nd case $\iff (D_1 < 0$ and ($a_2^2 - 4a_0 < 0$ or ($a_2^2 - 4a_0 \geq 0$ and $a_2 > 0$)))
 or ($a_1 = 0$ and $a_2^2 - 4a_0 = 0$ and $a_2 > 0$)
 3rd case $\iff D_1 \leq 0$ and $a_2^2 - 4a_0 \geq 0$ and $a_2 \leq 0$.

We get the quantity D_1 by using substitution $t = z - 2a_2/3$ in $P_3(t)$ that reduces it to

$$z^3 + pz + q = 0, \quad (5)$$

with

$$\begin{aligned} p &= -4a_0 - \frac{1}{3}a_2^2 \\ q &= \frac{8}{3}a_0a_2 - a_1^2 - \frac{2}{27}a_2^3, \end{aligned} \quad (6)$$

and finally

$$D_1 = \frac{q^2}{4} + \frac{p^3}{27}. \quad (7)$$

This is a known procedure that leads to the Cardano's formula (see [3]). Before we formulate and prove the theorem about multiplicity correspondences between $P_4(x)$ and $P_3(t)$ we will show from which part of the theorem 1 proof comes the first indication for such theorem. In the proof of the "only if" part of the first statement we should first apply the factorization theorem for $P_4(x)$, so we get

$$P_4(x) = (x - x_1)(x - x_2)(x - a - bi)(x - a + bi). \quad (8)$$

Since the coefficient of the third power of x in $P_4(x)$ is zero, we obtain the following important relation

$$x_1 + x_2 + 2a = 0. \quad (9)$$

By using the (8) we can represent the $P_4(x)$ as a product of two quadratic polynomials in three different ways. In every such representation, the second power of the coefficient of x (no matter which one because they differ only in sign) is a root of $P_3(t)$ (see [6]). Thus, by using (8) we can find all roots of $P_3(t)$ but we have to distinguish two

different cases. In the first case we suppose that $x_1 = x_2$, and together with (9) we get $x_1 + a = x_2 + a = 0$. Finally, from this one and from the three representations of (8) as product of two quadratic polynomials (by taking the second power of a coefficient of x in every such representation) we obtain

$$t_1 = 4a^2 \geq 0; \quad t_2 = t_3 = -b^2 < 0. \quad (10)$$

Hence, in this case the multiplicity of the real roots of $P_4(x)$ implies the same degree of the multiplicity of the real negative root of $P_3(t)$. If $x_1 \neq x_2$, it can be shown (see [6]) that there is no multiplicity of roots of $P_3(t)$ (because in this case t_2 and t_3 are conjugate complex numbers). Further on, we will show that this correspondence among the multiplicity of the roots of $P_4(x)$ and $P_3(t)$ is not a random event. For this purpose we shall divide all the possibilities of double and triple multiplicities of $P_3(t)$ on seven cases and in all those cases we will find the corresponding multiplicity of $P_4(x)$. It is time to look at the following seven figures and to analyze every one of them.

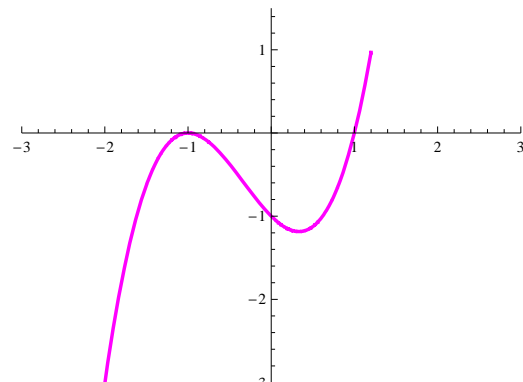


Fig. 1 a: 1st case

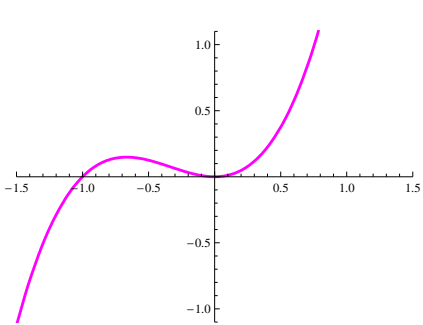


Fig. 1 b: 2nd case

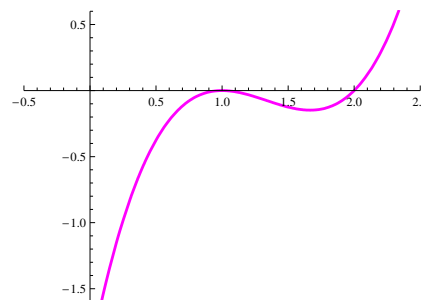


Fig. 1 c: 3rd case

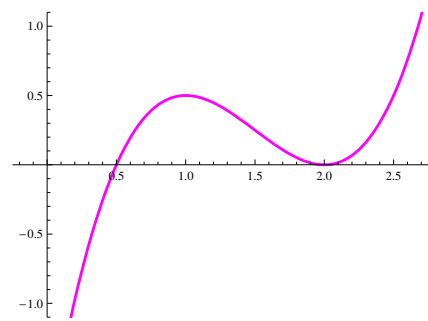


Fig. 1 d: 4th case

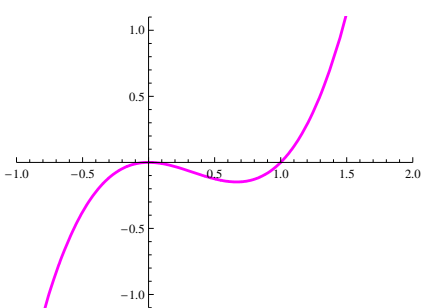


Fig. 1 e: 5th case

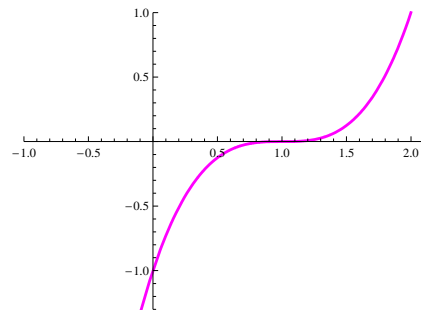


Fig. 1 f: 6th case

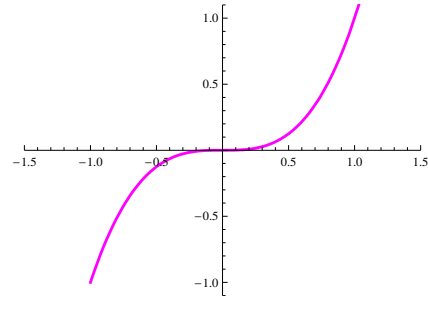


Fig. 1 g: 7th case

In the **1st case** (Fig. 1 a), $P_3(t)$ has a real negative double root and a real non-negative single root.

In the **2nd case** (Fig. 1 b), $P_3(t)$ has a zero as double root and a real negative single root.

In the **3rd case** (Fig. 1 c), $P_3(t)$ has a real positive double root which is smaller than the real positive single root.

In the **4th case** (Fig. 1 d), $P_3(t)$ has a real positive double root which is greater than the real non-negative single root.

In the **5th case** (Fig. 1 e), $P_3(t)$ has a zero as double root and a real positive single root.

In the **6th case** (Fig. 1 f), $P_3(t)$ has a real positive triple root.

In the **7th case** (Fig. 1 g), $P_3(t)$ has a zero as a triple root.

Now we can formulate and prove the main theorem.

Theorem 3.

- 1st case $\iff P_4(x)$ has two complex roots and one double real root.
- 2nd case $\iff P_4(x) = (x^2 + b^2)^2 \quad (b \neq 0)$
- 3rd case $\iff P_4(x)$ has three different real roots, but among them is only one double root and the other two single roots are on the same side of the double one.
- 4th case $\iff P_4(x)$ has three different real roots, but among them is only one double root and the other two single roots are on the opposite sides of the double one.
- 5th case $\iff P_4(x)$ has two double real roots.
- 6th case $\iff P_4(x)$ has two different real roots and one of them is a triple root.
- 7th case $\iff P_4(x)$ has only one fourfold real root which is zero.

Proof: At the bargaining we shall do some general considerations. It is known (see [7]) that the roots of $P_4(x)$ and $P_3(t)$ are connected by the following relations

$$\begin{aligned} t_1 &= -(x_1 + x_2)(x_3 + x_4) \\ t_2 &= -(x_1 + x_3)(x_2 + x_4) \\ t_3 &= -(x_1 + x_4)(x_2 + x_3). \end{aligned} \quad (11)$$

In the further considerations we shall use also the first Vieta's formula for the roots of $P_4(x)$ $x_1 + x_2 + x_3 + x_4 = 0$ (because the coefficient of the third power of x is zero). From these formulas we can get

$$\begin{aligned} t_1 &= (x_1 + x_2)^2 = (x_3 + x_4)^2 \\ t_2 &= (x_1 + x_3)^2 = (x_2 + x_4)^2 \\ t_3 &= (x_1 + x_4)^2 = (x_2 + x_3)^2. \end{aligned} \quad (12)$$

Now we shall consider the case when two roots of $P_4(x)$ are real and the other two roots are complex. Let $x_3 = a + bi$ and $x_4 = a - bi$ ($b \neq 0$). Then $t_2 = (x_1 + x_3)^2 = (x_1 + a + bi)^2$ must be a real number (because t_i for $i = 1, 2, 3$ are always real numbers in all seven cases) but that is only possible iff $x_1 + a = 0$ respectively $x_1 + x_2 + x_3 + x_4 = x_1 + a + x_2 + a = x_2 + a = 0$ thus $x_1 = x_2 = -a$. From (12) immediately follows $t_2 = t_3 = -b^2 < 0$. In the case when all four roots of $P_4(x)$ are complex numbers, let $x_1 = a + bi$, $x_2 = a - bi$, $x_3 = c + di$, $x_4 = c - di$, then from $x_1 + x_2 + x_3 + x_4 = 2a + 2c = 0$ we get $a + c = 0$. Hence from (12) it follows $t_2 = -(b+d)^2$ and $t_3 = -(b-d)^2$. From the fact that both numbers b and d are different from zero we conclude that $t_2 \neq t_3$ and at least one of them is less than zero. If a and c are both different from zero, then it follows from (12) $t_1 = 4a^2 > 0$, which means that all three roots of $P_3(t)$ are mutually different. If we want that at least two roots of $P_3(t)$ be the same, then it is necessary and sufficient that $a = c = 0$ and $b = d$ or $b = -d$, which implies $x_1 = bi$, $x_2 = -bi$, $x_3 = bi$, $x_4 = -bi$. According to this all four roots are purely imaginary with two equal pairs. On the basis of all these considerations we conclude that

$$t_i \geq 0 \quad (i = 1, 2, 3) \iff x_i \in \mathbf{R} \quad (i = 1, 2, 3, 4). \quad (13)$$

So we proved the first two statements of our theorem and in the remaining five statements are all four roots of $P_4(x)$ only real numbers. From (12) and from $x_1 + x_2 + x_3 + x_4 = 0$ we get

$$\begin{aligned} t_1 = t_2 < t_3 &\iff (x_2 - x_3)(x_1 - x_4) = 0 \\ &\quad (x_3 - x_4)(x_1 - x_2) < 0 \\ &\quad (x_2 - x_4)(x_1 - x_3) < 0. \end{aligned} \quad (14)$$

So there are two possibilities

$$\begin{aligned} I &\quad x_1 = x_4 \quad \text{and} \quad (x_2, x_3 < x_4 \quad \text{or} \quad x_2, x_3 > x_4) \\ II &\quad x_2 = x_3 \quad \text{and} \quad (x_1, x_4 < x_2 \quad \text{or} \quad x_1, x_4 > x_2). \end{aligned} \quad (15)$$

The case $x_1 = x_4$ and $x_2 = x_3$ is impossible because from $t_1 = -(x_1 + x_2)(x_3 + x_4) = -(x_1 + x_2)^2 \leq 0$ we get a contradiction. Analogously in the case of fourth statement we get

$$\begin{aligned} t_1 < t_2 = t_3 &\iff (x_3 - x_4)(x_1 - x_2) = 0 \\ &\quad (x_2 - x_3)(x_1 - x_4) < 0 \\ &\quad (x_2 - x_4)(x_1 - x_3) < 0. \end{aligned} \quad (16)$$

So there are two possibilities

$$\begin{aligned} I &\quad x_1 = x_2 \quad \text{and} \quad (x_3 < x_1 < x_4 \quad \text{or} \quad x_4 < x_1 < x_3) \\ II &\quad x_3 = x_4 \quad \text{and} \quad (x_1 < x_3 < x_2 \quad \text{or} \quad x_2 < x_3 < x_1). \end{aligned} \quad (17)$$

The case $x_1 = x_2$ and $x_3 = x_4$ is impossible because from $t_2 = -(x_1 + x_3)(x_2 + x_4) = -(x_1 + x_3)^2 \leq 0$ we get a contradiction. In the case of 5th statement we get again using (12) and $x_1 + x_2 + x_3 + x_4 = 0$

$$0 = t_1 = t_2 < t_3 \iff x_1 = -x_2 = -x_3 = x_4 \neq 0. \quad (18)$$

In the case of 6th statements we get analogously

$$\begin{aligned} t_1 = t_2 = t_3 &\iff (x_2 - x_3)(x_1 - x_4) = 0 \\ &\quad (x_3 - x_4)(x_1 - x_2) = 0 \\ &\quad (x_2 - x_4)(x_1 - x_3) = 0 \\ &\iff x_1 = x_2 = x_3 \\ &\quad x_1 = x_2 = x_4 \\ &\quad x_1 = x_3 = x_4 \\ &\quad x_2 = x_3 = x_4. \end{aligned} \quad (19)$$

If we supposed $x_1 = x_2 = x_3 = x_4$ we get that all four roots are equal to zero, which is a contradiction. In the case of 7th case by considerations of previous case we easily get $x_1 = x_2 = x_3 = x_4 = 0$. \square

Remark. As we have noted before, the proof of the "first case" in the theorem 1 is an indication for the existence of the theorem 3. Yet one indication for the theorem 3 is a fact that the discriminants of $P_4(x)$ and $P_3(t)$ are equal (see [7]).

It remains only to formulate and prove the theorem about the characterizations of all those seven cases.

Theorem 4.

$$\begin{aligned}
1st \text{ case} &\iff a_2^2 + 12a_0 > 0 \quad \text{and} \quad -2a_2 < \sqrt{a_2^2 + 12a_0} \quad \text{and} \quad 2(a_2^2 + 12a_0)^{\frac{3}{2}} = 2a_2^3 - 72a_2a_0 + 27a_1^2 \\
2nd \text{ case} &\iff a_1 = 0 \quad \text{and} \quad a_2^2 - 4a_0 = 0 \quad \text{and} \quad a_2 > 0 \\
3rd \text{ case} &\iff a_2 < 0 \quad \text{and} \quad a_2^2 - 4a_0 > 0 \quad \text{and} \quad a_2^2 + 12a_0 > 0 \quad \text{and} \quad 2(a_2^2 + 12a_0)^{\frac{3}{2}} = 2a_2^3 - 72a_2a_0 + 27a_1^2 \\
4th \text{ case} &\iff a_2 < 0 \quad \text{and} \quad a_2^2 - 4a_0 > 0 \quad \text{and} \quad a_2^2 + 12a_0 > 0 \quad \text{and} \quad 2(a_2^2 + 12a_0)^{\frac{3}{2}} = -2a_2^3 + 72a_2a_0 - 27a_1^2 \\
5th \text{ case} &\iff a_1 = 0 \quad \text{and} \quad a_2^2 - 4a_0 = 0 \quad \text{and} \quad a_2 < 0 \\
6th \text{ case} &\iff a_2^2 + 12a_0 = 0 \quad \text{and} \quad 8a_2^3 + 27a_1^2 = 0 \quad \text{and} \quad a_2 < 0 \\
7th \text{ case} &\iff a_0 = a_1 = a_2 = 0.
\end{aligned} \tag{20}$$

Proof:

$$\begin{aligned}
P_3(t) &= t^3 + 2a_2t^2 + (a_2^2 - 4a_0)t - a_1^2 \\
P'_3(t) &= 3t^2 + 4a_2t + a_2^2 - 4a_0 \\
P''_3(t) &= 6t + 4a_2.
\end{aligned} \tag{21}$$

In the 1st case $P'_3(t)$ should have two different real roots and the smaller one should be double real root of $P_3(t)$. For $P'_3(t)$ to have different real roots, the necessary and sufficient condition is

$$a_2^2 + 12a_0 > 0. \tag{22}$$

If condition (22) is satisfied then the smaller real root of $P'_3(t)$ is

$$t_1 = \frac{-2a_2 - \sqrt{a_2^2 + 12a_0}}{3}. \tag{23}$$

The condition necessary and sufficient for $P_3(t_1) = 0$ is

$$2(a_2^2 + 12a_0)^{\frac{3}{2}} = 2a_2^3 - 72a_2a_0 + 27a_1^2. \tag{24}$$

Finally, the condition for t_1 to be a negative real number is equivalent to

$$-2a_2 < \sqrt{a_2^2 + 12a_0}. \tag{25}$$

In the 2nd case $t = 0$ is a double real root of $P_3(t)$ which is evidently equivalent to

$$a_1 = 0 \quad \text{and} \quad a_2^2 - 4a_0 = 0. \tag{26}$$

As the second single real root of $P_3(t)$ is negative, we easily conclude that

$$a_2 > 0. \tag{27}$$

In the 3rd case $P'_3(t)$ has two different positive real roots which is equivalent to

$$\begin{aligned}
P'_3(0) &= a_2^2 - 4a_0 > 0 \quad \text{and} \\
P''_3(0) &= 4a_2 < 0 \quad \text{and} \\
a_2^2 + 12a_0 &> 0.
\end{aligned} \tag{28}$$

The last condition is obtained by analogous reasoning like in the 1st case. Finally, analogously as in the 1st case, it must be $P_3(t_1) = 0$ where t_1 is given by (23), so we get the relation (24) again.

In the 4th case we get the conditions (28) using the same reasoning like in the 3rd case. But now $P_3(t_2) = 0$ where t_2 is the greater real root of $P'_3(t)$ i. e.

$$t_2 = \frac{-2a_2 + \sqrt{a_2^2 + 12a_0}}{3}. \tag{29}$$

Condition $P_3(t_2) = 0$ is equivalent to the following condition

$$2(a_2^2 + 12a_0)^{\frac{3}{2}} = -2a_2^3 + 72a_2a_0 - 27a_1^2. \tag{30}$$

In the 5th case, analogously as in the 2nd case, $t = 0$ must be the double real root of $P_3(t)$ which is equivalent to the conditions (26). But now, since the second single real root of $P_3(t)$ is positive, we conclude easily that

$$a_2 < 0. \tag{31}$$

In the 6th case

$$P_3(t) = 0, \quad P'_3(t) = 0, \quad P''_3(t) = 0 \tag{32}$$

must be for the same value of t . From $P''_3(t) = 0$ we easily get

$$t = -\frac{2}{3}a_2. \tag{33}$$

From (33) we get immediately

$$a_2 < 0, \tag{34}$$

and

$$P'_3\left(-\frac{2}{3}a_2\right) = 0 \quad \text{and} \quad P_3\left(-\frac{2}{3}a_2\right) = 0, \tag{35}$$

which is equivalent to

$$a_2^2 + 12a_0 = 0 \quad \text{and} \quad 8a_2^3 + 27a_1^2 = 0. \quad (36)$$

In the 7th case it should be

$$P_3(0) = 0; \quad P'_3(0) = 0; \quad P''_3(0) = 0, \quad (37)$$

which is equivalent to

$$a_0 = 0; \quad a_1 = 0; \quad a_2 = 0. \quad (38)$$

□

Now, there is question left about the conditions that give the answer in the 3rd and the 6th case to the question on which side of the double (triple) root are two single roots (one single root). That problem is solved in the next lemma.

Lemma 5. Let $P_3(t)$ have a real positive double root and a real single root which is greater than that double one. Then

$$x_{1,2} = \frac{a_1(a_2^2 + 12a_0)}{8a_0a_2 - 2a_2^3 - 9a_1^2} \quad (39)$$

is double root of $P_4(x)$ and

$$a_1 > 0 (< 0) \iff x_3 \text{ and } x_4 \text{ are on the left (right) side of } x_{1,2}. \quad (40)$$

Let $P_3(t)$ have a positive triple root. Then

$$x_{1,2,3} = -\frac{8}{3} \frac{a_0}{a_1} \quad (41)$$

is a triple root of $P_4(x)$ and

$$a_1 > 0 (< 0) \iff x_4 \text{ is on the left (right) side of } x_{1,2,3}. \quad (42)$$

Proof: From the theorem 3 it follows that $P_4(x)$ has only one double real root. We will find that double root by eliminating the members with higher powers of x between the following two equations

$$\begin{aligned} P_4(x) &\equiv x^4 + a_2x^2 + a_1x + a_0 = 0 \\ P'_4(x) &\equiv 4x^3 + 2a_2x + a_1 = 0. \end{aligned} \quad (43)$$

By eliminating the member with x^4 between these two equations we get

$$2a_2x^2 + 3a_1x + 4a_0 = 0. \quad (44)$$

By eliminating the member with x^3 between (44) and the second equations of (43) we get

$$6a_1x^2 + (8a_0 - 2a_2^2)x - a_1a_2 = 0. \quad (45)$$

Finally, by eliminating the member with x^2 between (44) and (45) we get

$$(8a_0a_2 - 2a_2^3 - 9a_1^2)x - a_1a_2^2 - 12a_0a_1 = 0. \quad (46)$$

From the equation (46) the formula (39) follows. Using the relations which characterize the 3rd case in the theorem 4 we will prove that

$$8a_0a_2 - 2a_2^3 - 9a_1^2 > 0. \quad (47)$$

So we get

$$\begin{aligned} a_2^2 - 4a_0 &> 0 \implies 12a_2^2 - 48a_0 > 0 \implies \\ 16a_2^2 &> 4(a_2^2 + 12a_0) \implies \\ \implies 2(a_2^2 + 12a_0)^{\frac{3}{2}} &< -4a_2(a_2^2 + 12a_0) \implies \\ \implies 2(a_2^2 + 12a_0)^{\frac{3}{2}} &= 27a_1^2 + 2a_2^3 - 72a_0a_2 < \\ < -4a_2(a_2^2 + 12a_0) &\implies 8a_0a_2 - 2a_2^3 - 9a_1^2 > 0. \end{aligned} \quad (48)$$

From $a_2^2 + 12a_0 > 0$ and (47) it follows that the sign of $x_{1,2}$ is the same as of a_1 . It remains only to prove that a_1 cannot be zero. Suppose conversely that a_1 is zero. Then from

$$x_1 = x_2 = 0 \quad \text{and} \quad x_1 + x_2 + x_3 + x_4 = 0 \quad (49)$$

we conclude that $x_4 = -x_3$ which is in contradiction with the 3rd case (because x_3 and x_4 are on the opposite sides of double root zero). Now, if the sign of $x_{1,2}$ is positive ($a_1 > 0$) then from

$$x_{1,2} = -\frac{x_3 + x_4}{2} \quad (50)$$

we conclude that x_3 and x_4 lie on the left side of $x_{1,2}$. Completely analogously we reason in the case when $x_{1,2}$ is negative ($a_1 < 0$).

If $P_3(t)$ has positive triple root then according to theorem 3, $P_4(x)$ has a triple real root. We will get it by eliminating the members of higher powers of x among the following three equations

$$\begin{aligned} P_4(x) &\equiv x^4 + a_2x^2 + a_1x + a_0 = 0 \\ P'_4(x) &\equiv 4x^3 + 2a_2x + a_1 = 0 \\ P''_4(x) &\equiv 12x^2 + 2a_2 = 0. \end{aligned} \quad (51)$$

From the first two equations we get

$$2a_2x^2 + 3a_1x + 4a_0 = 0. \quad (52)$$

From the (52) and the last equation of (51) we get finally

$$9a_1x + 12a_0 - a_2^2 = 0. \quad (53)$$

From (53) it follows

$$x_{1,2,3} = \frac{a_2^2 - 12a_0}{9a_1}. \quad (54)$$

Using the relations which characterize the 6th case in the theorem 4 we easily get that a_1 cannot be zero and secondly that

$$x_{1,2,3} = -\frac{8}{3} \frac{a_0}{a_1}. \quad (55)$$

From relations $a_2^2 + 12a_0 = 0$ and $a_2 < 0$ it follows $a_0 < 0$.

From

$$x_4 = -3x_{1,2,3} \quad \text{and} \quad a_0 < 0 \quad (56)$$

we easily get (42). \square

References

- [1] W. W. RAUZE BALL, *A Short Account of the History of Mathematics*, Dover Publications, New York, 1960.
- [2] A. B. BASSET, *An Elementary Treatise on Cubic and Quartic Curves*, Deighton Bell and Co., Cambridge, 1901.
- [3] B. PAVKOVIĆ, D. VELJAN, *Elementarna matematika I*, Tehnička knjiga, Zagreb, 1992.
- [4] J. PLEMELJ, *Algebra in teorija števil*, Slovenska akademija znanosti in umetnosti, Ljubljana, 1962.
- [5] V. SEDMAK, *Uvod u algebru*, Sveučilište u Zagrebu, Zagreb, 1961.

[6] R. VIHER, The Consequences of Descartes's Method for Factorization of 4th Degree Polynomial, KoG no. 5, Zagreb, 2001.

[7] S. WARNER, *Modern Algebra*, Dover Publications, New York, 1990.

Radimir Viher

Faculty of Civil Engineering, University of Zagreb
Kačićeva 26, 10000 Zagreb, Croatia
e-mail: viher@master.grad.hr

Professional paper

Accepted 23.11.2007.

TATIANA OLEJNÍKOVÁ*

Cyclical Surfaces Created by a Conical Helix

Cyclical Surfaces Created by a Conical Helix

ABSTRACT

The paper describes cyclical surfaces created by revolution of a circle about an edge of the trihedron of a conical helix that is moving evenly along the helix. This Euclidean metric transformation is composed from revolution about one of the coordinate axes and transformation of the right-handed coordinate system to the right-handed system of the moving trihedron in every point of the conical helix. This transformation is analytically represented by a functional matrix of 4th order. These surfaces are determined at particular parameter values which have influence on the surface shape. The vector equation of surfaces and some illustrations of this group of surfaces are presented in the paper. The surfaces are illustrated and modelled in the programme Maple.

Key words: cyclical surface, conical helix, trihedron

MSC 2000: 15A04, 53A05, 14J26

1 The vector equation of the cyclical surface created by a conical helix

Let the conical helix s in right-handed coordinate system $(O; x, y, z)$ be located on the circular conical surface with the meridian defined analytically by the vector function $(r_1 + u(r_2 - r_1), 0, uv, 1), u \in \mathbb{R}, (r_1 \neq 0, r_2 \neq 0, v \neq 0)$ (Figure 1).

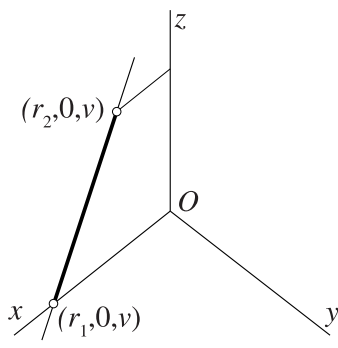


Figure 1: Meridian of the conical surface

Kružne plohe izvedene pomoću zavojnice na stošcu

SAŽETAK

Članak prikazuje kružne plohe koje nastaju rotacijom kružnice oko jednog brida trobrida pratioca na zavojnici stošca, koji se jednoliko giba duž zavojnice. Ova euklidska metrička transformacija sastoji se od rotacije oko jedne od koordinatnih osi i transformacije desno orientiranog koordinatnog sustava u desno orientirani sustav gibajućeg trobrida u svakoj točki zavojnice na stošcu. Ta je transformacija analitički prikazana funkcionalnom matricom 4. reda. Plohe su određene posebnim vrijednostima parametra koji utječe na njihov oblik. U članku je predstavljena vektorska jednadžba i nekoliko primjera ove grupe ploha. Primjeri su konstruirani pomoću računalnog programa Maple.

Ključne riječi: kružne plohe, zavojnica na stošcu, trobrid pratilac

The helix has the parametrical equations (1), where l is a number of helix screws and the parameter $q = +1$ for right-turned helix and $q = -1$ for left-turned one (Figure 2) [3].

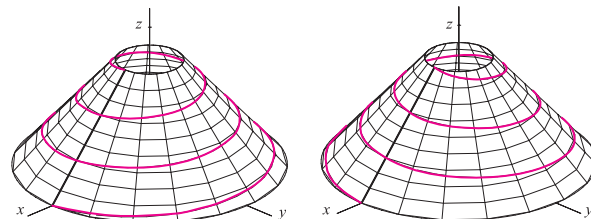


Figure 2: Conical helix right-turned and left-turned

$$\begin{aligned} x &= \left(r_1 + \frac{\varepsilon(r_2 - r_1)}{2l\pi} \right) \cos \varepsilon \\ y &= q \left(r_1 + \frac{\varepsilon(r_2 - r_1)}{2l\pi} \right) \sin \varepsilon, \quad \varepsilon \in (0, 2\pi). \\ z &= \frac{v\varepsilon}{2l\pi} \end{aligned} \quad (1)$$

* The paper was supported by the grant VEGA 1 / 4002/07

The trihedron $(R; t, n, b)$ in the coordinate system $(O; x, y, z)$ is given in every point $R \in s$ with coordinates determined in equation (2), where t is the tangent, b is the binormal and n is the principal normal of the conical helix s (Figure 3). The unit vectors of the trihedron are expressed in equations (3) and (4) [1].

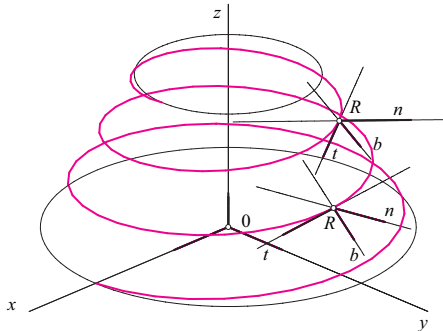


Figure 3: Trihedron $(R; t, n, b)$ with unit vectors

$$\begin{aligned} R(x_R, y_R, z_R) = & \\ & \left(\left(r_1 + \frac{\varepsilon(r_2 - r_1)}{2l\pi} \right) \cos \varepsilon, \left(r_1 + \frac{\varepsilon(r_2 - r_1)}{2l\pi} \right) \sin \varepsilon, \frac{v\varepsilon}{2l\pi} \right). \end{aligned} \quad (2)$$

$$\begin{aligned} \mathbf{t} &= (a_t, b_t, c_t), \\ a_t &= -\frac{1}{h} ((r_2 - r_1) \cos \varepsilon - (2r_1 l\pi + \varepsilon(r_2 - r_1)) \sin \varepsilon), \\ b_t &= -\frac{1}{h} (q(r_2 - r_1) \sin \varepsilon + (2r_1 l\pi + \varepsilon(r_2 - r_1)) \cos \varepsilon), \\ c_t &= -\frac{1}{h} (v), \text{ where} \\ h &= \sqrt{(r_2 - r_1)^2 + (2r_1 l\pi + \varepsilon(r_2 - r_1))^2 + v^2}. \end{aligned} \quad (3)$$

$$\begin{aligned} \mathbf{n} &= (a_n, b_n, c_n) = \frac{\mathbf{tp} \times \mathbf{t}}{|\mathbf{tp} \times \mathbf{t}|}, \\ \mathbf{b} &= (a_b, b_b, c_b) = \frac{\mathbf{t} \times \mathbf{n}}{|\mathbf{t} \times \mathbf{n}|}. \end{aligned} \quad (4)$$

$\mathbf{tp} = ((r_2 - r_1) \cos \varepsilon, q(r_2 - r_1) \sin \varepsilon, v)$ in equation (4) is the direction vector of the generator of the conical surface passing through the point R .

We will revolve the circle $k_0 = (S, r)$ represented by the vector function $\mathbf{r}(u) = (x(u), y(u), z(u), 1)$, $u \in \langle 0, 2\pi \rangle$ through the angle $\varepsilon' = m\varepsilon$ about the local coordinate axis x (resp. y , resp. z). The corresponding rotation is represented by the matrix function $T_x(\varepsilon'(\varepsilon))$ (resp. $T_y(\varepsilon'(\varepsilon))$,

resp. $T_z(\varepsilon'(\varepsilon))$) in equation (5) [2]. The parameter m is a multiple of the radian velocity of the point R moving on the helix. Right-handed rotation of the circle about the corresponding axis x , y , or z is represented by the parameter $q' = +1$ and left-handed rotation by the parameter $q' = -1$.

$$\begin{aligned} T_x(\varepsilon'(\varepsilon)) &= \begin{pmatrix} 1 & 0 & 0 & 0 \\ 0 & \cos \varepsilon'(\varepsilon) & q' \sin \varepsilon'(\varepsilon) & 0 \\ 0 & -q' \sin \varepsilon'(\varepsilon) & \cos \varepsilon'(\varepsilon) & 0 \\ 0 & 0 & 0 & 1 \end{pmatrix}, \\ T_y(\varepsilon'(\varepsilon)) &= \begin{pmatrix} \cos \varepsilon'(\varepsilon) & 0 & q' \sin \varepsilon'(\varepsilon) & 0 \\ 0 & 1 & 0 & 0 \\ -q' \sin \varepsilon'(\varepsilon) & 0 & \cos \varepsilon'(\varepsilon) & 0 \\ 0 & 0 & 0 & 1 \end{pmatrix}, \\ T_z(\varepsilon'(\varepsilon)) &= \begin{pmatrix} \cos \varepsilon'(\varepsilon) & q' \sin \varepsilon'(\varepsilon) & 0 & 0 \\ -q' \sin \varepsilon'(\varepsilon) & \cos \varepsilon'(\varepsilon) & 0 & 0 \\ 0 & 0 & 1 & 0 \\ 0 & 0 & 0 & 1 \end{pmatrix}. \end{aligned} \quad (5)$$

Then we will transform the rotated circle k' given in the local coordinate system $(O; x, y, z)$ into the circle k in the coordinate system $(R; t, n, b)$ where are expressed in (4) (Figure 4) by the transformation given by $\mathbf{M}(\varepsilon)$.

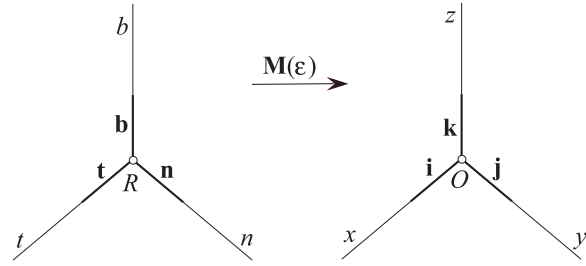


Figure 4: Transformation $(R; t, n, b)$ into $(O; x, y, z)$

The entries in the rows 1, 2 and 3 of $\mathbf{M}(\varepsilon)$ are the coordinates of the unit vectors of the trihedron expressed in equations (3), (4) and the entries in the 4th row are the coordinates of the point R in equation (2)

$$\mathbf{M}(\varepsilon) = \begin{pmatrix} a_t & b_t & c_t & 0 \\ a_b & b_b & c_b & 0 \\ a_n & b_n & c_n & 0 \\ x_R & y_R & z_R & 1 \end{pmatrix}. \quad (6)$$

The vector equation of the cyclical surface created by the conical helix is expressed as a product of three matrices for $i = x, y, z$.

$$\mathbf{p}(u, \varepsilon) = \mathbf{r}(u) \cdot \mathbf{T}_i(\varepsilon'(\varepsilon)) \cdot \mathbf{M}(\varepsilon). \quad (7)$$

2 Classification of the cyclical surfaces created by a conical helix

The three basic types of cyclical surfaces described above can be characterised with respect to the axis of revolution of the moved circle:

- I the circle rotates about the tangent t ,
- II the circle rotates about the binormal b ,
- III the circle rotates about the principal normal n

in the point R of the conical helix s .

The circle k_0 in dependence on the axis of revolution $o = x$ (resp. $o = y$, resp. $o = z$) is in:

- A meridian plane,
- B normal plane. (Figure 5)

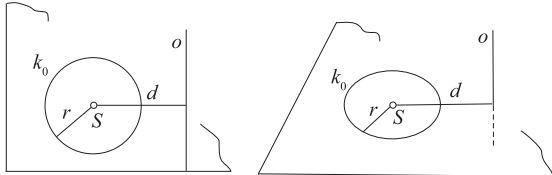


Figure 5: The circle k_0 in the meridian or normal plane

The distance $d = |S, o|$ between the centre S of the circle $k_0 = (S, r)$ and the axis of revolution o can be:

- a $d > r$ the circle k_0 does not intersect the axis o ,
- b $d = r$ circle k_0 is tangent to the axis o ,
- c $d = 0$ the centre of the circle k_0 is on the axis o .

3 Display of the cyclical surfaces created by a conical helix

In this chapter we will display only these cyclical surfaces created by the conical helix, which are applicable in technical practice. Hence we will display cyclical surfaces of types IA, IB, IIA, IIIA. The surfaces of types IIB and IIIB are inapplicable in technical practice in due to their forms.

In Figure 6 the cyclical surfaces of the named types are shown by rotating the circle k_0 about the corresponding coordinate axis in $(R; t, n, b)$ of the right-turned conical helix with $l = 1$ screw then transformed into the coordinate system $(O; x, y, z)$.

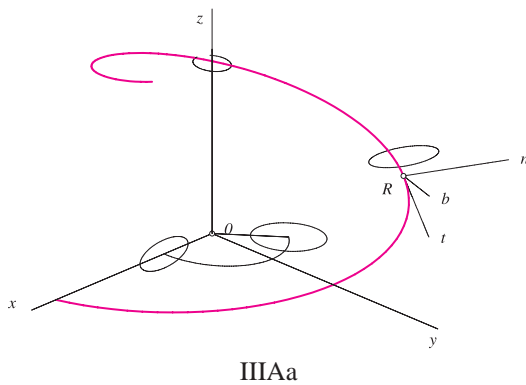
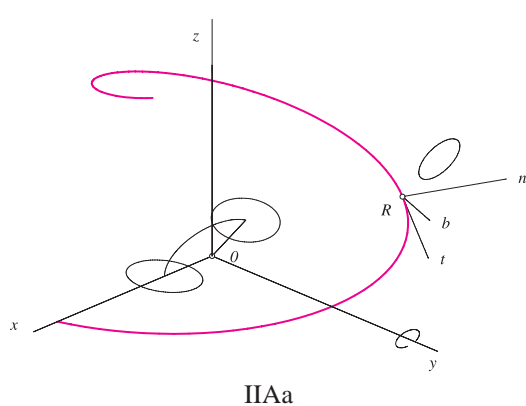
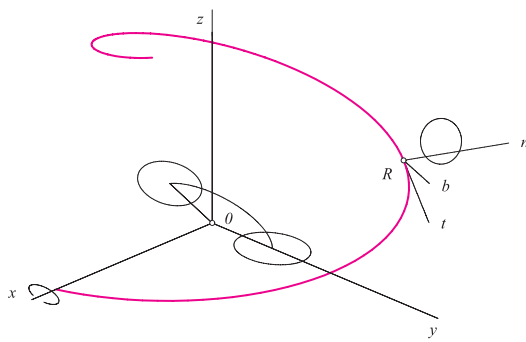
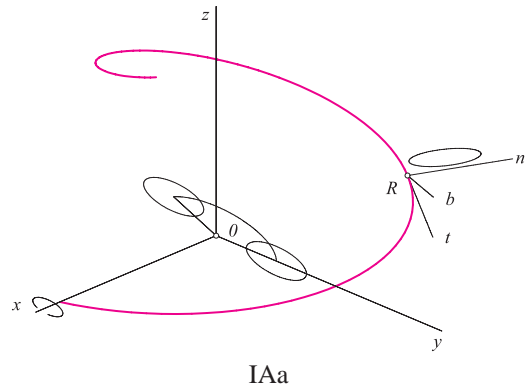


Figure 6: Types of the cyclical surfaces created by a conical helix

In Figure 7 a cyclical surfaces of type IA is shown, where the circle k_0 is in the normal plane to the axis of revolution $o = x$. All surfaces shown in Figure 7 have the same parameters $l = 3$, $m = 1$ but different parameter d . If $d > r$ the helix s is not on the surface, if $d = r$ the helix is on the surface and if $d = 0$, then the centre S of the revolving circle is on the helix s . The parameter $q' = +1$ for first three surfaces, $q' = -1$ for forth and fifth surface.

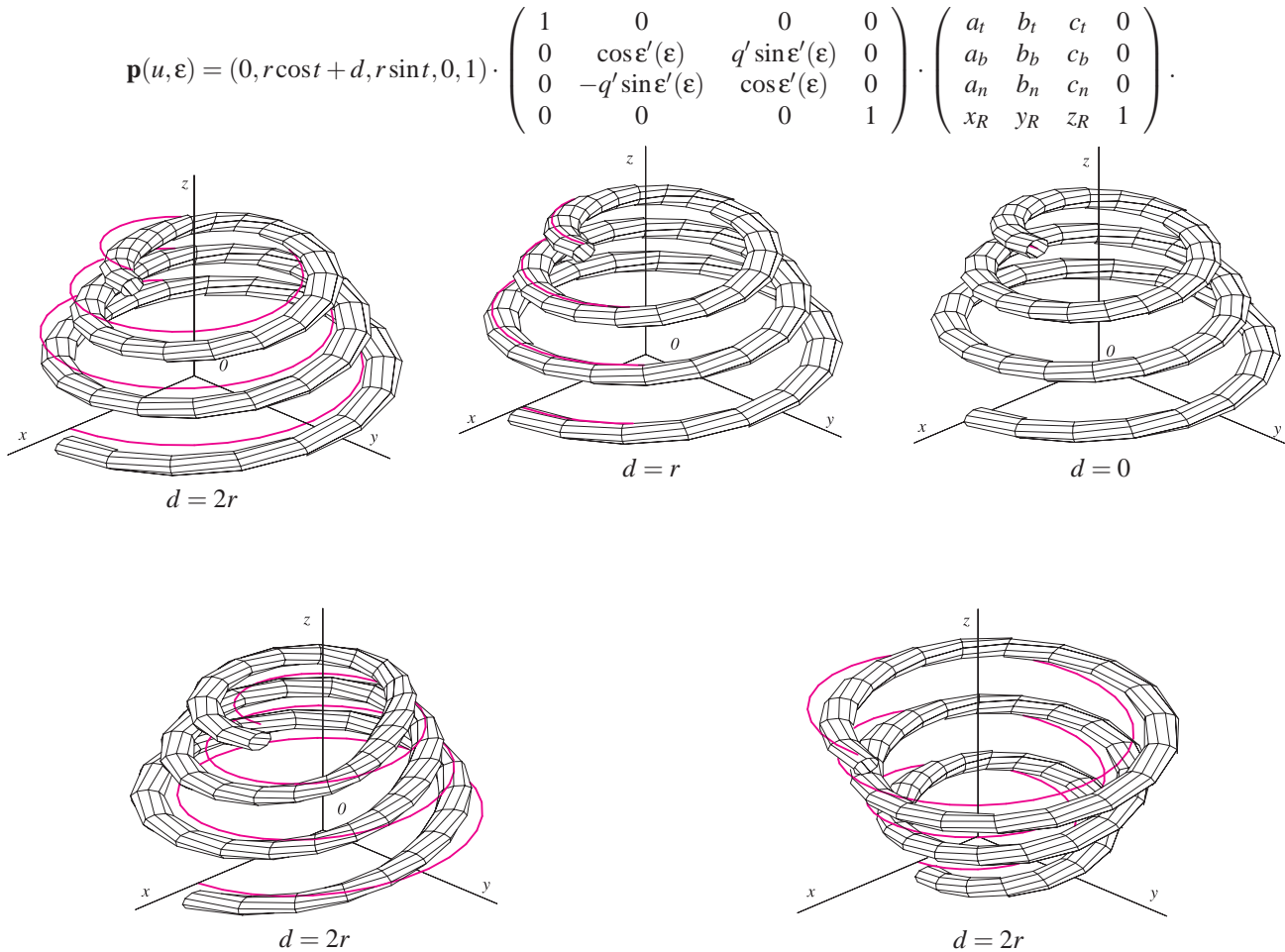


Figure 7: Cyclical surfaces of type IA

In Figure 8 cyclical surfaces of type IB are shown, where the circle k_0 is in the meridian plane of the axis of revolution $o = x$. The first two surfaces displayed in Figure 8 have the same parameters $l = 3, m = 10, d > r$, and $q = +1$ or $q = -1$. The helix s is not on these surfaces. Third and fourth surfaces have parameters $l = 3, m = 15, q = +1$ or $q = -1$. These surfaces are applicable only with parameter $m > 1$ in technical practice.

We may express the vector equation of this cyclical surface of type IA from equation (7), where the vector function of the circle k_0 in the normal plane to the axis $o = x$ is $\mathbf{r}(u) = (0, r \cos u + d, r \sin u, 1)$, $u \in \langle 0, 2\pi \rangle$ and we get the corresponding matrix for $i = x$ from equations (5), where a_t, b_t, \dots, c_n are expressed in equations (3), (4), x_R, y_R, z_R are the coordinates of the point R in the equation (2)

We may express the vector equation of this cyclical surface of type IB similarly as for the surface of type IA, where the vector function of the circle k_0 lying in the meridian plane of the axis $o = x$ is $\mathbf{r}(u) = (r \cos u + d, r \sin u, 0, 1)$, $u \in \langle 0, 2\pi \rangle$.

In Figure 9 cyclical surfaces of types IIB and IIIB are shown, where the circle is in the meridian plane of the axis of revolution $o = y$ or $o = z$. First three surfaces are created

by a circle rotating about the binormal and other two about the principal normal of the conical helix s . All surfaces are displayed with the helix s with parameters $l = 3, q = +1$.

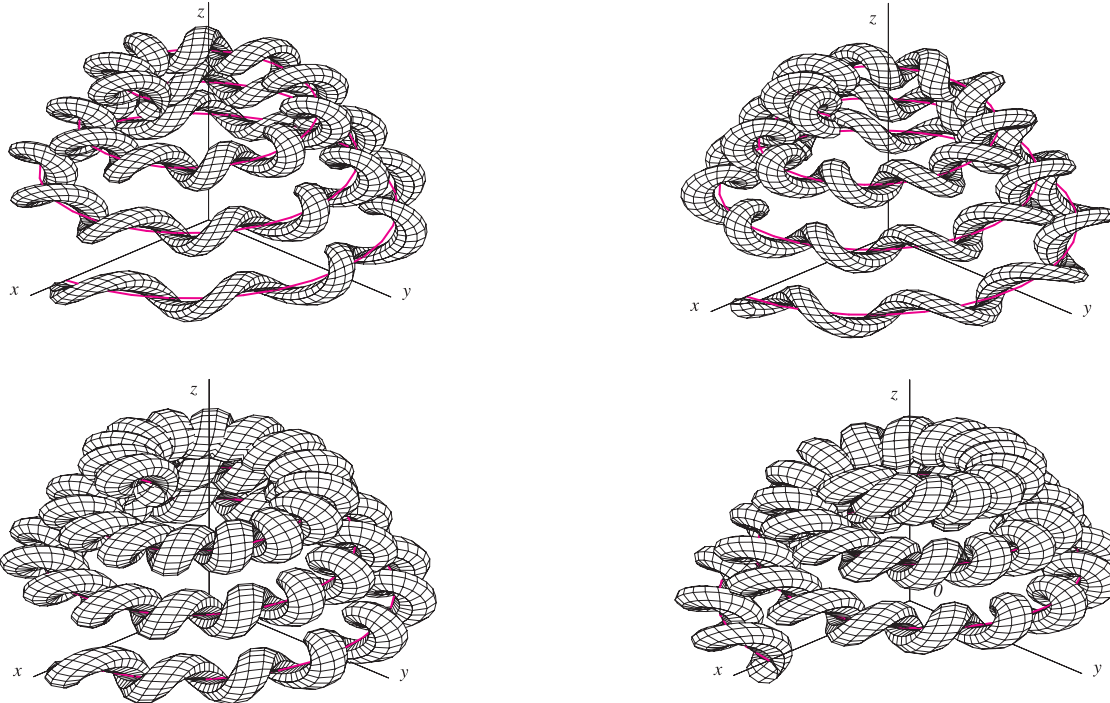


Figure 8: Cyclical surfaces of type IB

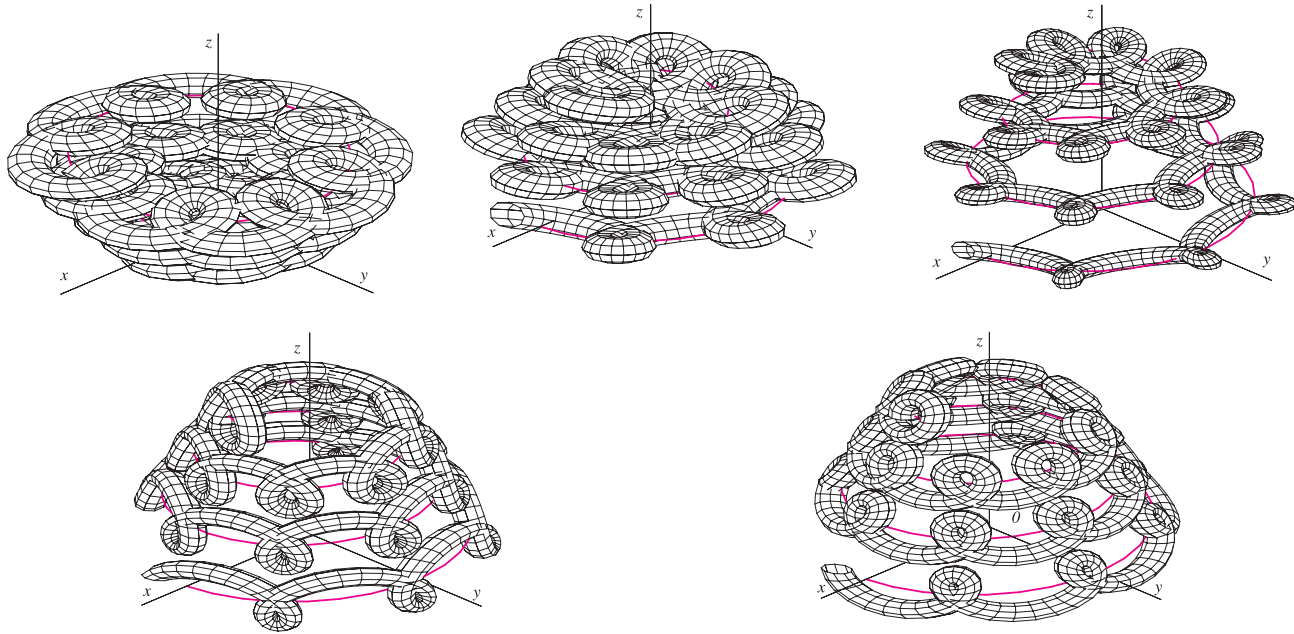


Figure 9: Cyclical surfaces of type IIB and IIIB

4 Conclusion

Many of these surfaces may be used in design practice as constructive or ornamental structural components. In Fig-

ure 10 there are displayed some illustrations of combinations of these cyclical surfaces with interesting and beautiful aesthetic forms.

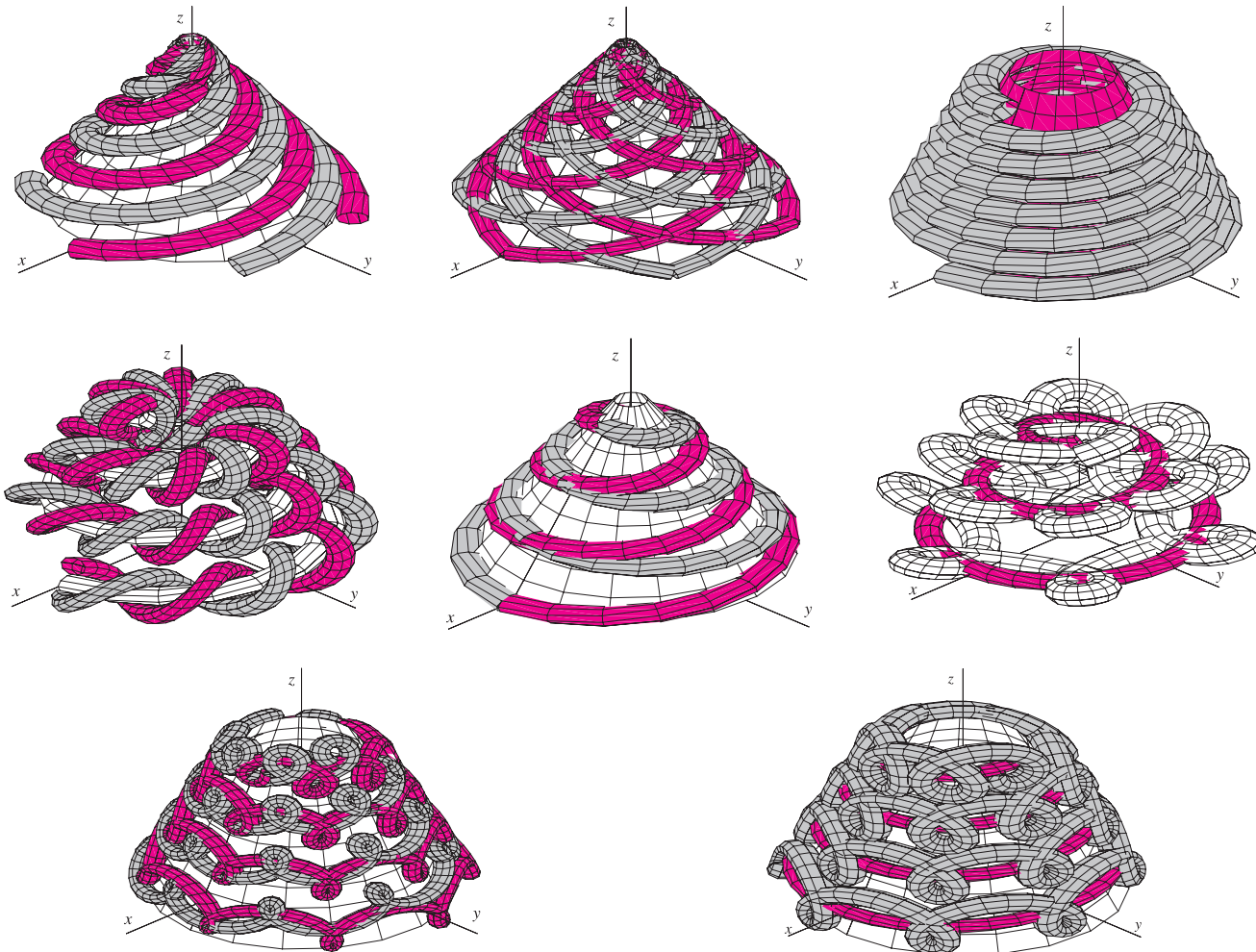


Figure 10: Combinations of cyclical surfaces of different types

References

- [1] BUDINSKÝ, B., KEPR, B., *Basic of Differential Geometry with Technical Applications*, SNTL - Publishers of Technical Literature, Praha, 1970
- [2] GRANAT, L., SECHOVSKÝ, H., *Computer Graphics*, SNTL - Publishers of Technical Literature, Praha, 1980
- [3] MEDEK, V., ZAMOŽIK, J., *Knots and Surfaces, Constructive geometry for technics*, ALFA - Publishers of Technical and Economical Literature, Bratislava, 1974

Tatiana Olejníková

Department of Applied Mathematics
Faculty of Civil Engineering
Technical University in Košice, Slovakia
e-mail: tatiana.olejnikova@tuke.sk

Professionelle Arbeit
Angenommen am 20.12.2007.

HANS GÜNTHER KOPETZKY
HANS SACHS

Quadratische Kegel und AutoCAD

Quadratic Cones and AutoCAD

ABSTRACT

Oblique circular cones and quadratic cones are discussed mainly with respect to implementations in Computer Algebra systems and CAD systems especially AutoCAD.

Key words: quadratic cones, oblique circular cones, elliptic cones

MSC 2000: 65D17

Bekanntlich existieren im dreidimensionalen euklidischen Raum E_3 bezüglich der 6-parametrischen euklidischen Bewegungsgruppe genau zwei Typen von quadratischen Kegeln: Schiefe Kreiskegel und Drehkegel (vgl. [3] p.158f). Gibt man also als Leitkurve einen Kegelschnitt vor und wählt eine Kegelspitze $S \notin \alpha$, so lässt sich der Verbindungskegel von S mit ℓ stets als *schiefer Kreiskegel* erzeugen.

Wir verstehen nun unter einem *elliptischen Kegel* einen Kegel mit elliptischer Leitkurve ℓ , dessen Kegelspitze S auf einer Normalen durch den Ellipsenmittelpunkt U auf die Trägerebene α von ℓ liegt (vgl. die Abbildung).

Schiefe Kreiskegel spielen in der Technik eine wichtige Rolle (vgl. z.B. [2]). Umso erstaunlicher ist es, daß z.B. in AutoCAD (zumindest bis zur Version 2007) keine Möglichkeit besteht *schiefe Kreiskegel* als Solids zu erzeugen; das Programm erlaubt nur die Konstruktion von Drehkegeln und elliptischen Kegeln. Zwar lassen sich schiefe Kreiskegel als verbindende Regelfläche zwischen einem Punkt S und einem Leitkreis ℓ mit diesem Programm als *Oberflächenmodelle* herstellen, doch bieten diese Objekte wenig Bearbeitungsmöglichkeiten, insbesondere z.B. keine Boole'schen Verknüpfungen oder ähnliche Operationen.

In dieser Arbeit wird mittels einfacher mathematischer Methoden die Erzeugung eines schiefen Kreiskegels für eine Computerimplementation hergeleitet.

Ein schiefer Kreiskegel mit dem Leitkreis k (Mittelpunkt O , Radius r) Trägerebene ε und der Spitze S (vgl. Kreuzriss in der Abbildung) kann wie folgt festgelegt werden:

Stočci 2. stupnja i AutoCAD

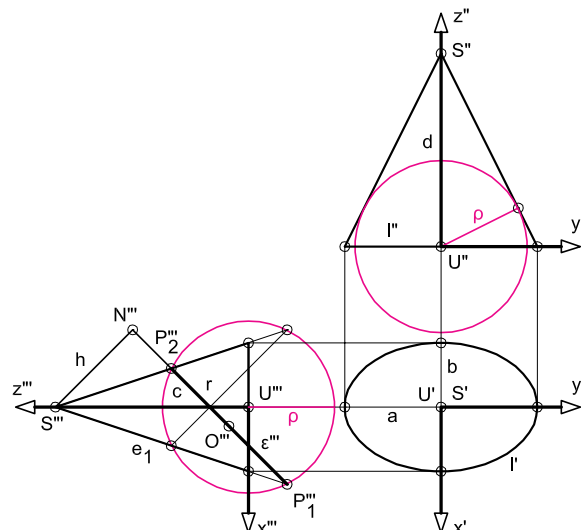
SAŽETAK

Raspravlja se o kosim kružnim stočcima i stočcima 2. stupnja, uglavnom s obzirom na izvedbu u računalnim algebarskim i CAD sistemima, posebno AutoCAD-u.

Ključne riječi: stožac 2. stupnja, kosi kružni stožac, eliptički stožac

Man bestimmt die Normalprojektion N von S auf ε und misst die beiden Abstände $h = \overline{SN}$ und $c = \overline{ON}$. Die Größe h ist die *Kegelhöhe*, c soll *Zentralabstand* heißen. Durch $\{r, c, h\}$ ist der Kreiskegel bis auf eine unwesentliche Spiegelung eindeutig festgelegt.

Für unsere Untersuchungen gehen wir nun von einem elliptischen Kegel Γ aus (vgl. die Abbildung), wobei die Leitellipse ℓ in der xy -Ebene liegt und die Halbachsenlängen a und b , $a > b$ besitzt; die Höhe von Γ sei $d = \overline{US}$, wobei U der Ellipsenmittelpunkt ist.



Hauptriss eines elliptischen Kegels

Zur Ermittlung der Kreisschnittebenen von Γ verwenden wir gemäß [3], p.249f eine Hilfskugel κ mit dem Mittelpunkt U , welche die Umrisszeugenden von Γ im Aufriß berührt. Wie aus [4] p.179 bekannt, zerfällt dann die Schnittkurve von Γ mit der Kugel κ in zwei Kurven zweiter Ordnung, die als Kurven auf κ somit Kreise sein müssen. Wir bezeichnen mit ρ den Radius dieser Hilfskugel.

Man findet unschwer

$$\rho = ad/\sqrt{a^2 + d^2}, \quad (1)$$

und als Gleichung von Γ

$$\frac{x^2}{a^2} + \frac{y^2}{b^2} = \left(1 - \frac{z}{d}\right)^2. \quad (2)$$

Schneidet man Γ mit der Ebene $y = 0$, so ergeben sich die beiden Umrisszeugenden e_1 und e_2 für den Kreuzriss zu

$$x = \pm b(1 - z/d) \quad (3)$$

und diese liefern im Schnitt mit dem Umriss der Kugel κ bezüglich des Kreuzrisses nach einigen Rechnungen vier Punkte von denen lediglich zwei benötigt werden. Die beiden anderen Punkte ergeben sich aus einer Spiegelung um die z -Achse. Zwei der benötigten Punkte sind z.B.

$$P_1\left(\frac{d^2b(1+W)}{b^2+d^2}, 0, \frac{d(b^2-d^2W)}{b^2-d^2}\right), \quad (4a)$$

$$P_2\left(\frac{-d^2b(1-W)}{b^2+d^2}, 0, \frac{d(b^2+d^2W)}{b^2+d^2}\right), \quad (4b)$$

wobei als Abkürzung

$$W := \sqrt{(a^2 - b^2)/(a^2 + d^2)} \quad (5)$$

verwendet wurde. Diese Punkte legen eine der *reellen* Kreisschnittebenen fest (vgl. die Abbildung). Die zweite würde sich natürlich aus den gespiegelten Punkten ergeben. Aus (4a) und (4b) erhält man als Gleichung der drittprojizierenden Kreisschnittebene

$$z = -\frac{d}{b}Wx + \frac{da^2}{a^2 + d^2}. \quad (6)$$

Als Nächstes muss der Mittelpunkt O des Schnittkreises k von Γ mit ϵ , der Radius r von k , der Zentralabstand c und die Kegelhöhe h berechnet werden. Für O erhält man

$$O\left(\frac{d^2bW}{b^2+d^2}, 0, \frac{db^2}{b^2+d^2}\right). \quad (7)$$

Wir verwenden noch die Abkürzung

$$Q := 1/\sqrt{(a^2 + d^2)(b^2 + d^2)}. \quad (8)$$

Aus (7) folgt dann mittels (4a)

$$r = ad^2 Q. \quad (9)$$

Für den Normalenfußpunkt N gewinnt man nach einigem Rechnen die Koordinaten

$$N\left(-\frac{d^4bW}{a^2(b^2+d^2)}, 0, \frac{da^2b^2+d^3(a^2-b^2)}{a^2+d^2}\right), \quad (10)$$

woraus sich $c = \overline{ON}$ bestimmen lässt zu

$$c = (d^2 Q/a) \sqrt{(a^2 - b^2)(a^2 + d^2)}. \quad (11)$$

Schließlich ergibt sich $h = \overline{SN}$ aus $S(0, 0, d)$ und wieder aus (10) als

$$h = d^3 b Q/a. \quad (12)$$

Zur Lösung der geometrischen Fragestellung muss das Gleichungssystem (9), (11) und (12) nach a , b und d aufgelöst werden. Dazu eliminieren wir als erstes die Größe Q aus den Gleichungen (11) und (12) mit Hilfe der Beziehung $Q = r/ad^2$ aus (9), quadrieren um die Wurzel in (11) zu vermeiden und erhalten unmittelbar aus (11) und (12) nach Division durch d^4 die beiden Gleichungen

$$\left(\frac{a^2}{d^2}\right)^2 c^2 = \left(\frac{a^2}{d^2} - \frac{b^2}{d^2}\right) \left(\frac{a^2}{d^2} + 1\right) r^2, \quad (13a)$$

$$\left(\frac{a^2}{d^2}\right)^2 h^2 = \left(\frac{b^2}{d^2}\right)^2 r^2. \quad (13b)$$

Setzt man nun

$$x := a^2/d^2 \quad \text{und} \quad y := b^2/d^2, \quad (14)$$

so erhalten wir schließlich die Gleichungen

$$c^2 x^2 = r^2(x^2 - xy + x - y), \quad (15a)$$

$$h^2 x^2 = r^2 y, \quad (15b)$$

Durch Elimination von y erhält man eine kubische Gleichung in x . Nach Ausscheiden der uninteressanten Lösung $x = 0$ hat man als Lösungen der verbleibenden quadratischen Gleichung mit $q = c^2 + h^2 - r^2$ dann

$$x_{1,2} = (-q \pm \sqrt{q^2 + 4h^2r^2})/2h^2, \quad (16)$$

wobei das positive Vorzeichen zu wählen ist. Aus (14) und (15b) lassen sich sofort a/d und b/d bestimmen zu

$$\frac{a}{d} = \sqrt{x} \quad \text{und} \quad \frac{b}{d} = \frac{h}{r}x, \quad (17)$$

wenn x nun die Lösung mit positivem Vorzeichen bei der Wurzel bedeutet.

Um d explizit zu bestimmen verwenden wir (8) und (12) und erhalten

$$d = \frac{1}{Qd^2} \frac{a}{b} h. \quad (18)$$

In diesem Ausdruck ist bereits alles bekannt, d kann daher sofort berechnet werden. Ausgedrückt durch die Lösung x erhält man

$$d = \sqrt{(x + 1/x)(h^2 x^2 + r^2)}, \quad (19)$$

und dann mit Hilfe von (17) sofort auch a und b .

Für die praktische Konstruktion mittels AutoCAD ist zunächst der dem schießen Kreiskegel zugeordnete elliptische Kegel zu bestimmen und dieser sodann mit der Kreisschnittebene ε zu schneiden. Die Gleichung von ε ist gegeben durch die Beziehung (6), woraus sich für den Neigungswinkel σ von ε gegen die xy -Ebene mit W aus (5) die Formel

$$\tan \sigma = -\frac{d}{b} W = -\frac{d}{b} \sqrt{\frac{a^2 - b^2}{a^2 + d^2}} \quad (20)$$

ergibt. Dieser *Kippwinkel* σ wird benötigt um die Basisfläche des schießen Kreiskegels parallel zur xy -Ebene drehen zu können.

Zur praktischen Durchführung werden zunächst also die Werte $\{a, b, d\}$ berechnet und der zugeordnete elliptische Kegel Γ z.B. als Solid dargestellt. Die weiteren Konstruktionen ergeben sich dann aus der Abbildung und den Beschreibungen und sollten für jemand, der einigermaßen mit den Grundkonstruktionen in AutoCAD vertraut ist unter Verwendung geeigneter Benutzerkoordinatensysteme keine Probleme mit sich bringen.

Zu bedenken ist aber Folgendes. Da die Berechnung von $\{a, b, d\}$ nicht zu vermeiden ist, kann man auch die Punkte P_1 und P_2 mit (4a) und (4b) direkt berechnen um sich aufwändigere Konstruktionen zu ersparen. Die Punkte werden dann mit Koordinaten eingegeben. Einen dritten Punkt von ε erhält man dann aus P_1 durch Änderung der y -Koordinate. Diese Möglichkeit ist auch deshalb interessant, weil sich unsere Kegelkonstruktion mit einer der internen Programmiersprachen von AutoCAD in einfacher Weise implementieren lässt, sodass die Erstellung eines schießen Kreiskegels dann durch einen eigenen Befehl aufrufbar wird.

Literatur

- [1] AUTODESK, INC: AutoCAD Benutzerhandbuch, www.autodesk.de
- [2] HOHENBERG, F.: *Konstruktive Geometrie in der Technik*, Springer Verlag, Wien 1966
- [3] KOMMERELL, K.: *Vorlesungen über Analytische Geometrie des Raumes*, K.F.Koehler Verlag, Stuttgart 1950
- [4] WUNDERLICH, W.: *Darstellende Geometrie I*, B.I.Hochschultaschenbücher, Bd. 96/96a, Mannheim, Wien, Zürich 1966

Hans Günther Kopetzky

e-mail: kopetzky@unileoben.ac.at

Hans Sachs

e-mail: sachs@unileoben.ac.at

Lehrstuhl für Angewandte Geometrie

Montanuniversität Leoben

A-8700 Leoben, Österreich

Professional paper
Accepted 28.12.2007.

DANIELA VELICOVÁ

Knotted Tori

Knotted Tori

ABSTRACT

Paper presents a family of surfaces called knotted tori, which can be regarded as special subset of two-axial surfaces of revolutions of Euler type. Analytic representation of surfaces and some of their specific geometric properties are derived, shaping parameters are discussed and several representatives of interesting shapes are illustrated.

Key words: knotted tori, Euler trajectory, two-axial surfaces of revolution

MSC 2000: 14J26, 15A04, 53A05

1 Introduction

Theory of knots is a part of algebraic topology, which studies problem known as "embeddings" of one topological space into another one. Embedding of space X into the space Y is an injective continuous mapping $f : X \rightarrow Y$ such that the restriction of f on

$$f : X \rightarrow f(X) \subseteq Y \quad (1)$$

is a homeomorphism of spaces X and $f(X)$.

The easiest form of the above mentioned problem is e.g. inclusion of a unit circle into the three-dimensional Euclidean space E^3 . In practical terms, this means that: "we take a circle, cut it, knot the created thread and finally glue together again both free ends". Closed space curve created in the described way is a topologically embedded circle into the three-dimensional space.

In the presented paper, the knotted tori will be understood as a regular surface created by a similar knotting of a torus like surface (not solid) in the three-dimensional space E^3 . Knotted torus is a surface with no self-intersections and singular points, it is closed, and its envelope is again a torus. This means that by knotting a torus no new type of topological structure will be created, or no new type of knot will arise than the original one. Consequently, there exist infinitely many different forms of the knotted tori in the three dimension space.

Torusni čvorovi

SAŽETAK

U članku se prikazuje porodica ploha pod nazivom torusni čvorovi, koja se može promatrati kao podskup dvoosnih rotacijskih ploha Eulerovog tipa. Izvode se analitička prezentacija tih ploha te neka od njihovih geometrijskih svojstava. Raspravlja se o parametrima oblika, a na nekoliko se primjera ilustriraju zanimljivi oblici ploha.

Ključne riječi: torusni čvorovi, Eulerova trajektorija, dvoosne rotacijske plohe

From the geometric point of view we can assume that a knotted torus is an envelope surface created by the continuous movement of the sphere in the space with the trajectory located on the torus of revolution in such way that no self-intersecting might occur. This curve is in the general case trajectory of the specific composite revolutionary movement about the two skew axes called Euler movement known as the Euler trajectory and described in details in [1].

Simple Euler trajectory in the basic form is a closed space curve without any multiple points illustrated in fig. 1, on the left; its orthographic view in the plane perpendicular to the axis of revolution 2o is a symmetric plane curve, Limaçon of Pascal.

Let $A = (a, 0, 0, 1)$ be a given point on the coordinate axis x that moves in the Euler movement composed from two revolutions, about coordinate axis $z = {}^1o$ and simultaneously about axis 2o parallel to the coordinate axis x in the distance $d \neq 0, {}^2o \parallel x$ determined by equations $y = d, z = 0$. Trajectory of the point movement can be analytically represented by continuous differentiable point function in one real variable v , which is on the interval $I = \langle 0, 1 \rangle \subset R$ in the following form:

$$\begin{aligned} \mathbf{r}(v) = & (a \cos k\pi v, a \sin k\pi v \cos l\pi v + d(1 - \cos l\pi v), \\ & a \sin k\pi v \sin l\pi v - d \sin l\pi v, 1). \end{aligned}$$

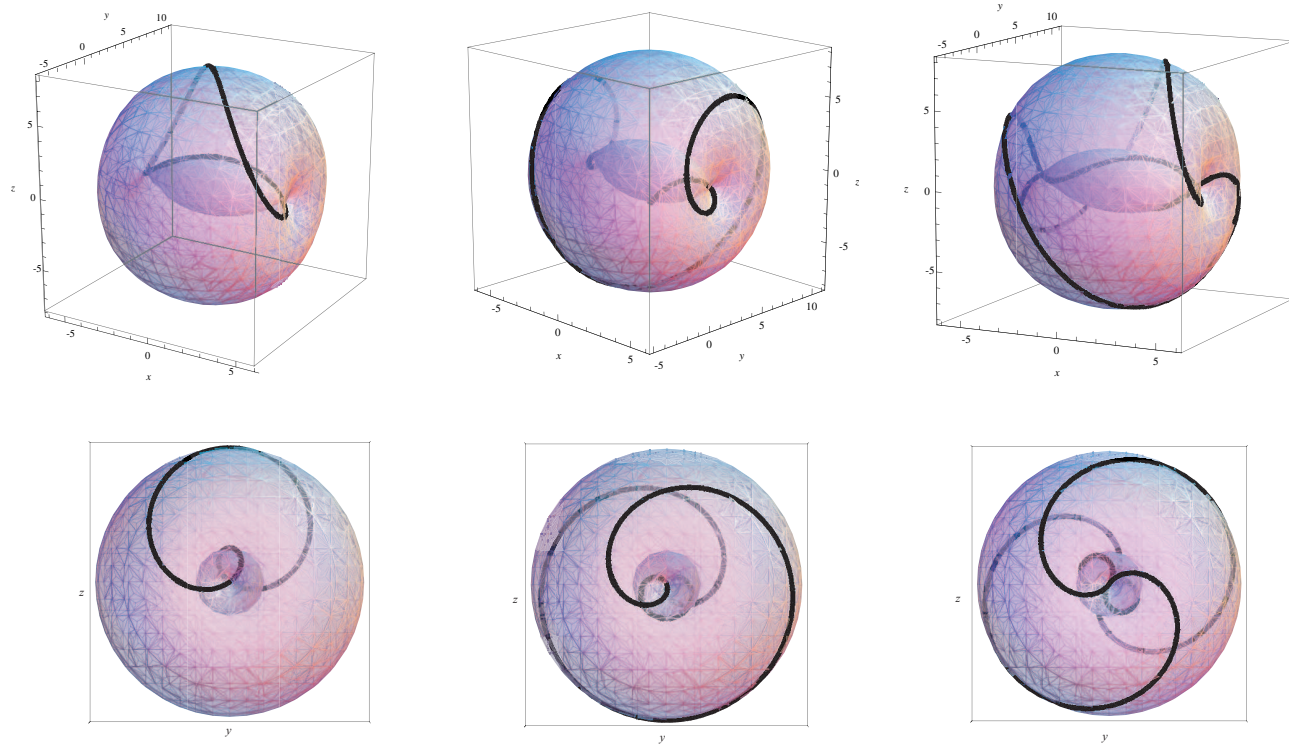


Figure 1: Forms of Euler trajectories.

Euler trajectory is located on torus of revolution with the axis in the axis of revolution 2o , centre in the point $S = (0, d, 0, 1)$ on the coordinate axis y and radius equal to the distance a of the moving point from the axis of revolution 1o . Coordinates of the Euler trajectory points satisfy the implicit equation of the torus

$$(x^2 + (y - d)^2 + z^2 + d^2 - a^2)^2 = 4d^2((y - d)^2 + z^2).$$

Several forms of the Euler trajectory determined by multiples k and l of angular velocities of separate revolutions are illustrated in fig. 1 on the left, in the middle and on the right, with pairs of parameters $a = 5, d = 3, (k, l) = (2, 2), (2, 6), (4, 6)$.

2 Knotted tori as cyclical two-axial surfaces of revolution of Euler type, the 1st form

Surfaces in the group of general two-axial surfaces of revolution of the Euler type (complete classification is presented in [2]) can be generated by the movement of the basic circle g located in the plane passing through the first - interior axis of revolution 1o , and they are represented by vector function

$$\mathbf{r}(u, v) = (a + r \cos 2\pi u, 0, b + r \sin 2\pi u, 1), \\ u \in \langle 0, 1 \rangle, a, b, r \in R, r \neq 0.$$

Parametric equations of surfaces in this subgroup of surfaces of Euler type are for $(u, v) \in \langle 0, 1 \rangle^2 \subset R^2$ in the form

$$\begin{aligned} x(u, v) &= (a + r \cos 2\pi u) \cos k\pi v \\ y(u, v) &= (a + r \cos 2\pi u) \sin k\pi v \cos l\pi v - \\ &\quad -(b + r \sin 2\pi u) \sin l\pi v + d(\cos l\pi v - 1) \\ z(u, v) &= (a + r \cos 2\pi u) \sin k\pi v \sin l\pi v + \\ &\quad +(b + r \sin 2\pi u) \cos l\pi v + d \sin l\pi v \end{aligned}$$

Knotted tori can be created by choosing values of shaping parameters satisfying the following relations

$$b = 0, a < d, a > r, k \text{ and } l \text{ are even numbers.}$$

Different modifications of knotted tori can be achieved by the choice of other shaping characteristics, multiples of separate angular velocities k and l . Number of windings in the direction of the revolution about the second axis is the number of arms equal to $l/2$, number of windings in the direction of the first axis of revolution defines the number of knots, $k/2$.

Simple non-trivial knotted torus (trefoil) is illustrated in fig. 2 on the left, shaping characteristics are $a = 5, b = 0, d = 10, r = 3, (k, l) = (6, 4)$. Other illustrated forms are determined by the same shaping parameters a, b, d, r, r , and by values $(k, l) = (10, 4), (14, 4)$, surfaces have two knotted arms; number of knots is 3, 5 and 7.

In fig. 3 knotted tori with values of shaping characteristics $a = 5, b = 0, d = 12, r = 3, (k, l) = (8, 6), (10, 6), (14, 6)$ are illustrated, which are created by knotting of three arms 4, 5 and 7 times.

By knotting four arms the next modification of the knotted torus can be created, shaping parameters of the illustrated surfaces are $a = 5, b = 0, d = 17, r = 2, (k, l) = (6, 8), (10, 8), (14, 8)$, so the four arms are knotted 3, 5 and 7 times.

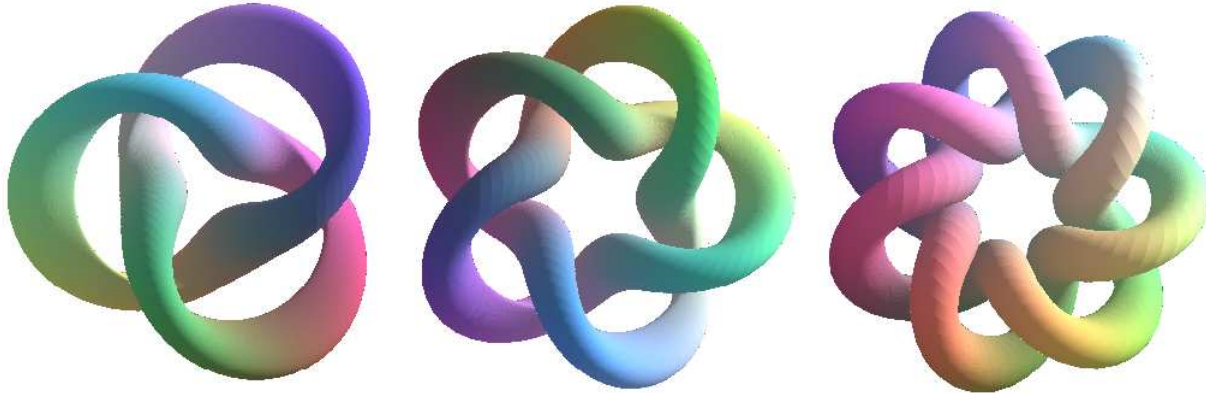


Figure 2: *Knotted tori of the 1st form, with 2 threads.*

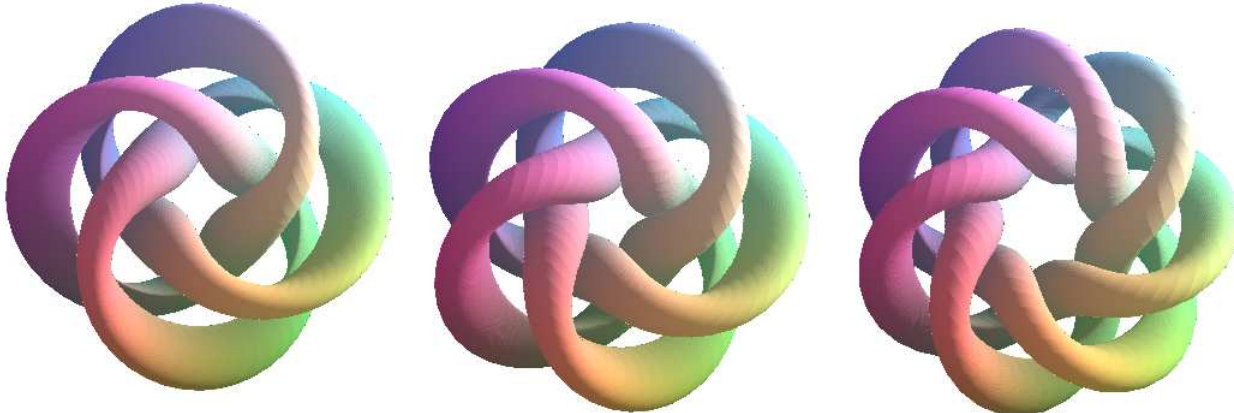


Figure 3: *Knotted tori of the 1st form, with 3 threads.*

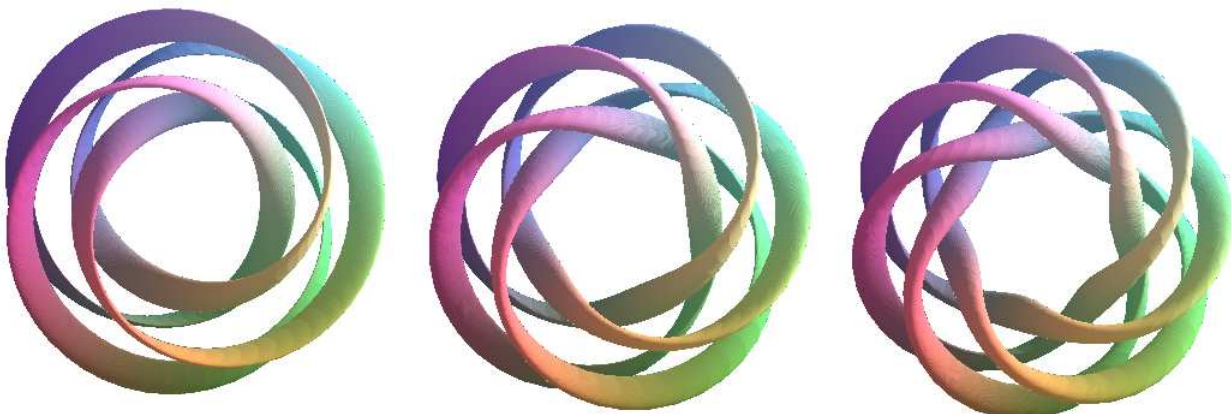


Figure 4: *Knotted tori of the 1st form, with 4 threads.*

3 Knotted tori as cyclical two-axial surfaces of revolution of Euler type, the 2nd form

Basic circle of the knotted torus located in the plane of the exterior axis of revolution 2o defined by vector function

$$\mathbf{r}(u) = (a + r \cos 2\pi u, b + r \sin 2\pi u, 0, 1), \\ u \in \langle 0, 1 \rangle, a, b, r \in R, r \neq 0.$$

determines subgroup of surfaces of Euler type of the second form represented analytically by parametric equations for $(u, v) \in \langle 0, 1 \rangle^2 \subset R^2$ in the form

$$x(u, v) = (a + r \cos 2\pi u) \cos k\pi v - (b + r \sin 2\pi u) \sin k\pi v \\ y(u, v) = (a + r \cos 2\pi u) \sin k\pi v \cos l\pi v + \\ + (b + r \sin 2\pi u) \cos k\pi v \cos l\pi v + d(\cos l\pi v - 1) \\ z(u, v) = (a + r \cos 2\pi u) \sin k\pi v \sin l\pi v + \\ + (b + r \sin 2\pi u) \cos k\pi v \sin l\pi v + d \sin l\pi v.$$

Different modifications of knotted torus of the 2nd form can be created by shaping characteristics, where $b = 0$, and

multiples of angles of revolutions are k and l . Number of turns about the second axis of revolution defines the number of arms $l/2$, number of turns about the first axis of revolution gives the number of knots $k/2$.

Knotted tori of the second form are illustrated in fig. 5, values of parameters for corresponding forms illustrated from the left to the right are: $a = 10, b = 0, d = 17, r = 3, (k, l) = (4, 6), (4, 10), (4, 14)$.

In fig. 6, samples of modifications determined by parameters $a = 10, b = 0, d = 17, r = 3, (k, l) = (6, 8), (6, 10), (6, 14)$ are presented, in fig. 7 illustrations of knotted tori determined by multiples of angular velocities $(k, l) = (8, 6), (8, 10), (8, 14)$ are presented.

Some complex forms of knotted tori are extremely interesting in shapes, and they can be utilised as small artefacts, resembling mosaic motifs, laces and embroidered emblems. Samples of these aesthetic objects, which are freely modified forms of knotted tori, are illustrated in fig. 8.

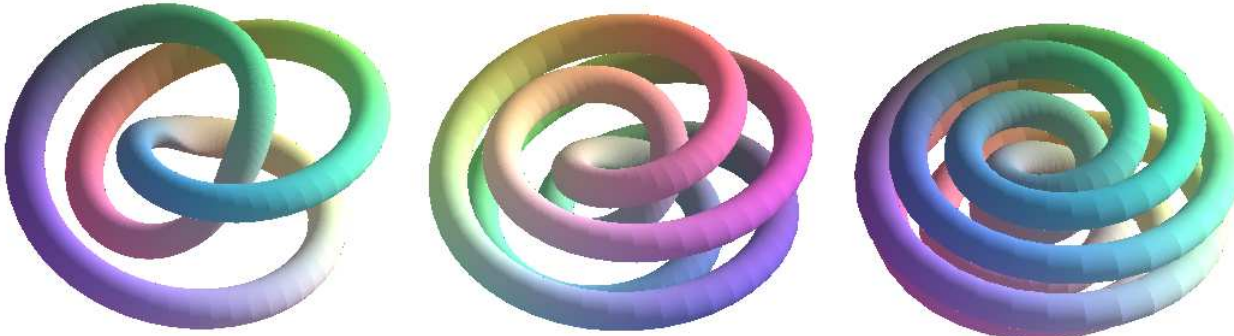


Figure 5: Knotted tori of the 2nd form, two-folded.

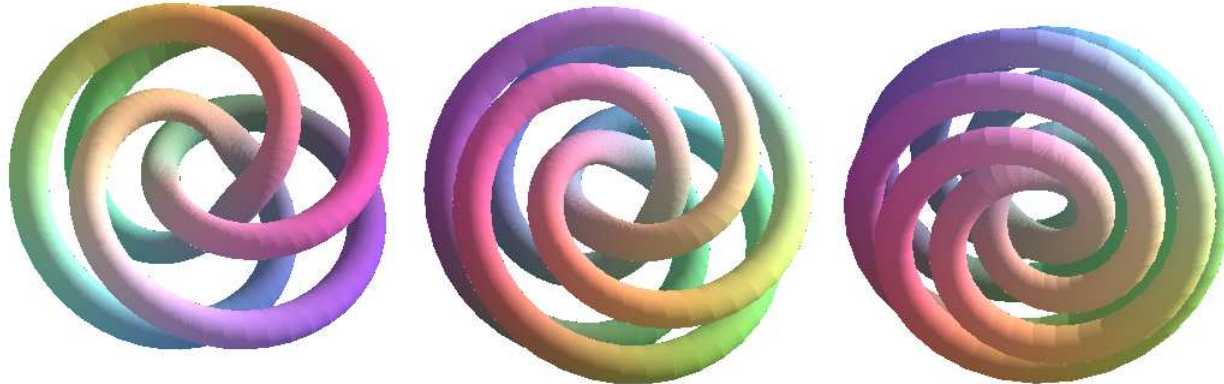


Figure 6: Knotted tori of the 2nd form, three-folded.

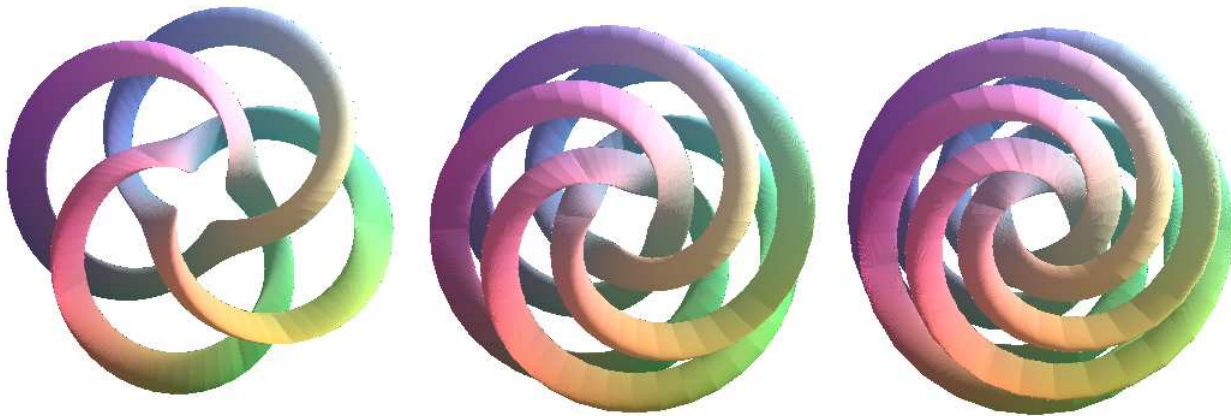


Figure 7: *Knotted tori of the 2nd form, four-folded.*

4 Conclusions

There exist infinitely many different forms of knotted tori, and not all of them can be created as special two-axial surfaces of revolution of Euler type, whereas many of them can be created on the base of other principles. There is available a rich source database of materials dealing with knotted tori, where this topic is discussed from different viewpoints and on different theoretical or practical levels. Book [3] is an introduction to the theory of knots and topology of surfaces, where common links between these two areas and their connections to the graph theory and theory of groups are given. Book is written in a very good style, there are a lot of illustrations in there, and just the basic knowledge of secondary school mathematics is

expected from readers. Book [4] brings a historical survey of the theory of knots, showing that creation of knots can be regarded as one of the oldest and most widespread techniques in art, weaving, sea-sailing, coding, ciphering, building and architecture, and in many other applications and practical activities influencing the development of human civilisation and culture.

Some interesting and inspiring sources can be found on Internet, where one can see also many interactive applications enabling modelling of knotted tori on-line on web. Web-page at address [5] is entirely designed for bringing information about available source materials with references to all aspects of knotted tori modelling - theory, art, computer modelling, video presentations, on-line galleries.

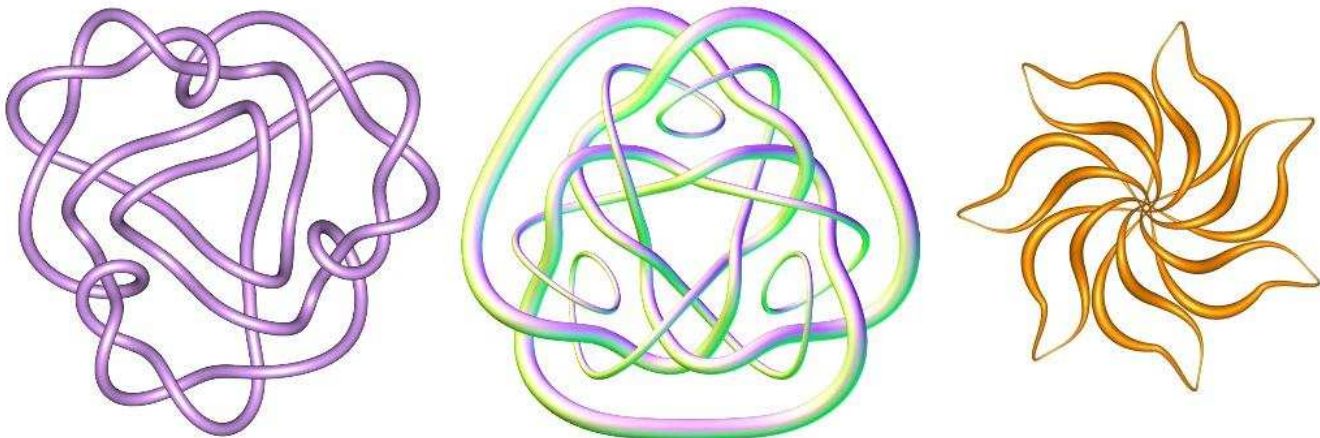


Figure 8 *Knotted tori, free forms.*

References

- [1] D. VELICOVÁ, Trajectories of composite rotational movements, G–Slovak Journal for Geometry and Graphics, ISSN 1335- X, Vol. 3, No. 5, 2006, pp. 47-64.
- [2] D. VELICOVÁ, Classification of two-axial surfaces, G - Slovak Journal of Geometry and Graphics, ISSN 1335- X, Vol. 4, No. 7, 2007, pp. 63-82.
- [3] N. D. GILBERT, T. PORTER, *Knots and Surfaces*, Oxford University Press, 1997 (original 1994).
- [4] J. C. TURNER, P. VAN DE GRIEND, *History and Science of Knots*, World Scientific Publishing Co., 1996.
- [5] <http://www.earlham.edu/~peters/knotlink.htm>

Daniela Velichová

Department of Mathematics, Mechanical Engineering Faculty, Slovak University of Technology
Námestie slobody 17, 812 31 Bratislava, Slovakia
e-mail: daniela.velichova@stuba.sk

Stručni rad

Prihvaćeno 29.12.2007.

ŽELJKO GJURANIĆ

Modeliranje terena pomoću Delaunayeve triangulacije

Terrain Modelling by Using Delaunay Triangulation

ABSTRACT

Delaunay triangulation is a terrain modelling procedure out of irregular set of points, such as geodetic survey. This article discusses one of the computation methods with computation theory and some practical uses. It also discusses some uses for Voronoi diagram as well as computation method.

Key words: Delaunay triangulation, Voronoi diagram, terrain modelling, geodetic survey

MSC 2000: 68W30, 86A30

1 Uvod

Prilikom projektiranja građevina, potrebno je uzeti u obzir, između ostalog, i geometriju terena na kojem će se graditi. Time se izbjegavaju troškovi suvišnih iskopa i nasipa, sanacije terena i sl. Iz tog razloga se prije projektiranja, poglavito većih građevina, naručuje geodetska izmjera postojecog terena. Navedenom izmjerom se određuju prostorne koordinate točaka. Pojedini softverski paketi, kao što su *Autodesk Civil 3d*, *Bentley PowerCivil i sl.*, imaju mogućnost generiranja modela terena iz niza točaka, međutim takvi paketi su znatno skuplji od klasičnih CAD alata, a često i komplikirani za uporabu.

Ovaj rad objašnjava jednu od metoda kako od izmjerjenih točaka dobiti trodimenzionalni model terena iz kojeg je moguće dobiti slojnice, presjeke, količine iskopa i nasipa i sl. Poznavajući metodu moguće je napisati samostalan računalni program za generiranje modela ili nadograditi postojeći CAD alat. Dobiveni trodimenzionalni model se sastoji od trokuta koji povezuju sve točke, a postupak generiranja trokuta se naziva Delaunayevom triangulacijom prema ruskom matematičaru Borisu Delaunayu (Boris Delone 1890-1980) [4].

Modeliranje terena pomoću Delaunayeve triangulacije

SAŽETAK

Delaunayova triangulacija je postupak modeliranja terena iz nepravilnog skupa točaka, kao što je geodetska izmjera. U članku je prikazana jedna od metoda proračuna triangulacije s teorijskom podlogom i nekoliko primjera upotrebe. Također je navedeno nekoliko primjera uporabe Voronoi-jevog dijagrama, i metoda proračuna.

Ključne riječi: Delaunayeva triangulacija, Voronoi-jev dijagram, modeliranje terena, geodetski snimak

2 Delaunayeva triangulacija

Polazimo od pretpostavke da teren ne može imati točke na istim x i y koordinatama i različitoj visini. Ova pretpostavka je nužna da bi se problem triangulacije mogao svesti na ravnički. Problem triangulacije je matematički analogan problemu *konveksne ovojnica* [1] u prostoru, odnosno razvlačenju elastične membrane kroz zadane točke.

Konkretno, Delaunayeva ravnička triangulacija je analoga problemu konveksne ovojnice točaka ravnine xy projiciranih na paraboloid $z = x^2 + y^2$ paralelno s osi z [1], (vidi sliku 1). Time se dobiva triangulacija s najmanje ostrih kutova, što je ujedno i optimalno rješenje.

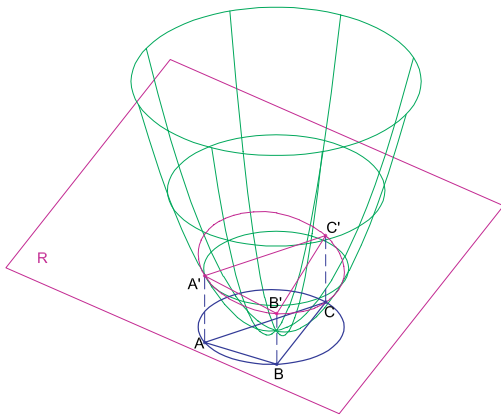
Ako proizvoljna ravničina R ima jednadžbu

$$z = \alpha x + \beta y + \gamma,$$

projekcija presjeka paraboloida $z = x^2 + y^2$ i te ravničine, na ravničinu xy , ima jednadžbu

$$x^2 + y^2 = \alpha x + \beta y + \gamma.$$

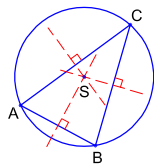
Iz jednadžbe je vidljivo da je, neovisno o presječnoj ravničini, projekcija presjeka kružnica. Budući da presjek sadrži vrhove trokuta $A'B'C'$, projekcija je upravo opisana kružnica trokuta ABC . Vidi sliku 1.



Slika 1: Paraboloid presječen ravninom

Da bi ovojnica bila konveksna, za svaki trokut $A'B'C'$ mora vrijediti da se sve zadane točke nalaze iznad ravnine trokuta. Projekcija bilo koje točke paraboloida iznad ravnine trokuta, na ravninu xy , nalazi se izvan presječnice paraboloida ravnom trokuta, dakle projekcija u xy ravnini se nalazi izvan opisane kružnice trokuta ABC .

Postavljamo uvjet triangulacije: Za svaki trokut ABC vrijedi da se sve zadane točke, osim A , B , i C , nalaze izvan opisane kružnice trokuta ABC . Ovim uvjetom triangulacija dobiva jedinstveno rješenje.



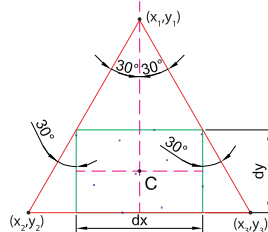
Slika 2: Trokut s opisanom kružnicom

3 Rastući algoritam za Delaunayjevu triangulaciju

Postoji nekoliko učinkovitih algoritama za Delaunayjevu triangulaciju, a jedan od najjednostavnijih i najbržih je tzv. *rastući algoritam* [2]. Osnova rastućeg algoritma je dodavanje točaka u postojeću mrežu. Algoritam također zahtjeva da se svaka točka koja se dodaje u mrežu nalazi unutar gabarita postojeće mreže. Dakle, početna mreža se definira kao trokut, unutar kojeg se nalaze sve zadane točke. Ovako dobivena triangulacija ima 3 točke više od zadanih, te je na kraju potrebno izbrisati sve trokute koji sadrže bilo koju od te 3 točke.

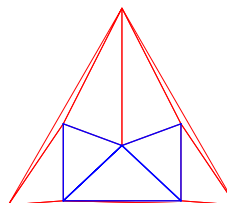
Numerički najpovoljniji trokut, koji sadrži sve točke, je istostraničan. Ako definiramo pravokutnik koji sadrži sve zadane točke sa stranicama dx i dy i točkom $C(C_x, C_y)$ kao središtem pravokutnika, možemo odrediti koordinate vrhova istostraničnog trokuta opisanog pravokutniku:

$$\begin{aligned}x_1 &= C_x & y_1 &= C_y + \frac{dy}{2} + \frac{dx}{2 \cdot \tan 30^\circ} \\x_2 &= C_x - \frac{dx}{2} - dy \cdot \tan 30^\circ & y_2 &= C_y - \frac{dy}{2} \\x_3 &= C_x + \frac{dx}{2} + dy \cdot \tan 30^\circ & y_3 &= C_y - \frac{dy}{2}.\end{aligned}$$

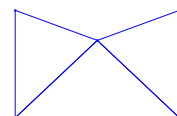


Slika 3: Jendakostraničan trokut opisan pravokutniku

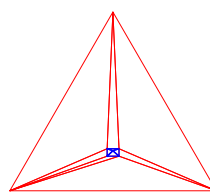
Ovako smo dobili najmanji istostraničan trokut koji sadrži pravokutnik opisan točkama. Međutim, prilikom triangulacije se mogu pojavit konkavni vanjski rubovi mreže, zbog čega se preporučuje definirati znatno veći trokut od minimalno potrebnog (barem 10 puta).



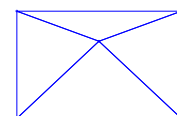
Slika 4: Trokut 10% veći od minimalnog



Slika 5: Neispravna triangulacija



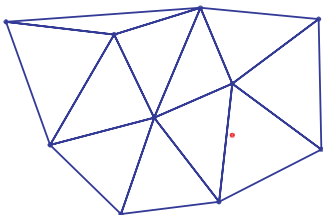
Slika 6: Trokut 10 puta veći od minimalnog



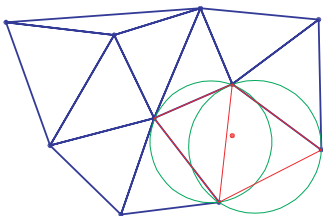
Slika 7: Ispravna triangulacija

Dodavanje točke se vrši na sljedeći način:

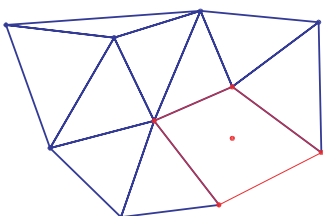
Prvo se provjeri koje je trokute potrebno ukloniti, a to su oni unutar čijih se opisanih kružnica nalazi točka koju treba dodati u mrežu (vidi sliku 9). Nakon uklanjanja trokuta iz mreže, točka se nalazi unutar poligona čiji broj stranica ovisi o broju i međusobnom položaju uklonjenih trokuta (vidi sliku 10). Novi trokuti koji se dodaju u mrežu sadrže po jednu stranicu navedenog poligona, i točku koju treba dodati (vidi sliku 11). Postupak se ponavlja za sve zadane točke i tako se dobije konačna mreža prikazana na slici 11.



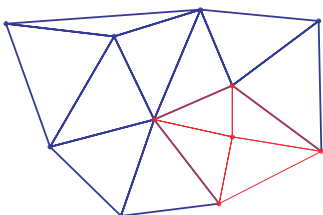
Slika 8: Mreža u koju treba dodati točku



Slika 9: Trokuti koji se brišu



Slika 10: Trokuti izbrisani



Slika 11: Dodana točka

Algoritam, napisan u pseudo kodu, izgleda ovako:

```

For i = 0 do broj_točaka
For j = 0 do broj_trokuta
If tocka_i unutar opisane kružnice trokuta_j
dodaj_rubove_trokuta_j_u_tablicu
briši_trokut_j_iz_mreže
End If
Next j
For j = 0 do broj_rubova ' broj rubova u
tablici
For k = j do broj_rubova
If rub_j = rub_k
briši_rub_j_iz_tablice
briši_rub_k_iz_tablice
End If
Next k
Next j
' U tablici su ostali vanjski rubovi poligona
For j = 0 do broj_rubova
dodaj_trokut-rub_j-točka_i
Next j
Next i

```

Ukoliko se izvodi na prosječnom računalu, ovaj algoritam je dovoljno brz za većinu primjena - triangulacija 10.000 točaka traje svega nekoliko sekundi. Međutim u slučaju posebnih potreba, npr. izvođenje na ručnom računalu, vrlo velik broj točaka (nekoliko milijuna) ili potreba za iterativnim postupkom, moguće je da izvođenje traje predugo za praktičnu uporabu. Postoje tri vrlo jednostavne metode ubrzavanja algoritma:

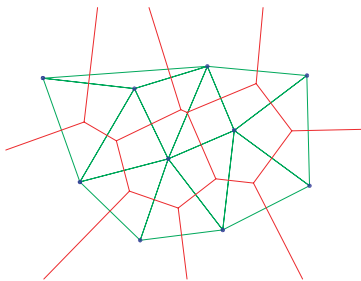
1. Memorirati uz svaki trokut koordinate središta i radijus opisane kružnice, da se izbjegne ponovno proračunavanje za svaki korak.
2. Sortiranje točaka po jednoj osi - smanjuje broj provjera.
3. Definirati sve trokute u istom smjeru, pa će rubovi koji se preklapaju u tablici uvijek biti okrenuti suprotno jedan drugom.

4 Voronoijev dijagram

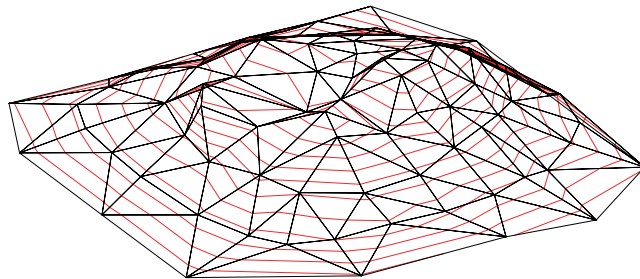
Rješavanjem Delaunayeve triangulacije ujedno je riješen još jedan problem, a to je Voronoijev dijagram [3] (ruski matematičar Georgi Voronoi 1868–1908).

Za niz točaka u ravnini, Voronoijev dijagram prikazuje područja kojima je pojedina točka najbliža. Dobiva se spajanjem središta opisanih kružnica trokuta, odnosno sastoji se od simetrala stranica Delaunayeve triangulacije. Voronoijev dijagram ima široku primjenu u više grana djelatnosti:

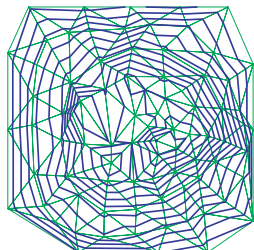
- Urbanizam - definiranje položaja važnih objekata.
- Cestogradnja - izbjegavanje prepreka.
- Gradnja velikih postrojenja - pronalaženje idealne lokacije.
- Arheologija - područja utjecaja skupina životinja.
- Biologija - površine tla koje koriste pojedine biljke, transport kisika u stanice.



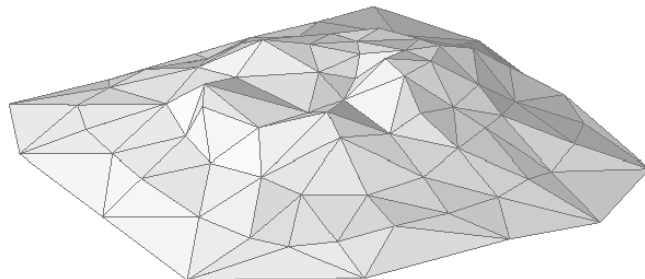
Slika 12: Voronoijev dijagram



Slika 14: Trodimenzionalni prikaz modela terena sa slojnicama



Slika 13: Model terena sa slojnicama



Slika 15: Osjenčani prikaz modela terena

Literatura

- [1] Computing a Delaunay triangulation,
<http://www.jouy.inra.fr/unites/miaj/public/vigneron/cs4235/110cs4235.pdf>
- [2] Efficient Triangulation Algorithm for Constructing the Model Surface from the Interpolation of Irregularly-Spaced Laser Scanned Data,
<http://ieg.or.kr/abstract/P080307.PDF>
- [3] Delaunay triangulation, http://en.wikipedia.org/wiki/Delaunay_triangulation

- [4] Boris Delaunay,
http://en.wikipedia.org/wiki/Boris_Delaunay

Željko Gjuranić

Hrvatske telekomunikacije d.d.

Savska cesta 32, 10000 Zagreb

e-mail: Zeljko.Gjuranic@t.ht.hr

GUIDE FOR AUTHORS

SCOPE. “KoG” publishes scientific and professional papers from the fields of geometry, applied geometry and computer graphics.

SUBMISSION. Scientific papers submitted to this journal should be written in English or German, professional papers should be written in Croatian, English or German. Only unpublished material can be accepted.

Two single-side copies of the manuscript with wide margins and double spaced should be sent to the one of the editors.

Sonja Gorjanc sgorjanc@grad.hr Faculty of Civil Engineering	Jelena Beban - Brkić jbeban@geof.hr Faculty of Geodesy
---	--

Kačićeva 26, 10000 Zagreb, Croatia

The first page should contain the article title, author and coauthor names, affiliation, a short abstract in English, a list of keywords and the Mathematical subject classification.

ELECTRONIC FORMATS. Accepted papers should be sent by electronic mail as ASCII files (\LaTeX format is recommended) to the address: sgorjanc@grad.hr

OFFPRINTS. The total of 20 reprints of each contribution will be sent to its first mentioned author (if not otherwise desired) free of charge.

How to get KoG?

The easiest way to get your copy of KoG is by contacting the editor's office:

Nikoleta Sudeta
nsudeta@arhitekt.hr
Faculty of Architecture
Kačićeva 26, 10 000 Zagreb, Croatia
Tel: (+385 1) 4639 219
Fax: (+385 1) 4828 079

The price of the issue is €15 + mailing expenses €5 for European countries and €10 for other parts of the world.

The amount is payable to:

ACCOUNT NAME: Hrvatsko društvo za geometriju i grafiku
Kačićeva 26, 10000 Zagreb, Croatia
IBAN: HR862360000-1101517436

UPUTE ZA AUTORE

PODRUČJE. "KoG" objavljuje znanstvene i stručne rade iz područja geometrije, primijenjene geometrije i računalne grafike.

UPUTSTVA ZA PREDAJU RADA. Znanstveni rade trebaju biti napisani na engleskom ili njemačkom jeziku, a stručni na hrvatskom, engleskom ili njemačkom. Rad treba biti neobjavljen.

Dva primjera rukopisa sa širokim marginama i dvostrukim proredom treba poslati na adresu jedne od urednica:

Sonja Gorjanc sgorjanc@grad.hr Građevinski fakultet	Jelena Beban - Brkić jbeban@geof.hr Geodetski fakultet
---	--

Kačićeva 26, 10000 Zagreb

Prva stranica treba sadržavati naslov rada, podatke o autoru i koautorima, sažetak na hrvatskom i engleskom, ključne riječi i MSC broj.

ELEKTRONIČKI FORMATI. Prihvaćene rade autoru dostavljaju elektronskom poštom kao ASCII datoteke (preporučuje se \LaTeX format) na adresu: sgorjanc@grad.hr

POSEBNI OTISCI. Autori dobivaju 20 otisaka svog rada koji se šalju prvom koautoru, ukoliko nije dukčije dogovorenno.

Kako nabaviti KoG?

KoG je najjednostavnije nabaviti u uredništvu časopisa:

Nikoleta Sudeta
nsudeta@arhitekt.hr
Arhitektonski fakultet
Kačićeva 26, 10 000 Zagreb
Tel: (01) 4639 219
Fax: (01) 4828 079

Za Hrvatsku je cijena primjera 100 KN + 10 KN za poštarinu.

Nakon uplate za:

HDGG (za KoG), Kačićeva 26, 10000 Zagreb
žiro račun broj **2360000-1101517436**

poslati ćemo časopis na Vašu adresu.

Ako Vas zanima tematika časopisa i rad našega društva, preporučamo Vam da postanete članom HDGG (godišnja članarina iznosi 100 KN). Za članove društva časopis je besplatan.

Visual rhythms

Tamás F. Farkas is one of the most significant contemporary geometrical artists, whose works appear not merely at exhibitions from Paris to Tokio, but also at scientific conferences and workshops, as it has been e.g. at the 12th Scientific-Professional Colloquium of Croatian Society for Geometry and Graphics.

His visual researches are motivated by the intention to create new structures and "constructions that have never been seen before". His paintings and graphics reflect ardent desire to beauty and harmony. All these motivations lead to different realizations in two, three or even higher dimensional arrangements of forms, both real and imaginary (not constructable in the tangible world).

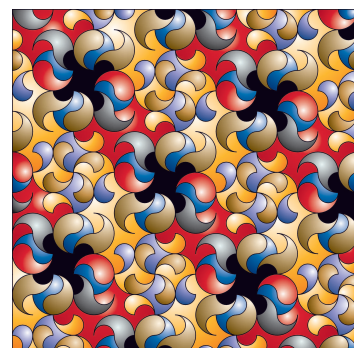
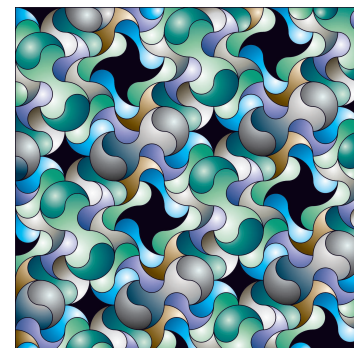
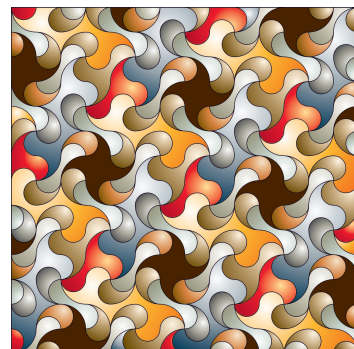
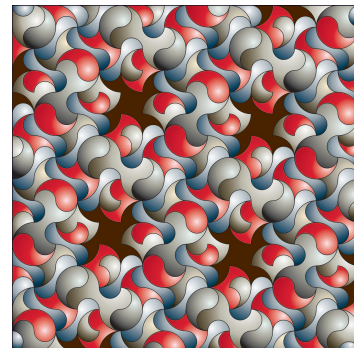
The cover page of this issue of KoG shows some Tamás F. Farkas's brand new planar creations. From mathematical point of view all these belong to discrete geometry, more precisely to periodic patterns and tilings. This area has a wide literature from the classical results of planar crystallographic groups e.g. to classification results of color groups. Not only mathematics, but physics, chemistry, crystallography and engineering sciences operate with the mentioned concepts and theories.

The fascinating, artistically formulated graphics are created empirically by Tamás, who works as an intuitive geometer in a way that is very rich in ideas.

T. F. Farkas's newest inventions, the admiring forms randed by circular arcs constitute a coherent, connected, yet undiscovered visual world. The objects we see express different relations: they rotate, whirl and wave. Structure, periodicity and symmetry makes the figures moving in an almost vivid way. The way of coloring just heighten the spatial imagination and the dynamics. The arrangements are full of life, it is easy to associate to exotic flowers or cells under the object glass of a microscope. The patterns of circular arcs recall images of petals, blooms, fruits and lush tropical vegetation. The forms swirl here and there, they wave and we think to see drops between the leaves.

Sometimes we feel to see frills, cloth making a fluttering movement and we are already at the dance, rhythm and music. If we let the pictures to lead us into the world of fantasy, then we may hear a melody from a far distance or discover the strange poesy of forms, full of youth and life. Tamás F. Farkas often refers to his pictures as "visual melodies", and indeed, the rhythm and the composing connects the two areas.

We do mention that this new geometric-artistic imagination may inspire the scientist, initiating new thoughts and helps to discover new relations between different layers of life.



ATTILA BÖLCSKEI

ISSN 1331-1611



9 771331 161005

